Tareq Anwar Shikdar

Data-Driven Advanced Forecasting, Planning, and Market Operation of Hybrid PV-BESS Power Plant

Master's Thesis

School of Technology and Innovations
Master of Science in Technology
Master's Degree in Smart Energy
Erasmus Mundus Joint Masters in Smart Cities and Communities

Vaasa 2026

UNIVERSITY OF VAASA

School of Technology and Innovations

Author:	Tareq Anwar Shikdar
Title of the thesis:	Data-Driven Advanced Forecasting, Planning, and Market Operation of Hybrid PV-BESS Power Plant
Degree:	Master of Science in Technology
Degree Programme:	Erasmus Mundus Joint Master Degree in Smart Cities and Communities (SMACCs)
Supervisor:	Hannu Laaksonen
Partner Co-Supervisor	Tauno Kekäle (Merinova)
2nd Partner Co-Supervisor	Simon Björkman (EPV Energia Oy)
Year:	2026 **Pages:** 117

ABSTRACT:

This study aims to develop a unified, data-driven framework that integrates probabilistic photovoltaic (PV) forecasting, risk-aware battery energy storage system (BESS) planning, and market-oriented operational control under uncertainty. The research addresses the following key questions: (i) how forecast uncertainty can be effectively utilized in operational decision-making, (ii) how it influences optimal BESS sizing, and (iii) how it affects economic performance and risk in electricity markets. The proposed framework enables end-to-end propagation of probabilistic information across decision layers, transforming forecast uncertainty into a quantifiable decision variable. The framework is validated using real data from a utility-scale PV plant in Finland. Probabilistic forecasting based on quantile regression achieves reliable calibration (prediction interval coverage ≈ 0.88–0.93). Forecast accuracy degrades with increasing prediction horizon defined as day-ahead (D1), two-day-ahead (D2), and three-day-ahead (D3) with root mean square error (RMSE) increasing from approximately 8.4 MW (D1) to 12.9 MW (D3). This degradation significantly increases the probability of extreme imbalance events, referred to as tail-risk exposure. Incorporating this uncertainty into planning, a Conditional Value-at-Risk (CVaR)-based optimization where CVaR represents the expected loss under worst-case conditions consistently identifies a compact BESS configuration within the evaluated

design space and considered market conditions (2 MW / 2 MWh). This design maximizes economic value (≈ €4.18 M annual profit, ≈ €35 M net present value (NPV), where NPV represents long-term investment profitability) under controlled risk (≈ €2.38 M CVaR), indicating that optimal sizing is governed by marginal value saturation rather than capacity scaling. Operational results show that uncertainty-aware dispatch reduces extreme imbalance exposure and reserve volatility, at the cost of moderate reductions in short-term profit (≈10–20%) and increased curtailment. A critical nonlinear regime is observed at intermediate horizons (D2), where imbalance cost peaks (~450 k€), indicating maximum sensitivity to forecast error. Long-term evaluation demonstrates that optimized control reduces battery cycling by approximately 50%, significantly extending asset lifetime. The main contribution of this study is the development of a unified, decision-oriented PV–BESS framework that explicitly links forecast uncertainty to economic value, operational risk, and storage efficiency. The results demonstrate that optimal system performance emerges from selective, risk-aware utilization of flexibility rather than maximum energy throughput, providing a scalable foundation for real-time digital twin applications in renewable-dominated power systems

KEYWORDS: Probabilistic modeling; BESS optimization; CVaR; uncertainty propagation; energy markets; PV–BESS systems; decision-oriented optimization; digital twin

Contents

Figures

Tables

Use of Artificial Intelligence

During the preparation of this thesis, the author used AI tools including **ChatGPT, QuillBot, and Grammarly** to support language improvement, grammar checking, paraphrasing assistance, text refinement, and overall readability enhancement. These tools were used only for improving the clarity and presentation of the written content.

The author of the thesis takes full responsibility for the content of the thesis and confirms that all analysis, interpretations, results, and conclusions were developed independently by the author.

ABBREVIATIONS

Abbreviation	Full Form
ANN	Artificial Neural Network
API	Application Programming Interface
AR	Autoregressive
ARIMA	Autoregressive Integrated Moving Average
BESS	Battery Energy Storage System
CAPEX	Capital Expenditure
CNN	Convolutional Neural Network
CVaR	Conditional Value-at-Risk
D1	Day-ahead forecast horizon (24 h)
D2	Two-day-ahead forecast horizon (48 h)
D3	Three-day-ahead forecast horizon (72 h)
ECDF	Empirical Cumulative Distribution Function
ENTSO-E	European Network of Transmission System Operators for Electricity
FMI	Finnish Meteorological Institute
FCR	Frequency Containment Reserve
HV	High Voltage
IRR	Internal Rate of Return
LSTM	Long Short-Term Memory
MAE	Mean Absolute Error
MILP	Mixed-Integer Linear Programming
MPPT	Maximum Power Point Tracking
MPC	Model Predictive Control
MV	Medium Voltage
NASA POWER	Prediction Of Worldwide Energy Resources
NPV	Net Present Value
NWP	Numerical Weather Prediction
PoC	Point of Connection
RMSE	Root Mean Square Error
SOC	State of Charge

1 Introduction

1.1 Background and Challenges of PV Integration

The global energy system is undergoing a structural transition toward low-carbon and sustainable operation, driven by decarbonization targets, policy commitments, and increasing electricity demand. Within this transition, photovoltaic (PV) generation has emerged as a dominant technology due to its modularity, declining costs, and scalability (IEA, 2025). Consequently, PV is expected to constitute a significant share of future electricity generation and play a central role in achieving net-zero emission targets. However, PV generation is inherently stochastic, as it depends on meteorological variables such as solar irradiance, cloud dynamics, ambient temperature, and seasonal patterns. This results in substantial temporal variability and uncertainty in generation profiles, directly affecting system balancing and operational reliability under high renewable penetration (Luo et al., 2025; Ejuh Che et al., 2025). In electricity markets, generation must be scheduled ahead of delivery, and deviations between scheduled and actual output lead to imbalance settlements and associated economic penalties. Therefore, forecasting accuracy and more critically, uncertainty representation is essential for both operational efficiency and market participation (Agakishiev et al., 2025). At higher penetration levels, PV integration introduces interconnected technical and economic challenges. Forecast uncertainty leads to both underproduction and overproduction, increasing imbalance exposure and degrading economic performance (Luo et al., 2025; Mystakidis et al., 2024). In addition, grid constraints, particularly point-of-connection (PoC) export limits, result in curtailment during high-generation periods, reducing renewable utilization and revenue (IEA, 2025). A further limitation arises from the temporal mismatch between PV generation and market price signals, which constrains value capture when peak production does not align with high-price periods (Pavlík et al., 2025). Together, these challenges highlight the need for coordinated strategies to manage uncertainty while improving system flexibility and economic efficiency.

1.2 Role of Battery Energy Storage Systems in PV Integration

Battery Energy Storage Systems (BESS) provide a critical flexibility mechanism for mitigating PV variability and enhancing system performance. Advanced hybrid storage architectures and energy-management strategies have further expanded the operational role of BESS in modern hybrid power systems (Baccino & Santarelli, 2023). By enabling temporal energy shifting, BESS reduces curtailment, compensates for forecast deviations, and improves dispatchability (Rezaeimozafar et al., 2024; Yang et al., 2024). In addition, storage systems enable participation in multiple market layers, including energy arbitrage and ancillary services such as frequency containment reserves, allowing value stacking and improved economic performance. Beyond economic benefits, BESS contributes to system stability through fast-response services such as frequency regulation and voltage support (Ejuh Che et al., 2025; Gardemeister et al., 2025). However, its value is highly sensitive to system design and operational strategy. Oversizing increases capital costs, while undersizing limits flexibility. Similarly, inefficient operation accelerates degradation and reduces lifecycle profitability. Therefore, effective PV–BESS integration requires coordinated optimization across forecasting, system design, and operational control.

1.3 Research Motivation and Problem Statement

Despite extensive research in PV forecasting, BESS planning, and operational control, these domains are largely studied in isolation. Forecasting studies typically focus on statistical accuracy metrics (e.g., RMSE, MAE) without explicitly linking predictions to operational or economic outcomes (Chen et al., 2024). Similarly, BESS sizing approaches often rely on deterministic assumptions, neglecting forecast uncertainty, while operational strategies frequently depend on point forecasts, limiting robustness under uncertainty (Tkac et al., 2023). In practice, these components are inherently interdependent. Forecast uncertainty directly influences operational risk, market participation, and the value of system flexibility, while system design constrains operational decisions and economic outcomes. However, existing literature lacks integrated, data-driven frameworks that consistently connect forecasting, planning, and operation within a unified decision-

making structure. To address this gap, this thesis develops a multi-phase framework linking probabilistic forecasting, risk-aware BESS sizing, and market-oriented dispatch. The central objective is to transform forecast uncertainty from a source of risk into a quantifiable and exploitable component of system value (Wang et al., 2024).

1.4 Objectives, Research Questions, and Contributions

1.4.1 Objectives

The primary objective of this thesis is to develop an integrated PV–BESS decision framework that enables uncertainty-aware forecasting, risk-informed planning, and optimized market participation. Specifically, the study aims to:

- Develop a probabilistic PV forecasting model capturing uncertainty across multiple horizons
- Design a risk-aware BESS sizing methodology incorporating economic and operational constraints
- Formulate an optimization-based operational strategy for PV–BESS systems in electricity markets
- Evaluate system performance in terms of economic value and operational robustness
- Establish a unified data-driven pipeline linking forecasting, planning, and operation.

1.4.2 Research Questions

This thesis addresses the following research questions:

1. How can probabilistic forecasting improve operational decision-making in PV systems?
2. How does forecast uncertainty influence BESS sizing and system design?
3. What constitutes an optimal market-oriented operational strategy for PV–BESS systems?
4. How does forecast quality affect economic performance and imbalance risk?
5. What is the long-term techno-economic benefits of PV–BESS integration?

1.4.3 Scientific Contributions

The key contributions of this thesis are:

- A probabilistic forecasting framework explicitly designed for decision-making applications
- A risk-aware BESS sizing methodology incorporating uncertainty and market dynamics
- A market-oriented operational strategy integrating energy and reserve participation
- A unified multi-phase framework linking forecasting, planning, and operation
- Quantification of forecast value in terms of economic performance and risk reduction
- Comprehensive evaluation of PV–BESS system performance under uncertainty

1.5 Thesis Organization

The remainder of this thesis is structured as follows. Chapter 2 reviews the literature on PV forecasting, energy storage systems, and operational strategies. Chapter 3 presents the data and methodological framework. Chapter 4 introduces the mathematical formulation and the proposed integrated system. Chapter 5 provides the simulation results and integrated analysis across all phases. Finally, Chapters 6 presents the discussion and conclusions of this research.

2 Literature Review

2.1 PV Forecasting and Uncertainty Modeling

Accurate photovoltaic (PV) power forecasting is essential for maintaining system balance, ensuring reliable grid operation, and enabling efficient market participation. However, PV generation is inherently stochastic due to its dependence on meteorological variables, making forecasting a challenging task in modern power systems. Early approaches relied on statistical models such as autoregressive (AR), ARIMA, and linear regression (Iheanetu, 2022; Al-Dahidi et al., 2024). While computationally efficient and interpretable, these methods struggle to capture the nonlinear and non-stationary behavior of solar irradiance, particularly under rapidly changing weather conditions. To improve physical consistency, numerical weather prediction (NWP)-based models were introduced, incorporating irradiance, temperature, and cloud cover (Wang et al., 2026; Visser et al., 2024). However, their performance remains constrained by upstream weather forecast errors. More recently, data-driven approaches have demonstrated superior performance. Machine learning models such as artificial neural networks (ANNs), support vector machines (SVMs), and ensemble methods effectively capture nonlinear relationships (Sweeney et al., 2020; Maciejowska et al., 2024), while deep learning architectures, including long short-term memory (LSTM) and convolutional neural networks (CNNs), further enhance temporal and spatiotemporal modeling (Meng et al., 2022; Wang et al., 2026). To address inherent uncertainty, probabilistic forecasting has emerged as a robust alternative. Unlike deterministic models, it provides prediction intervals or full distributions, offering a more comprehensive representation of PV output (Maciejowska et al., 2024; Sweeney et al., 2020). Common approaches include quantile regression, Bayesian methods, and ensemble techniques, with quantile regression widely adopted due to its flexibility in estimating conditional distributions without strong assumptions (Maciejowska et al., 2024; Visser et al., 2024). Despite these advances, forecasting performance is still predominantly evaluated using statistical metrics such as RMSE and MAE, which do not reflect operational or economic impact. In market environments, even small forecast errors can lead to imbalance penalties and suboptimal dispatch (Visser et al., 2024).

Similarly, probabilistic forecasts are often assessed using calibration and sharpness metrics, with limited integration into decision-making processes (Sweeney et al., 2020; Maciejowska et al., 2024)**.**

2.2 BESS Planning and Sizing Approaches

Battery Energy Storage Systems (BESS) are essential for enhancing the flexibility and economic performance of PV-integrated systems. By enabling energy shifting, peak shaving, curtailment reduction, and ancillary service participation, BESS improves both system stability and market competitiveness (IEA, 2025; Čović et al., 2024). Lithium-ion batteries dominate current deployments due to high efficiency, scalability, and declining costs (IEA, 2025), while alternative technologies such as supercapacitors and hybrid storage systems are used in high-power or fast-response applications (Čović et al., 2024). The value of BESS depends strongly on system design, particularly sizing strategies. Technical approaches focus on grid compliance and power smoothing objectives, such as ramp-rate control (Lappalainen & Valkealahti, 2022; Abdalla et al., 2026), but often neglect economic performance. Data-driven approaches extract representative patterns from historical data using clustering or motif analysis (Yang et al., 2025), though they struggle with extreme events and lack integration with uncertainty modeling (Allahvirdizadeh et al., 2021). Recurring-pattern-based approaches have also been proposed to improve hybrid energy storage sizing under repetitive operational conditions (Karrari et al., 2022). Techno-economic optimization methods, typically based on mixed-integer linear programming (MILP), aim to maximize economic performance under operational constraints (Cao et al., 2022; Gao et al., 2025). Recent hybrid power plant studies have also explored surrogate-based energy management and sizing approaches to improve computational efficiency in large-scale optimization problems (Assaad et al., 2025). However, these models often rely on deterministic inputs, limiting robustness under uncertainty. Stochastic and reliability-based approaches incorporate uncertainty using risk measures such as Conditional Value at Risk (CVaR), improving robustness (Mottola et al., 2024; Xuan et al., 2021; Domínguez & Vitali, 2021), but are generally confined to planning stages and rarely linked to forecasting or real-time operation. Hybrid renewable storage studies emphasize variability and resource complementarity (Talvi & Lappalainen,

2024;Ruan et al., 2025; Holttinen et al., 2025) yet often lack economic depth and market integration.

2.3 PV–BESS Operation and Market Participation

Operational strategies determine the real-time utilization of BESS and significantly influence system performance. Common approaches include rule-based control, optimization-based strategies, and model predictive control (MPC) (Gao et al., 2019; Lindberg et al., 2024). Rule-based methods are simple but suboptimal under dynamic conditions, while optimization-based approaches improve performance but depend heavily on forecast accuracy and are often based on deterministic inputs. BESS enables participation in multiple electricity markets, including day-ahead, intraday, and ancillary services (IEA, 2025; Ruiz-Abellón et al., 2024). Risk-constrained participation strategies for energy and reserve markets have also gained increasing attention in virtual power plant and active distribution network research (Jadidoleslam, 2025). Through value stacking combining energy arbitrage and reserve provision storage systems can significantly enhance profitability (Hofbauer et al., 2022). However, market participation is typically modeled independently of forecasting and planning processes, limiting the ability to fully exploit market opportunities under uncertainty.

2.4 Risk-Aware Optimization in Energy Systems

Risk-aware optimization methods, particularly those based on Conditional Value at Risk (CVaR), are widely used to manage uncertainty in energy systems (Wang et al., 2024; Xuan et al., 2021). These approaches balance expected returns with downside risk, improving decision robustness. However, they are typically applied in isolated stages, such as planning or operation, without integration across forecasting, system design, and dispatch. This limits their ability to capture the full propagation of uncertainty across multi-stage decision processes.

2.5 Research Gap and Thesis Positioning

The literature reveals several critical limitations. Existing studies largely treat forecasting, BESS sizing, and operation as separate components, with minimal cross-layer integration

(Ali et al., 2025). While probabilistic methods effectively quantify uncertainty, they are seldom propagated into system design and operational decision-making, and BESS planning often remains based on deterministic assumptions. Thus,

High statistical accuracy and uncertainty quantification do not necessarily translate into operational or economic value, as uncertainty is quantified but not effectively utilized in decision-making.

To address these limitations, this thesis proposes a unified data-driven framework that integrates probabilistic forecasting, risk-aware BESS sizing, and market-oriented operation within a single decision pipeline. The framework enables end-to-end uncertainty propagation, where quantile-based forecasts (q05–q95) directly inform both planning and dispatch. A CVaR-based sizing strategy balances expected return against downside risk, while a market-integrated optimization framework supports coordinated participation in energy and reserve markets. The approach further captures multi-horizon uncertainty evolution across D1–D3 and extends to a digital twin layer for real-time monitoring and adaptive control. In this way, the thesis moves beyond accuracy-driven forecasting toward decision-oriented optimization, offering a coherent and practically deployable framework for PV–BESS systems operating under uncertainty

Table 1. Comparative Analysis of Existing Studies

Domain	Aspect	Existing Approaches	Limitations	Proposed Framework
Forecasting	Output	Deterministic; probabilistic (Iheanetu, 2022; Visser et al., 2024; Maciejowska et al., 2024)	Uncertainty ignored or not utilized	Quantile-based probabilistic forecasts
	Uncertainty	Limited/implicit (Sweeney et al., 2020)	Not propagated to decisions	Fully integrated into decision-making
	Metrics	RMSE, MAE (Al-Dahidi et al., 2024)	No economic relevance	Cost-, imbalance-, profit-based metrics
	Decision Link	Decoupled from operation (Visser et al., 2024; Lindberg et al., 2024)	Weak linkage	Integrated with sizing and dispatch

BESS Sizing	Objective	Technical or economic (Lappalainen & Valkealahti, 2022; Cao et al., 2022)	Fragmented objectives	Unified techno-economic + risk-aware
	Uncertainty	Deterministic inputs (Gao et al., 2025)	Ignores variability	Driven by probabilistic forecasts
	Market	Simplified models (IEA, 2024; Gao et al., 2025)	Limited realism	Full energy + reserve integration
	Forecast Link	Weak linkage (Allahvirdizadeh et al., 2021)	Disconnected decisions	Multi-horizon (D1–D3) driven
	Robustness	Moderate (Xuan et al., 2021)	Not linked to operation	Risk-aware + operational coupling
Operation	Control	Rule-based / MPC (Gao et al., 2019)	Deterministic inputs	Risk-aware optimization (MPC)
	Uncertainty	Limited use (Lindberg et al., 2024)	Poor robustness	Fully uncertainty-aware
	Market	Separate modeling (IEA, 2023)	No coordination	Integrated multi-market
	Adaptability	Static/semi-dynamic (Ruiz-Abellón et al., 2024)	Limited flexibility	Dynamic scenario-based
	Economics	Suboptimal value (Hofbauer et al., 2022)	Inefficient flexibility use	Profit-maximizing with risk control
System Integration	Integration	Disjoint stages (Ali et al., 2025)	No end-to-end pipeline	Fully integrated framework
	Decision	Component-level (Bernecker et al., 2026)	No coordination	Multi-phase architecture
	Risk	Isolated handling (Xuan et al., 2021)	Not propagated	End-to-end CVaR-based
	Applicability	Moderate (IEA, 2024)	Limited deployment	Market-aligned, deployable

3 Data and Methodology Framework

3.1 System Description and Dataset Overview

This study is based on the Heinäneva Solar Park (EPV Energia Oy, Finland), a utility-scale photovoltaic (PV) plant with an installed capacity of approximately 80 MW and an annual generation of about 80 GWh. The system operates under Nordic climatic conditions characterized by strong seasonal variability. The plant comprises approximately 123,000 panels over 120 hectares and follows a modular architecture consisting of ten main blocks and one dual-axis tracker block. Each block operates with a dedicated inverter and medium-voltage (MV) transformer, and all blocks are aggregated through an MV network to a central substation for high-voltage (HV) grid integration, as illustrated in Fig.1.

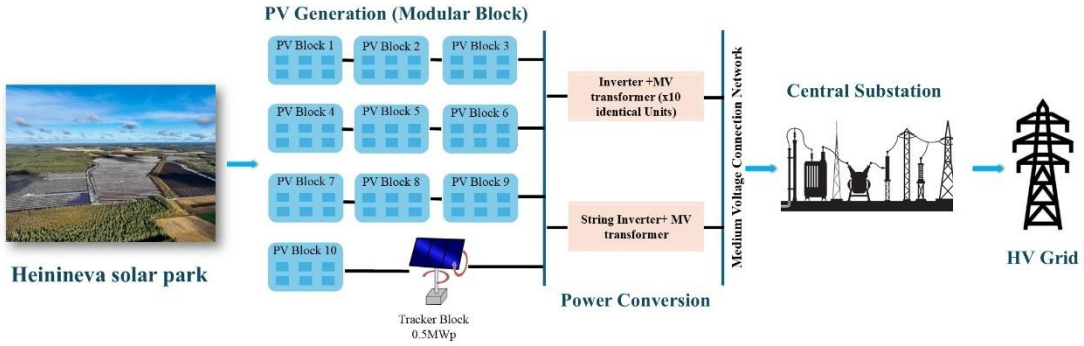

Figure 1. **Structural and Electrical Architecture of the Heinineva Solar Park.**

The system employs a hybrid inverter topology combining central and string inverters, enabling multi-level maximum power point tracking (MPPT) at both sub-array and string levels. Approximately 85.3 MWp is installed as fixed-tilt systems, while 0.5 MWp uses dual-axis tracking, improving irradiance capture while introducing additional variability. A hierarchical control structure supports centralized dispatch, grid compliance, and energy management functions. Grid exports are constrained by a 60 MW point-of-connection (PoC) limit, leading to curtailment during high-generation periods and directly influencing dispatch, storage sizing, and economic performance (Esmaeili Aliabadi & Pinto, 2025). All dataset variables are aligned to a 15-minute resolution, consistent with electricity market settlement intervals. The dataset integrates PV generation, environmental conditions, and operational signals, providing a structured representation of system

behavior for forecasting and decision-making. Key characteristics are summarized in Table 2. The dataset is constructed through multi-source integration. PV generation data is obtained from EPV Energia Oy, while meteorological inputs are collected from on-site measurements and the Finnish Meteorological Institute (FMI). Additional solar radiation and atmospheric variables are sourced from NASA POWER (Finnish Meteorological Institute, 2025; NASA POWER, 2025). Electricity market data are incorporated from Nord Pool, ENTSO-E, and Fingrid, enabling representation of both energy and reserve market conditions (Nord Pool, 2025; ENTSO-E, 2025; Fingrid, 2025).

Table 2. Dataset Summary

Category	**Variable**	**Value**
Dataset	Type	Multi-source processed dataset
Size	Observations	12,725
	Features	77
Time	Resolution	15 minutes
	Period	16 Jun 2025 – 27 Oct 2025 (~4.5 months)
PV Output	Target Variable	Power (MW)
	Mean	10.14 MW
	Max	72.44 MW
	Min	0 MW
Operational Signals	Risk Indicator	deficit_MW
	Commitment Flag	commitment_defined
Features	Categories	Meteorological, Temporal, Forecast, Risk

3.2 Data Processing and Feature Engineering

A structured data processing and feature engineering pipeline is applied to ensure dataset consistency and suitability for probabilistic forecasting and optimization.

All data streams are synchronized and resampled to a unified 15-minute resolution. Missing values are handled through interpolation for short-duration gaps, while anomalous or physically inconsistent observations are removed using rule-based filtering based

on domain constraints, including non-negative irradiance, feasible PV output limits, and realistic meteorological ranges.

Feature normalization and scaling are applied to improve numerical stability and model generalization (Xiong et al., 2025).

Feature engineering captures the temporal, physical, and operational drivers of PV generation:

- **Temporal features** (hour, day, season) capture periodic patterns
- **Meteorological variables** (irradiance, temperature, cloud indicators) represent physical drivers
- **Historical PV features** (lagged values) capture temporal dependencies
- **Market variables** (spot and reserve prices) represent economic signals
- **Operational signals and risk indicators** (e.g., commitment status, imbalance) link forecasting to decision-making

In addition, derived features such as rolling statistics and variability indicators are included to improve robustness under fluctuating conditions. The unified feature structure is summarized in Table 3. The selected features represent system-level behavior; localized effects such as panel degradation or shading are not explicitly modeled.

Table 3. Unified Feature Categories and Modeling Role

Feature Category	**Variables**	**Role in Model**	**Purpose**
Temporal	hour, day, month, seasonal indicators	Input features	Capture periodic patterns
Meteorological	irradiance, temperature, cloud indicators	Input features	Represent physical drivers of PV generation
Historical PV	lagged power values	Input features	Capture temporal dependency and persistence
Market	spot price, reserve price	Input features	Represent economic signals for decision-making
Operational Signals	commitment_defined	Input features	Support market-based decisions
Risk Indicators	deficit_MW	Input features	Represent imbalance risk

Derived Features	rolling statistics, variability metrics	Engineered features	Improve model robustness and stability
Target Variable	power (MW)	Output	PV generation prediction

The selected features represent temporal patterns, physical drivers, and economic signals relevant for forecasting and decision-making. Factors such as panel degradation, shading effects, or localized disturbances are not explicitly included, as the focus is on system-level modeling.

3.3 Probabilistic Forecasting Framework

The dataset supports multi-horizon forecasting within the proposed PV–BESS framework. Three forecast horizons are considered: day-ahead (D1), two-day-ahead (D2), and three-day-ahead (D3), enabling analysis of uncertainty propagation and forecast degradation with increasing lead time (Smyl et al., 2026).PV generation is modeled using a probabilistic approach based on conditional quantiles in the range q_{05}–q_{95}. This allows construction of prediction intervals and scenario trajectories used in planning and operational optimization (Visser et al., 2024; Wang et al., 2026). Model training is performed using quantile regression with the pinball loss function, enabling estimation of calibrated predictive distributions without strong distributional assumptions (Mystakidis et al., 2024). This is particularly suitable for PV generation, where uncertainty is non-Gaussian and driven by weather variability. Quantile outputs are transformed into representative scenarios (lower, median, upper) to enable efficient propagation into downstream decision-making stages (Sun et al., 2020). Forecast performance is evaluated using coverage probability and interval width, ensuring both calibration and sharpness (Wang et al., 2026). The forecasting configuration is summarized in Table 4.

Table 4. Phase-1 Forecasting Configuration and Data Structure

Component	**Variables / Description**	**Role in Framework**
Input Features	Temporal, meteorological, historical PV, market variables	Provide explanatory variables for forecasting model

Target Variable	PV power (MW)	Forecast output
Forecast Type	Probabilistic (quantile-based, q05–q95)	Represent uncertainty
Forecast Horizons	D1, D2, D3	Capture multi-horizon uncertainty propagation
Training Method	Quantile regression (pinball loss)	Estimate conditional quantiles
Output Representation	Prediction intervals and scenarios	Input to planning and dispatch
Scenario Reduction	Lower, median, upper trajectories	Reduce computational complexity
Evaluation Metrics	Coverage probability, interval width	Assess calibration and sharpness

3.4 Optimization and Simulation Methodology

The proposed methodology integrates planning and operational decision-making within a multi-stage optimization framework (Zhu et al., 2026; Das et al., 2025).

3.4.1 Planning Optimization

The planning stage determines the optimal battery energy storage system (BESS) configuration by evaluating candidate designs across power capacity, energy capacity, and duration. Uncertainty in PV generation is represented through scenario sets derived from the probabilistic forecasting framework (Section 3.3) (Sun et al., 2020). Each configuration is evaluated using a risk-aware objective combining expected annual profit, Net Present Value (NPV), and Conditional Value-at-Risk (CVaR) at a 95% confidence level. CVaR captures extreme adverse outcomes and provides a coherent risk measure for energy market applications (Rockafellar & Uryasev, 2000; Wang et al., 2024). The selected configuration (2 MW / 2 MWh) reflects a balance between profitability and risk under the considered conditions.

3.4.2 Operational Dispatch Optimization

The operational stage simulates system behavior using the selected BESS configuration. The dispatch problem is formulated as a constrained optimization model solved

sequentially over discrete time steps, consistent with rolling-horizon energy management strategies (Conejo et al., 2010). At each time step t, decision variables include charging power, discharging power, and reserve allocation. Constraints include battery limits, point-of-connection (PoC) export limits, and reserve requirements. The objective maximizes economic returns considering energy revenue, reserve revenue, imbalance penalties, and battery degradation costs (Yang et al., 2024; Amorim et al., 2024).

3.4.3 Time-Stepped Simulation Framework

System operation is simulated over the study horizon using a 15-minute time-stepped framework. At each time step:

- Retrieve probabilistic forecast inputs (Section 3.3)
- Update system states (e.g., state-of-charge)
- Solve dispatch optimization
- Apply charging, discharging, and reserve decisions
- Record performance indicators

The rolling-horizon structure enables adaptation to updated forecasts and system conditions, ensuring consistent propagation of forecast uncertainty into operational decisions (Conejo et al., 2010; Das et al., 2025).

3.4.4 Integrated Methodological Workflow

As shown in Fig. 2, the framework follows a structured pipeline from data ingestion to forecasting, optimization, and performance evaluation. The integration of these components ensures that uncertainty captured at the forecasting stage is consistently propagated into planning and operational decision-making. This unified workflow enables coordinated decision-making across multiple layers:

Raw Data → **Forecasting** → **Planning** → **Dispatch** → **Evaluation**.

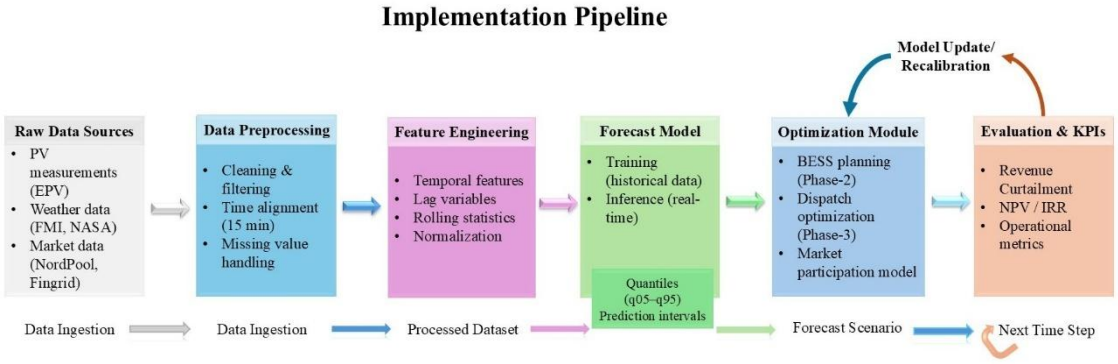

Figure 2. Overall Methodological Workflow

3.5 Performance Evaluation and Implementation Framework

System performance is evaluated using a structured set of operational, economic, strategic, and technical metrics derived from the mathematical formulation in Section 4, ensuring consistency between system modeling, optimization, and evaluation. Operational performance is characterized by exported energy, curtailment, and imbalance, capturing system behavior under uncertainty and grid constraints, while economic performance is quantified through energy market revenue, reserve market revenue, imbalance penalties, battery degradation cost, and net profit, reflecting financial outcomes of system operation. Strategic performance is assessed using Net Present Value (NPV) and Conditional Value-at-Risk (CVaR, 95%), enabling evaluation of long-term investment viability and downside risk exposure, whereas technical performance is represented by energy throughput and equivalent full cycles, capturing battery utilization and degradation. All metrics are computed at each time step and aggregated over the simulation horizon. Table 5 summarizes the selected metrics, providing a unified and decision-oriented evaluation basis for analyzing trade-offs between profitability, risk exposure, and operational efficiency. The framework is implemented as a modular computational pipeline integrating data processing, probabilistic forecasting, planning optimization, operational dispatch, and performance evaluation, with validation procedures ensuring data integrity and scenario consistency. The modular structure supports scalability and real-time integration through API-based data acquisition from platforms such as Nord Pool, ENTSO-E, Fingrid, Finnish Meteorological Institute, and NASA POWER, enabling the development

of a digital twin environment for real-time monitoring, probabilistic forecasting, and adaptive operational decision-making.

Table 5. Performance Evaluation Metrics

Category	Metric	Description
Operational	Exported Energy	Total energy delivered to grid
	Curtailment	Unused PV generation due to constraints
	Imbalance	Deviation between scheduled and actual generation
Economic	Energy Revenue	Income from energy market participation
	Reserve Revenue	Income from ancillary services
	Imbalance Cost	Penalty due to forecast error
	Net Profit	Total economic performance
Strategic	NPV	Long-term investment viability
	CVaR (95%)	Downside risk measure
Technical	Energy Throughput	Total battery energy processed
	Equivalent Cycles	Battery usage intensity

4 Problem Formulation and Proposed Framework

4.1 System Modeling Overview

This study considers a grid-connected photovoltaic (PV) power plant integrated with a battery energy storage system (BESS), operating under electricity market conditions with a constrained point-of-connection (PoC). The system is characterized by three interacting components: (i) uncertainty in PV generation, (ii) operational flexibility provided by energy storage, and (iii) economic signals derived from electricity markets. The objective of this chapter is to establish a unified mathematical framework that captures the interactions between generation uncertainty, system constraints, and market participation. The formulation integrates probabilistic forecasting, battery operation, and market-based decision-making within a consistent structure, enabling direct linkage between uncertainty, operational actions, and economic outcomes.

The proposed framework is structured into multiple decision layers, including probabilistic forecasting, risk-aware planning, operational dispatch, and strategic evaluation, ensuring consistent propagation of uncertainty from forecast inputs to planning and real-time operational decisions. The overall structure of the multi-phase PV–BESS framework is summarized in Table 6 and illustrated in Fig. 3.

Table 6. Summary of the Multi-Phase Framework

Phase	**Input**	**Output**	**Purpose**
Phase-1	PV + Weather Data	Quantile Forecasts	Uncertainty modeling
Phase-2	Forecast Scenarios	Optimal BESS Size	Risk-aware planning
Phase-3	Forecast + BESS	Dispatch Decisions	Market optimization
Phase-4	Dispatch Results	NPV, IRR, KPIs	Strategic evaluation
Phase-5	Real-Time Data	Control Actions	Digital twin operation

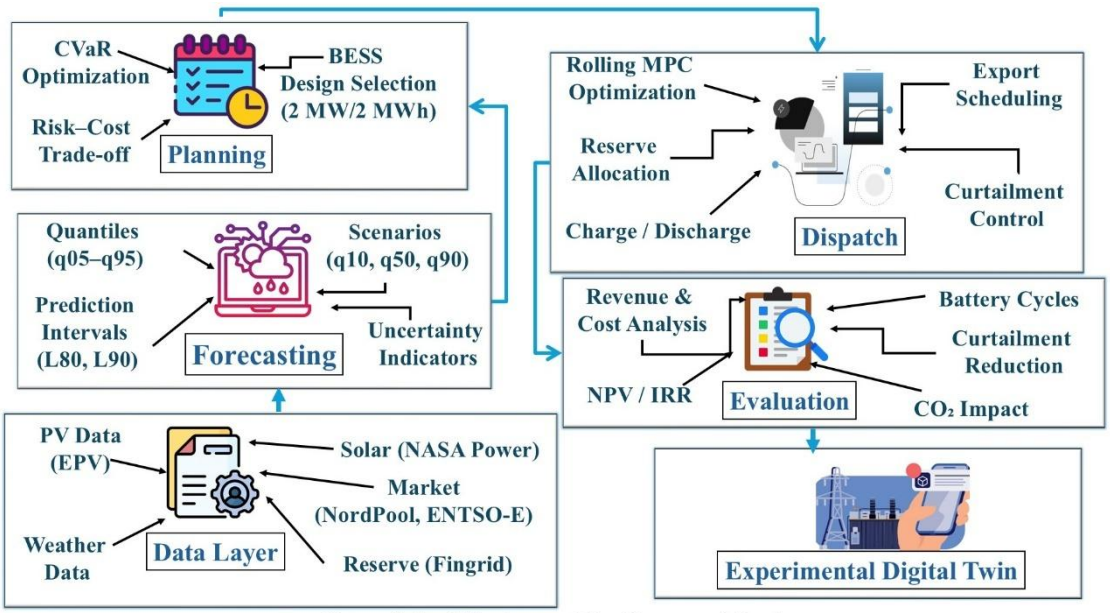

Figure 3. **Overall Architecture of the Proposed Multi-Phase PV–BESS Framework.**

4.2 Probabilistic PV and Imbalance Modeling

Photovoltaic (PV) generation is inherently uncertain due to variability in meteorological conditions. To represent this uncertainty, a probabilistic forecasting approach is adopted using conditional quantiles. Let:

$$\hat{Q}_{\tau,t}, \tau \in \mathcal{T} \tag{1}$$

denote the predicted PV generation quantile at time t, where:

$$\mathcal{T} = \{0.05,0.10,0.20,0.25,0.30,0.40,0.50,0.60,0.70,0.80,0.90,0.95\} \tag{2}$$

The median forecast is:

$$P_{pv,t}^{med} = \hat{Q}_{0.50,t} \tag{3}$$

Prediction intervals are defined as:

$$[L90_t, U90_t] = [\hat{Q}_{0.05,t}, \hat{Q}_{0.95,t}] \tag{4}$$

$$[L80_t, U80_t] = [\hat{Q}_{0.10,t}, \hat{Q}_{0.90,t}] \tag{5}$$

To enable tractable optimization, representative scenarios are constructed as:

$$P_{pv,t}^{-},\ P_{pv,t}^{(0)},\ P_{pv,t}^{+} \tag{6}$$

corresponding to pessimistic, median, and optimistic PV generation levels derived from the quantile structure (Teixeira et al., 2024; Sun et al., 2020).

4.2.1 Imbalance Modeling

The committed power $b_t$is equivalent to the scheduled export P_t^{sched}, and both notations are used interchangeably in the formulation Electricity market participation requires advance commitment of generation. The system submits a scheduled export P_t^{sched}, while the actual export depends on scenario-based PV generation and battery operation. The realized export under scenario $s$is defined as:

$$P_{s,t}^{actual} = P_{s,t}^{PV} - P_{s,t}^{curt} - P_t^{ch} + P_t^{dis} \tag{7}$$

The resulting imbalance is:

$$\Delta_{s,t} = P_{s,t}^{actual} - P_t^{sched} \tag{8}$$

This deviation is decomposed into surplus and deficit components:

$$\Delta_{s,t}^{+} = \max\left(0, \Delta_{s,t}\right), \Delta_{s,t}^{-} = \max\left(0, -\Delta_{s,t}\right) \tag{9}$$

where $\Delta_{s,t}^{+}$represents overproduction and $\Delta_{s,t}^{-}$represents underproduction. The imbalance cost is given by:

$$C_{s,t}^{imb} = \Delta_{s,t}^{-} \cdot \pi_t^{up} + \Delta_{s,t}^{+} \cdot \pi_t^{down} \tag{10}$$

where $\pi_t^{up}$and π_t^{down}denote upward and downward regulation prices, respectively. In the absence of explicit imbalance prices, they are approximated as:

$$\pi_t^{up} = \gamma^{up} \cdot \pi_t^{spot}, \pi_t^{down} = \gamma^{down} \cdot \pi_t^{spot} \tag{11}$$

with $\gamma^{up} > 1$and $\gamma^{down} < 1$, reflecting higher penalties for underproduction. To capture extreme economic losses, Conditional Value-at-Risk (CVaR) is incorporated as a coherent risk measure widely used in stochastic optimization and energy system applications (Shapiro et al., 2021; Wang et al., 2024). The scenario loss is defined as:

$$L_s = -\Pi_s \tag{12}$$

and the CVaR measure is:

$$CVaR = \eta + \frac{1}{1-\beta}\sum_s p_s z_s \tag{13}$$

subject to:

$$z_s \geq L_s - \eta, z_s \geq 0 \tag{14}$$

where $\beta$is the confidence level, ηrepresents the Value-at-Risk (VaR), and $z_s$captures excess loss beyond VaR. For clarity, deterministic notation is used in conceptual

explanations, while scenario index $s$is explicitly included in operational and stochastic formulations. This formulation explicitly links forecast uncertainty to imbalance penalties and enables risk-aware operational decision-making. Additional details are provided in Appendix 1.

4.3 Battery Energy Storage System Model

The battery energy storage system (BESS) provides operational flexibility by enabling energy shifting, reserve provision, and mitigation of PV variability. Its behavior is modeled through state-of-charge (SOC) dynamics, operational constraints, and degradation representation.

4.3.1 State-of-Charge Dynamics

The SOC evolution is defined as:

$$SOC_{t+1} = SOC_t + \eta_c P_{ch,t} \Delta t - \frac{P_{dis,t}}{\eta_d} \Delta t \tag{15}$$

where $SOC_t$is the state of charge at time t, $P_{ch,t}$and $P_{dis,t}$denote charging and discharging power, and $\eta_c, \eta_d$are charging and discharging efficiencies.

4.3.2 Operational Constraints

The battery operates within physical and safety limits:

$$SOC^{min} \leq SOC_t \leq SOC^{max} \tag{16}$$

$$0 \leq P_{ch,t} \leq P_b^{max}, 0 \leq P_{dis,t} \leq P_b^{max} \tag{17}$$

To avoid simultaneous charging and discharging, a linear relaxation is adopted:

$$P_{ch,t} + P_{dis,t} \leq P_b^{max} \tag{18}$$

This formulation ensures computational efficiency while maintaining physically feasible operation.

4.3.3 Battery Sizing Context

The battery size is determined in Phase-2 using a risk-aware optimization framework. While a wide design space (up to ~30 MW) is explored, the optimal configuration is:

$$P_b^{max} = 2 \text{ MW}, E_b^{max} = 2 \text{ MWh} \quad (19)$$

The duration is:

$$h_b = \frac{E_b^{max}}{P_b^{max}} = 1 \text{ hour} \quad (20)$$

This selection reflects the trade-off between flexibility and cost under uncertainty.

4.3.4 Degradation Modeling

Battery degradation is approximated using energy throughput:

$$E_t^{through} = P_{ch,t} + P_{dis,t} \quad (21)$$

$$C_{deg,t} = c_{deg} \cdot E_t^{through} \cdot \Delta t \quad (22)$$

where $c_{deg}$is the degradation cost coefficient. This approach captures cycling-related wear and is widely used in system-level optimization models (e.g., Yang et al., 2024; Amorim et al., 2024).

4.4 Power Balance and Market Model

4.4.1 Power Balance and Curtailment

The system must satisfy power balance at each time step and under each scenario s:

$$P_{s,t}^{PV} - P_{ch,t} + P_{dis,t} = P_{s,t}^{grid} + P_{s,t}^{curt} \quad (23)$$

where $P_{s,t}^{PV}$is scenario-based PV generation, $P_{s,t}^{grid}$is exported power, and $P_{s,t}^{curt}$represents curtailed energy. Curtailment is implicitly determined as:

$$P_{s,t}^{curt} = \max\left(0,\ P_{s,t}^{PV} - P_{ch,t} + P_{dis,t} - P_{s,t}^{grid}\right) \quad (24)$$

4.4.2 Grid Export Constraint

The exported power is limited by point-of-connection (PoC)

$$P_{exp,t} \leq P_{PoC} \quad (25)$$

where:

$$P_{PoC} = 60 \text{ MW} \quad (26)$$

This constraint reflects real grid limitations and strongly influences system operation.

4.4.3 Scheduled and Actual Export

Electricity market participation requires advance commitment through scheduled export:

$$E_t^{sched} = P_t^{sched} \cdot \Delta t \tag{27}$$

The actual export under scenario $s$is:

$$E_{s,t}^{act} = P_{s,t}^{grid} \cdot \Delta t \tag{28}$$

The mismatch between scheduled and actual export is:

$$\Delta_{s,t} = E_{s,t}^{act} - E_t^{sched} \tag{29}$$

This formulation enables explicit modeling of market commitments and deviations under uncertainty.

4.4.4 Electricity Market Model

Energy Revenue

The energy revenue of this proposed system is denoted as:

$$R_{energy,t} = E_t^{act} \cdot \pi_{spot,t} \tag{30}$$

This represents revenue from energy sales in the spot market.

Reserve Participation

Reserve provision is constrained by battery power and energy availability:

$$0 \leq R_t \leq P_b^{max} \tag{31}$$

$$P_{dis,t} + R_t \leq P_b^{max} \tag{32}$$

$$SOC_t \geq SOC^{min} + R_t \cdot \Delta t \tag{33}$$

These constraints ensure that sufficient power and energy headroom are maintained for reserve activation

Reserve Revenue

Reserve revenue of this proposed system is denoted as :

$$R_{reserve,t} = R_t \cdot \pi_{reserve,t} \tag{34}$$

This captures revenue from providing reserve capacity, enhancing system profitability

Imbalance Cost

Mismatch is decomposed into surplus and deficit components:

$$\Delta_{s,t}^{+} = \max(0, \Delta_{s,t}), \Delta_{s,t}^{-} = \max(0, -\Delta_{s,t}) \quad (35)$$

The imbalance cost is defined as:

$$C_{s,t}^{imb} = \Delta_{s,t}^{-} \cdot \pi_t^{up} + \Delta_{s,t}^{+} \cdot \pi_t^{down} \quad (36)$$

where:

- π_t^{up}: penalty for underproduction
- π_t^{down}: penalty for overproduction

In the absence of explicit imbalance prices:

$$\pi_t^{up} = \gamma^{up} \cdot \pi_{spot,t}, \pi_t^{down} = \gamma^{down} \cdot \pi_{spot,t} \quad (37)$$

with $\gamma^{up} > 1$and $\gamma^{down} < 1$.

Curtailment Cost

Curtailment is penalized to discourage renewable energy loss:

$$C_{s,t}^{curt} = c_{curt} \cdot P_{s,t}^{curt} \cdot \Delta t \quad (38)$$

Battery utilization

Battery utilization is quantified as:

$$E^{through} = \sum_t (P_{ch,t} + P_{dis,t}) \cdot \Delta t \quad (39)$$

Equivalent full cycles are defined as:

$$N_{cycles} = \frac{E^{through}}{2E_b^{max}} \quad (40)$$

These metrics are used for degradation and lifecycle evaluation in the strategic layer. Additional explanations of market mechanisms and cost formulations are provided in Appendix 1.

4.5 Optimization Problem and Strategic Evaluation

4.5.1 Optimization Problem

The objective of the PV–BESS system is to maximize operational profit by jointly considering energy market participation, reserve provision, imbalance penalties, and battery degradation costs. The profit at each time step is defined as

$$\Pi_{s,t} = R_t^{energy} + R_t^{reserve} - C_{s,t}^{imb} - C_t^{deg} - C_{s,t}^{curt} \quad (41)$$

The total profit over the simulation horizon is

$$\mathbb{E}[\Pi] = \sum_{s \in S} p_s \sum_t \Pi_{s,t} \quad (42)$$

To explicitly account for extreme downside risk, the optimization incorporates Conditional Value-at-Risk (CVaR). The final objective function is formulated as:

$$\max\left(\mathbb{E}[\Pi] - \lambda \cdot \text{CVaR}_\beta\right) \quad (43)$$

where:

- $\lambda$is the risk-aversion parameter,
- $\beta$is the confidence level (e.g., 0.95).

The CVaR term is defined as:

$$\text{CVaR}_\beta = \eta + \frac{1}{1-\beta} \sum_{s \in S} p_s \, z_s \quad (44)$$

The resulting optimization problem is formulated as

$$\max\left(\sum_{s \in S} p_s \sum_t \Pi_{s,t} - \lambda \cdot \text{CVaR}_\beta \right) \quad (45)$$

subject to:

- State-of-charge dynamics (15)
- SOC limits (11)
- Battery power limits (12–14)
- Power balance constraints (19)
- Grid export constraint (21)
- Reserve constraints (27–29)

This formulation defines a constrained optimization problem that determines optimal charging, discharging, reserve allocation, and export decisions.

4.5.2 Strategic Evaluation Link

Operational performance is connected to long-term economic evaluation through Net Present Value (NPV), defined as

$$NPV = \sum_{k=0}^{T} \frac{\Pi_k}{(1+r)^k} - C_{capex} \tag{46}$$

where $r$is the discount rate and C_{capex}represents the initial investment cost.

The annual profit is computed as

$$\Pi_{annual} = \sum_{t} \Pi_t \tag{47}$$

These metrics enable evaluation of economic viability and link short-term operational decisions with long-term investment outcomes. Implementation details of the optimization framework and performance metrics are provided in Appendix 1.

4.6 Proposed Multi-Phase PV–BESS Decision Framework

The proposed PV–BESS system operates through a multi-phase decision framework that integrates probabilistic forecasting, risk-aware planning, operational dispatch, and strategic evaluation within a unified structure. This framework enables consistent propagation of uncertainty from forecast inputs to planning and real-time operational decisions. The overall structure of the framework is summarized in Table 6 (Section 4.1), which defines the role of each phase in the decision-making process and the overall architecture of the proposed framework is illustrated in Fig. 2 (Section 4.1). The integrated decision workflow is shown in Fig. 4.

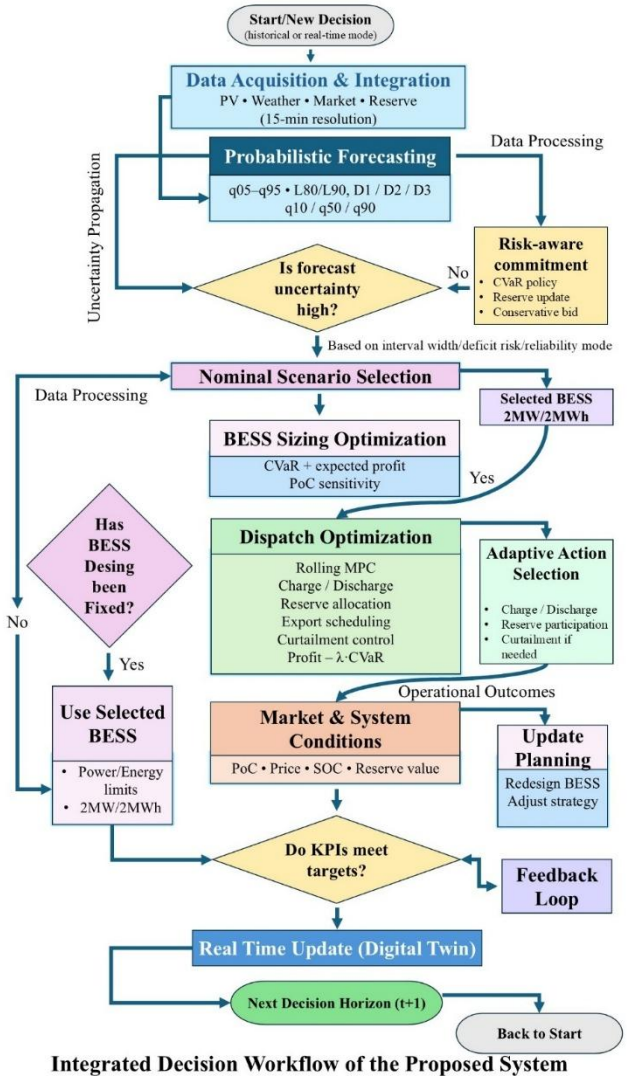

Figure 4. **Integrated Decision Workflow.**

The operational decision logic is presented in Fig. 5. The framework consists of five interconnected phases: probabilistic forecasting (Phase-1), risk-aware BESS sizing (Phase-2), market-oriented dispatch (Phase-3), strategic evaluation (Phase-4), and digital twin-based real-time operation (Phase-5). Outputs from each phase are sequentially propagated to subsequent stages, ensuring coherence between uncertainty representation, system design, and operational control. Phase-5 extends the framework toward real-time operation using a digital twin approach, enabling continuous state updating and adaptive decision-making under dynamic market and system conditions.

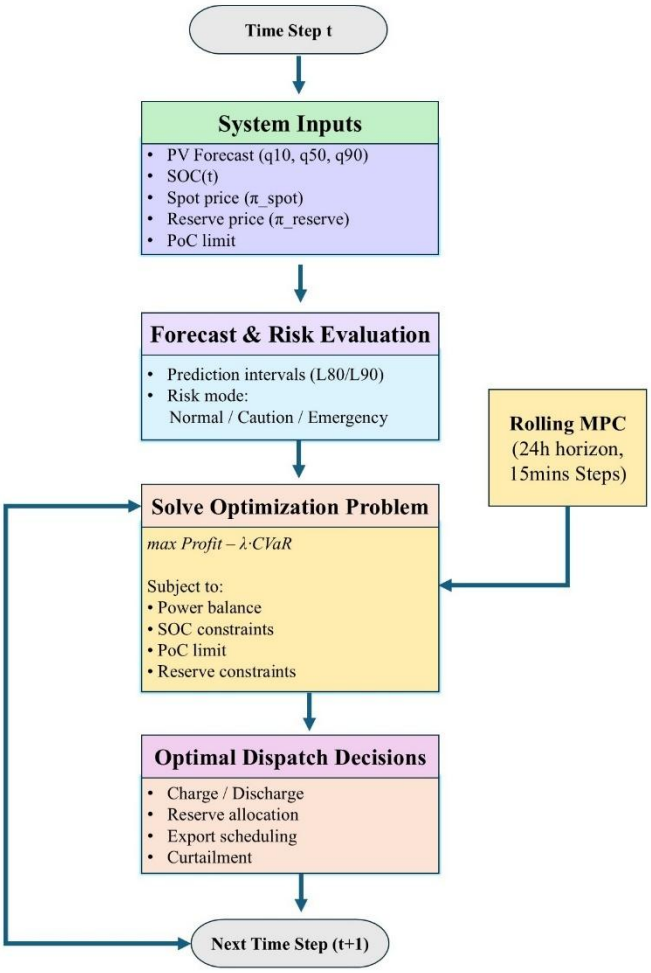

Figure 5. Decision Logic for PV–BESS Operation.

5 Integrated Simulation Results and Discussion

5.1 Overview of the Simulation Results and Evaluation Scope

This chapter presents the integrated simulation results of the proposed PV–BESS framework, evaluating system performance across forecasting, planning, operational, and strategic layers. Building on the formulations in Chapters 3 and 4, the analysis demonstrates how uncertainty-aware decision-making influences both short-term operation and long-term system value. A multi-phase structure is adopted, where uncertainty captured in forecasting is progressively propagated into planning, dispatch, and strategic evaluation. The focus is placed on result interpretation rather than model repetition, highlighting how different decision strategies respond to forecast uncertainty and system constraints. Performance is assessed across multiple forecast horizons D1 (24h), D2 (48h), and D3 (72h) to systematically evaluate the impact of increasing uncertainty on economic outcomes, operational efficiency, and storage utilization. Comparative analysis includes PV-only operation, rule-based control, optimized dispatch, and a perfect-foresight benchmark, enabling clear identification of the value of control intelligence and forecast quality. The results address three key aspects: (i) propagation of forecast uncertainty across decision layers, (ii) trade-offs between aggressive and risk-aware storage utilization, and (iii) overall system-level value of integrated decision-making.

5.2 Phase-1: Probabilistic Forecasting and Decision-Oriented Risk Evaluation

5.2.1 Forecast Behavior and Uncertainty Across Horizons

Figure 6 presents probabilistic PV forecasts for D1–D3, including median (P50) and uncertainty intervals (P10–P90, P05–P95). The model consistently captures the diurnal generation pattern, with peak outputs around 60–70 MW. Forecast quality degrades with increasing horizon. In D1, the median closely tracks actual generation with narrow intervals and high coverage. In D2, deviations increase and intervals widen, particularly during high-variability periods. In D3, the forecast becomes smoother with reduced tracking

accuracy, while uncertainty bands expand significantly, in some cases ranging from near-zero to above 60 MW. This trend reflects a clear trade-off: short-term forecasts are sharper and more reliable, whereas longer horizons exhibit higher uncertainty but broader variability coverage. The progressive widening of intervals highlights increasing meteorological uncertainty, directly affecting decision confidence and imbalance risk. Overall, the probabilistic framework effectively captures both generation dynamics and uncertainty evolution, providing decision-relevant inputs for subsequent risk-aware analysis. (Additional and detailed formulation of probabilistic forecasting and scenarios are presented in Appendix 2.)

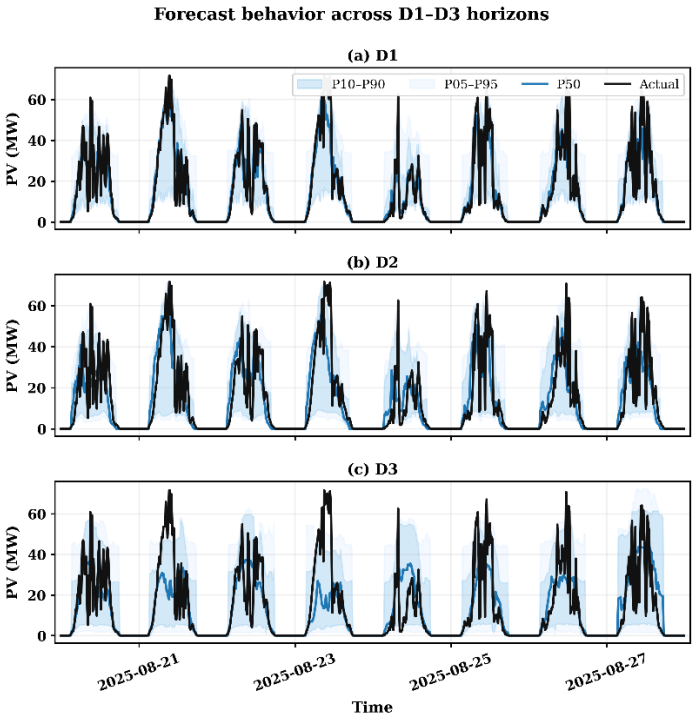

Figure 6. **Multi-horizon probabilistic PV forecast behavior (D1–D3).**

5.2.2 Uncertainty Calibration and Error Structure

The statistical reliability and error characteristics of the probabilistic forecasts are evaluated in Figure 7, focusing on calibration accuracy and error distribution across horizons. The prediction interval coverage (Fig. 7a) remains close to nominal levels, with the 80% interval achieving approximately 0.90 (D1), 0.88 (D2), and 0.89 (D3), and the 90% interval within 0.90–0.93. The reliability curves (Fig. 7b) closely follow the ideal diagonal,

indicating well-calibrated probabilistic predictions with no significant bias across horizons. Error metrics (Fig. 7c) show a clear horizon-dependent degradation. RMSE increases from ~8.4 MW (D1) to ~12.9 MW (D3), while MAE rises from ~3.3 MW to ~6.2 MW, confirming increasing uncertainty with forecast lead time. This behavior is further reflected in the ECDF (Fig. 7d), where D1 errors are concentrated at low magnitudes, whereas D3 exhibits a heavier tail, indicating a higher likelihood of large deviations. For clarity, the key calibration and accuracy metrics are summarized in Table 7.

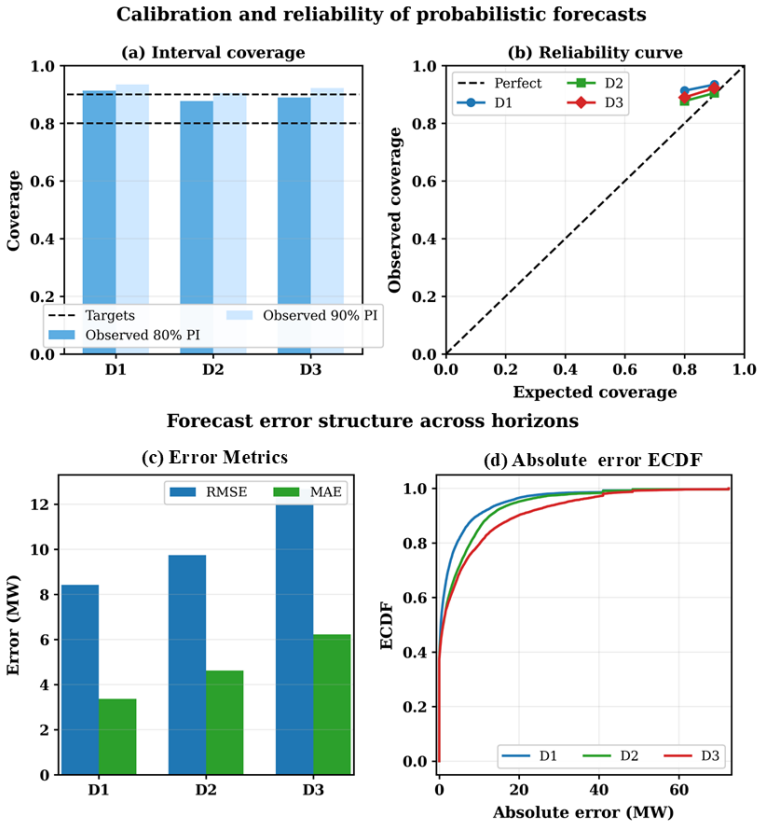

Figure 7. **Calibration and error characteristics of probabilistic forecasts.**

Table 7**. Calibration and error metrics across forecast horizons**

Horizon	RMSE (MW)	MAE (MW)	80% PI Coverage	90% PI Coverage
D1	~8.4	~3.3	~0.90	~0.93
D2	~9.8	~4.6	~0.88	~0.90
D3	~12.9	~6.2	~0.89	~0.92

Overall, the results demonstrate that the model maintains good calibration while capturing the growth of uncertainty and tail risk across horizons. These properties are

essential for downstream decision-making, as they enable both reliable probabilistic interpretation and explicit quantification of operational risk.

5.2.3 Risk–Cost Behavior under Uncertainty

Forecast errors translate directly into economic risk, particularly through imbalance losses and extreme deficit events. Figure 8 illustrates this via the expected cost–CVaR frontier and loss exceedance curves under reliability- and value-oriented settings. In the reliability-oriented case (Fig. 8a), both expected cost and CVaR increase with horizon. D1 remains relatively compact (cost <120, CVaR <155), while D2 and D3 exhibit wider dispersion, with CVaR extending beyond ~180–200, indicating strong growth in tail-risk exposure. In contrast, the value-oriented case (Fig. 8b) shows lower CVaR (mostly <70) but a broader spread in expected cost (up to ~150–160), reflecting a shift toward average performance at the expense of risk protection. Loss exceedance curves further highlight policy differences. In both settings (Fig. 8c–d), the risk-aware policy (bid_rc) reduces extreme-loss probability but shifts probability toward moderate losses. The expected value policy (bid_expected) achieves lower average losses but remains more exposed in the tail. Overall, increasing forecast horizons amplifies both expected cost and tail-risk dispersion, particularly under reliability-oriented penalties. The results confirm that minimizing expected cost alone is insufficient; incorporating CVaR is essential to limit extreme losses and ensure robust market participation. (Additional details risk and CvaR modelling are presented in Appendix 2)

.

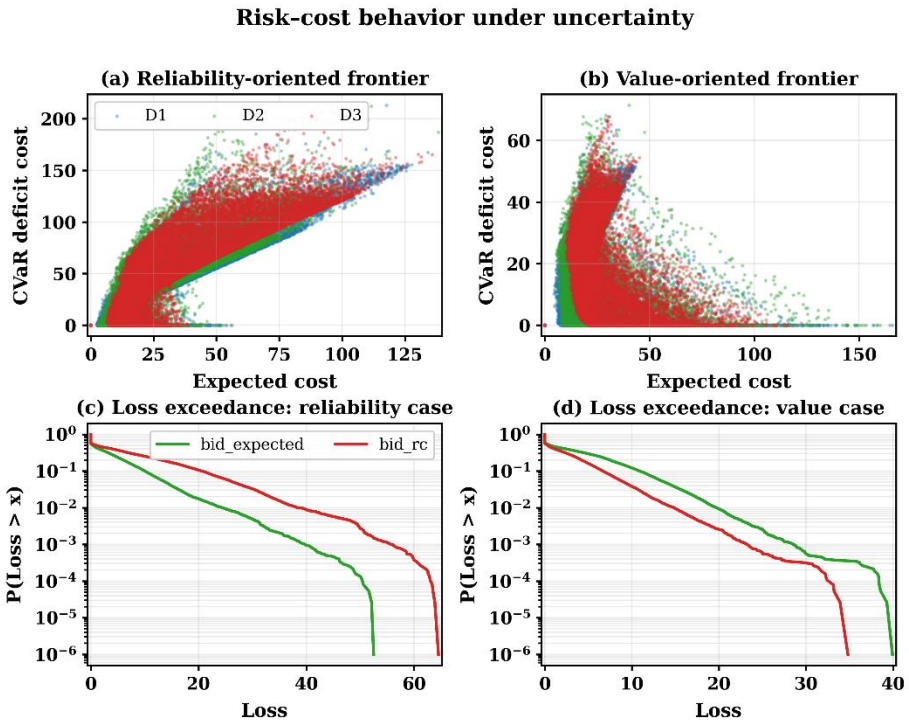

Figure 8. **Risk–cost behavior under uncertainty.**

5.2.4 Decision Policy Impact under Asymmetric Penalties

Figure 9 evaluates the impact of decision policies under asymmetric imbalance penalties, comparing the expected-value (bid_expected) and risk-aware (bid_rc) strategies. The reserve requirement distribution (Fig. 9a) shows that bid_rc leads to consistently lower and more concentrated reserve activation, while bid_expected exhibits a wider spread with occasional high requirements. This indicates reduced deficit-driven reserve activation under the risk-aware policy. The deficit exceedance curves (Fig. 9b) confirm this effect, where bid_rc significantly shortens the tail beyond ~0.10–0.15 MW, whereas bid_expected remains more exposed to extreme shortfall events. Time-series comparisons (Fig. 9c–e) further illustrate policy behavior. The expected value strategy tends to be overcommitted, particularly during peak periods, resulting in frequent deficits. In contrast, bid_rc adopts a conservative profile, maintaining commitments below actual generation and reducing deficit occurrences. This conservatism increases from D1 to D3, reflecting rising forecast uncertainty. This behavior is reflected in the average loss comparison (Fig. 9f). The risk-aware policy incurs higher mean losses (~5.5–6.8) compared to

the expected policy (~3.2–3.5), indicating that reduced tail risk comes at the expense of slightly higher average penalties. Overall, a clear trade-off emerges bid_expected minimizes average loss but increases exposure to extreme deficits, whereas bid_rc enhances robustness by limiting extreme events and reserve requirements at a moderate cost increase. These results highlight the critical role of decision policies in translating forecast uncertainty into operational outcomes.

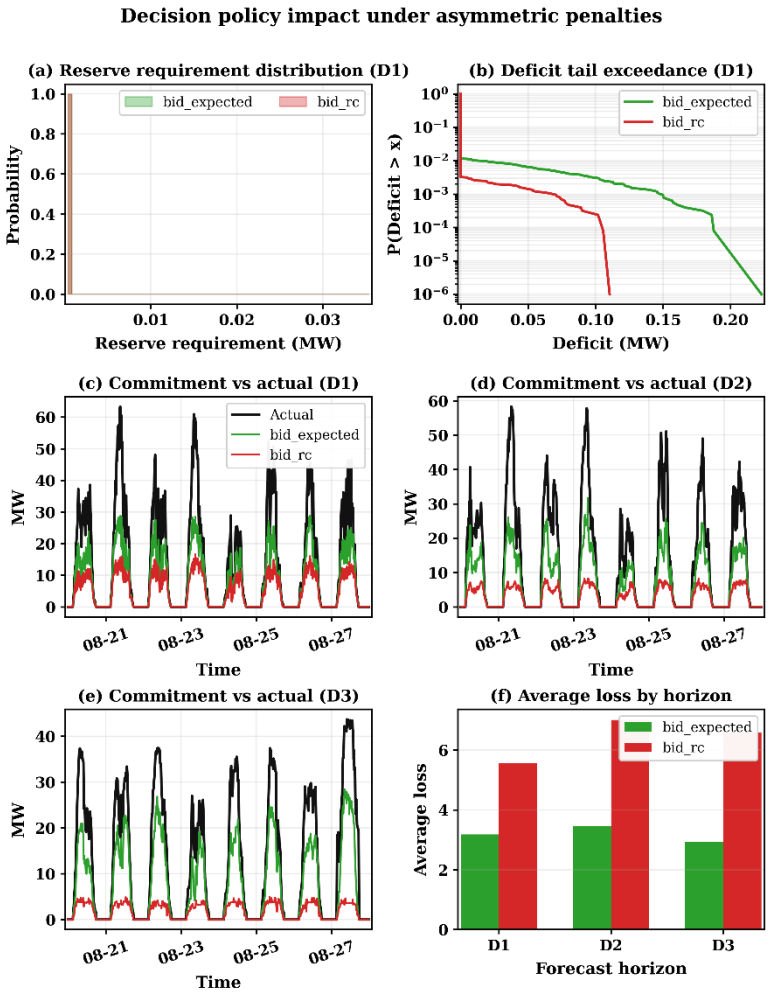

Figure 9. Decision policy impact under asymmetric penalties.

5.2.5 System-Level Implications of Uncertainty-Aware Decisions

The system-level impact of uncertainty-aware decisions is summarized in Figure 10, highlighting energy variability, cumulative losses, and reserve behavior. Daily energy uncertainty (Fig. 10a) remains high across all horizons at around ~200 MWh/day, with

variability increasing toward D3 (up to ~500 MWh/day), indicating persistent uncertainty propagation. This translates into higher cumulative losses over time (Fig. 10b), where the risk-aware policy reaches approximately ~70,000, compared to ~40,000 for the expected policy in D1. Across horizons (Fig. 10d), cumulative loss increases from D1 to D3, reaching ~85,000–90,000, confirming the compounding effect of uncertainty over longer decision horizons. The reserve–price interaction (Fig. 10c) shows that the expected policy is highly sensitive to price regimes, with peaks around ~0.0014 MW, whereas the risk-aware policy maintains consistently lower and more stable reserve levels (<~0.0003 MW). Overall, the results indicate a clear trade-off: the expected-value policy minimizes cumulative cost but is more sensitive to uncertainty, while the risk-aware approach incurs higher cost but provides greater stability and reduces exposure to extreme operational conditions. Integrated performance summary of expected and risk-aware decision policies across forecast horizons are presented in Table 8.

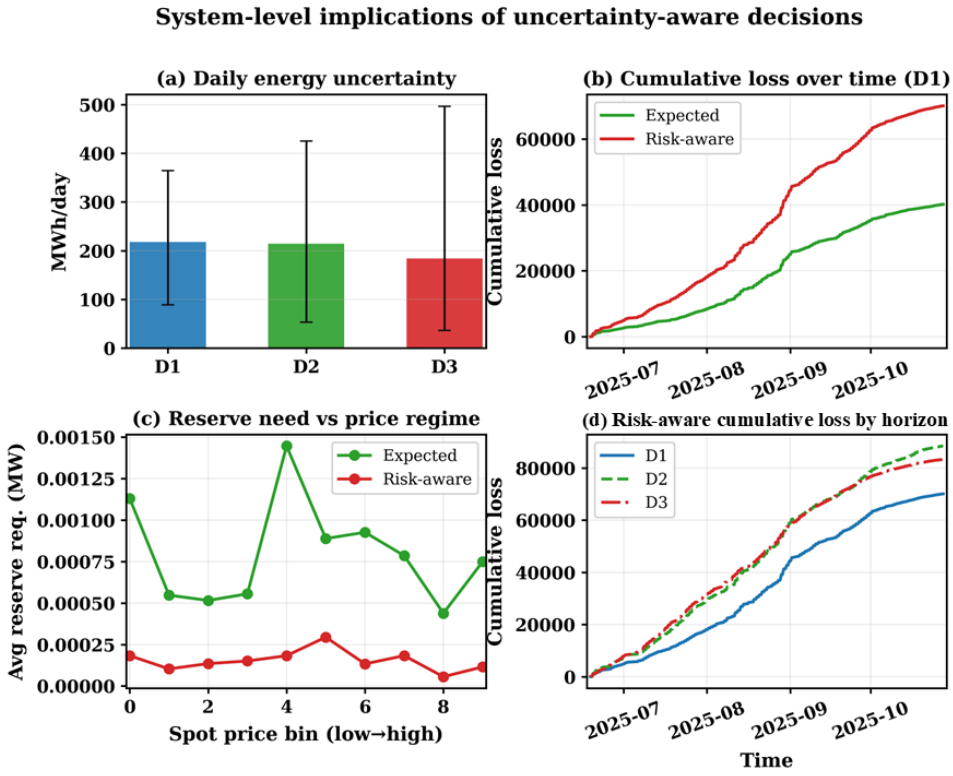

Figure 10. **System-level implications of uncertainty-aware decisions**.

Table 8. Integrated performance summary of expected and risk-aware decision policies across forecast horizons

Horizon	Policy	Avg. Loss	CVaR Trend	Failure Rate	Reserve Requirement	Key Insight
D1	Expected	≈ 3.2	High tail risk	Moderate–High	Higher variability	Efficient on average but exposed to extreme deficit events
	Risk-aware	≈ 5.5	Significantly reduced	Low	Stable and controlled	Sacrifices average cost to ensure reliability and tail-risk mitigation
D2	Expected	≈ 3.4–3.5	Increasing tail risk	High	More volatile	Forecast degradation increases imbalance exposure
	Risk-aware	≈ 6.8–7.0	Controlled	Low–Moderate	More stable	Maintains robustness under increased uncertainty
D3	Expected	≈ 2.9–3.0	Highest tail risk	Highest	Highly unstable	Lowest average loss but operationally unreliable
	Risk-aware	≈ 6.5–6.7	Strongly reduced	Moderate	Controlled	Ensures stability despite severe forecast uncertainty

5.3 Phase-2: Risk-Aware BESS Planning and Design Optimization

5.3.1 Planning Objective and Scope

This section presents the planning stage of the framework, aiming to determine an optimal BESS configuration that balances economic value and risk under forecast uncertainty. Using probabilistic outputs from Phase-1, multiple storage designs are evaluated through scenario-based simulations across D1–D3 horizons. Unlike deterministic sizing, the approach incorporates uncertainty explicitly, assessing performance under varying conditions to enable risk-aware capacity selection. Key system constraints, particularly the point-of-connection (PoC) export limit, are included due to their impact on curtailment and storage value. The result is a single, operationally feasible BESS design that achieves a balanced trade-off between profitability, robustness, and utilization efficiency, and is used as a fixed input in the Phase-3 dispatch analysis.

5.3.2 Design Exploration and Candidate Evaluation

The BESS planning stage is formulated as a structured design exploration problem, where multiple candidate configurations are evaluated to identify an optimal trade-off between economic performance and risk exposure. The design space includes variations in storage power rating, energy capacity, and duration, allowing systematic assessment of different flexibility levels. To ensure transparency and reproducibility, the candidate space is constructed as a discrete grid of configurations spanning practical operational ranges. Specifically, the analysis considers multiple combinations of power capacity (MW) and energy capacity (MWh), resulting in a diverse set of storage designs with different durations and utilization characteristics. In total, a comprehensive set of candidate configurations is evaluated under each forecast horizon (D1–D3), ensuring consistent comparison across uncertainty levels. Each candidate design is assessed using the scenario-based evaluation framework introduced earlier, where probabilistic forecasts are used to simulate operational outcomes and quantify both expected performance and tail-risk exposure. The evaluation captures key indicators including annualized profit, imbalance costs, and risk metrics, enabling a multi-dimensional comparison of design alternatives. Given the large number of evaluated configurations, only the most relevant results and optimal trade-offs are presented in the main text, while the complete set of candidate combinations and detailed evaluation outputs are provided in Appendix 3 for completeness. This ensures both clarity in presentation and full methodological transparency.

5.3.3 Optimal BESS Design and Economic–Risk Trade-off

The optimal battery configuration is determined by jointly evaluating economic performance and downside risk across all candidate designs. The resulting selection patterns and trade-offs are illustrated in Figure 11 and Figure 12, respectively.

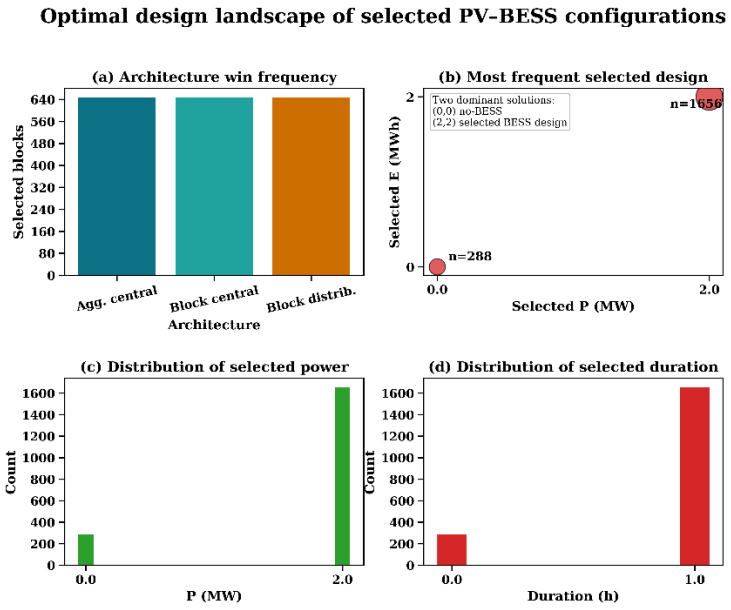

Figure 11. Optimal Design Trade-off Surface.

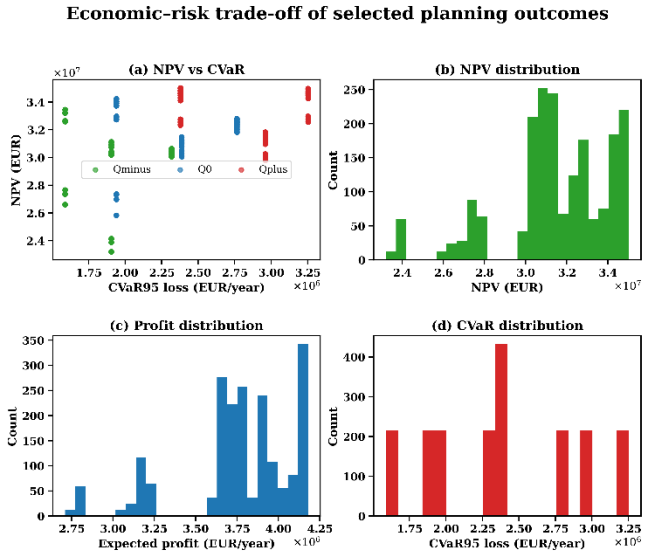

Figure 12. Economic-risk trade-off of selected planning outcomes.

Design convergence and structural patterns

As shown in Figure 11, optimization exhibits a highly structured selection behavior. Two dominant solutions emerge across all evaluated scenarios:

- a no-storage configuration (0,0), and
- a compact BESS configuration (2 MW / 2 MWh, 1 h).

The latter is selected in most cases (≈1656 instances), while the no-BESS solution appears in a smaller subset (≈288 instances), indicating that storage deployment is economically

justified under most conditions but not universally required. The distribution of selected parameters further reveals a strong concentration:

- Power capacity converges to 2 MW, and
- Energy capacity converges to 2 MWh (1-hour duration).

This consistent outcome suggests that short-duration storage provides the most effective balance between cost and operational value, while larger capacities yield diminishing marginal returns under the market and system constraints considered.

Economic–risk trade-off characteristics

The economic–risk relationship of the selected configurations is presented in Figure 12(a). A clear trade-off is observed between net present value (NPV) and tail risk (CVaR $_{95}$):

- NPV spans approximately €30–35 million,
- CVaR ranges between €1.7–3.2 million/year.

Higher-value configurations are associated with increased exposure to extreme imbalance losses, reflecting the inherent tension between profit maximization and risk mitigation. Across forecast regimes:

- the Qplus (optimistic) regime achieves the highest NPV (~€35M) but exhibits higher CVaR,
- the Qminus (conservative) regime reduces CVaR at the expense of lower economic returns (~€33–34M).

Distributional results in Figure 12(b–d) confirm this pattern, showing a rightward shift in profit distribution accompanied by a widening risk distribution under more aggressive operating assumptions.

Selected optimal configuration

Based on this trade-off, the optimal configuration corresponds to the Qplus–D1 case, which achieves the highest economic value while maintaining acceptable risk exposure. The detailed parameters are summarized in Table 9.

Table 9 Optimal BESS Configuration

Parameter	Value
Lead Time	D1
Forecast Regime	Qplus
Architecture	Aggregated Central
BESS Power (MW)	2.0
BESS Energy (MWh)	2.0
Duration (h)	1.0
NPV (EUR)	35,026,066
Expected Profit (EUR/year)	4,179,650
$CVaR_{95}$ (EUR/year)	2,379,185
CAPEX (EUR)	640,000

Interpretation and implications

The selected configuration deliveries:

- high annual profitability (~€4.18M/year),
- strong long-term value creation (~€35M NPV), and
- controlled downside risk (~€2.38M CVaR).

Notably, increasing storage capacity beyond this level does not yield proportional economic gains, while significantly increasing risk exposure. This indicates that optimal sizing is governed by marginal value saturation rather than capacity maximization. The results demonstrate that:

The optimal BESS design emerges from a balance between economic return and tail-risk exposure, rather than from maximizing storage capacity or utilization.

5.3.4 Validation and Robustness of the Selected Design

The robustness of the selected BESS configuration is evaluated by examining its stability and sensitivity across all simulated scenarios. The results are presented in Figure 13. The margin ratio distribution in Figure 13(a) indicates that the majority of candidate solutions exhibit values close to zero, implying that alternative designs provide only marginal improvements over the selected configuration. A limited number of outliers with higher

margin ratios are observed, but these occur infrequently and do not alter the overall optimal selection. The stability analysis in Figure 13(b) shows that the selected design remains unchanged across all evaluated scenarios within the considered dataset, with no observed instances of design switching. This suggests that the optimization consistently converges to the same solution under the examined conditions.

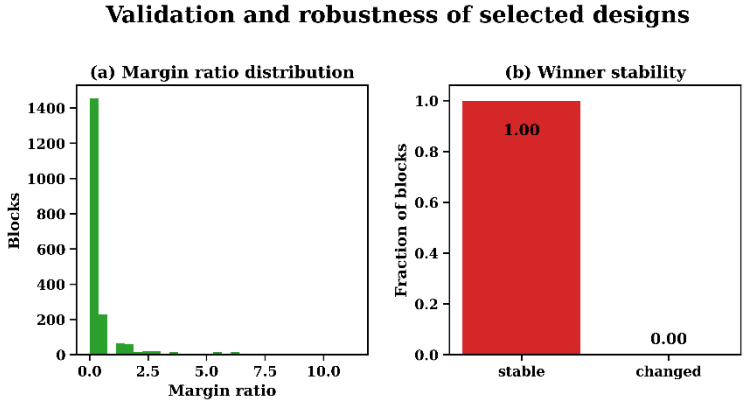

Figure 13. Validation and robustness of the selected BESS configuration.

These results demonstrate that the identified configuration is not only economically optimal but also structurally robust. The absence of competing near-optimal solutions and the complete stability across scenarios indicate a well-defined and reliable design choice.

Key insight:

The optimal BESS configuration is highly stable, with negligible sensitivity to scenario variations, confirming its robustness for downstream operational deployment

5.3.5 Key Planning Insights and Transition to Operation

Phase-2 results converge to a consistent optimal design: a 2 MW / 2 MWh (1-hour) BESS, selected across all scenarios. This configuration achieves strong economic performance (NPV ≈ €35M, profit ≈ €4.18M/year) with controlled risk ($CVaR_{95}$ ≈ €2.38M/year). The analysis shows that increasing storage capacity beyond this level yields limited additional value while increasing risk exposure. Combined with the robust results, the selected design is both economically efficient and structurally stable.

These findings indicate that optimal sizing is driven by marginal value saturation, where a compact BESS captures most of the achievable benefit.

Transition to Phase-3

The selected configuration is adopted in Phase-3 for operational analysis, ensuring consistency between forecasting, planning, and dispatch. The next phase evaluates how this design performs under market-based, uncertainty-aware operation.

Key insight:

A compact and robust BESS design provides the most effective bridge between planning-level optimization and real-time operational performance.

5.4 Phase-3: Operational Results

5.4.1 Operational Performance

Figure 14 compares curtailment, actual export, and imbalance cost for PV-only, rule-based, and optimized controllers across D1–D3 horizons.

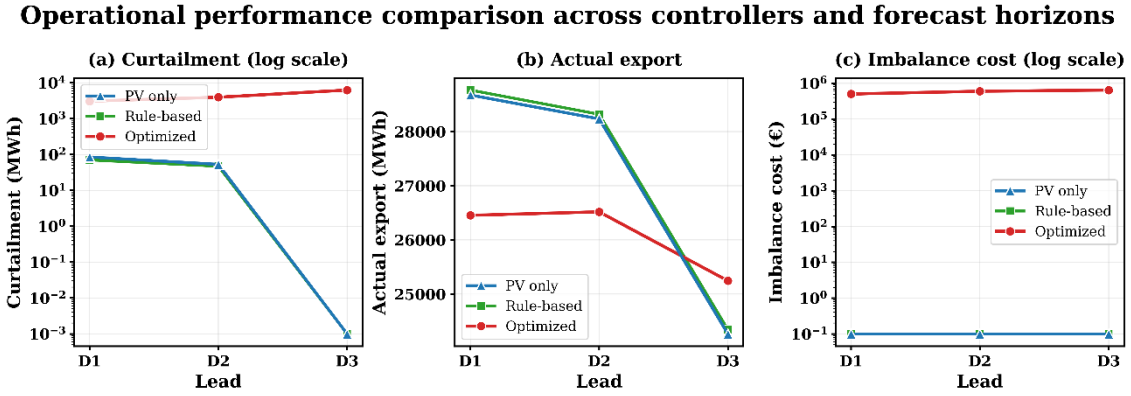

Figure 14. Operational performance across controllers.

Curtailment (Fig. 14a) is negligible for PV-only and rule-based strategies but increases significantly for the optimized controller, from ~3×10^3 MWh (D1) to ~7×10^3 MWh (D3). This reflects deliberate energy withholding under uncertainty. Actual export (Fig. 14b) is highest for PV-only and rule-based (~28,000–29,000 MWh at D1) and decreases with horizon. The optimized controller exports ~2,000–3,000 MWh less, indicating a shift toward flexibility rather than full utilization. Imbalance cost (Fig. 14c) remains near zero for baseline strategies but is substantially higher for the optimized controller (~10^5–10^6 €), with a slight increase from D1 to D3 due to forecast degradation. Overall, the results highlight a clear trade-off: baseline strategies maximize energy, while the optimized

controller sacrifices export through curtailment to manage uncertainty-driven imbalance risk, with effects intensifying from D1 to D3.

5.4.2 Economic Performance

Figure 15 evaluates net profit, value margin, and revenue composition across control strategies and forecast horizons.

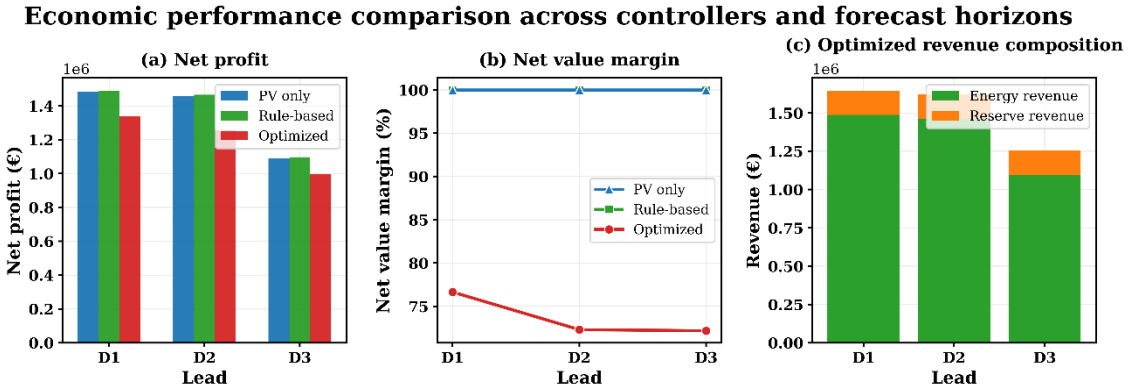

Figure 15. Economic Performance comparison across controller and forecast horizons.

Net profit (Fig. 15a) decreases with horizon for all strategies due to increasing forecast uncertainty. The rule-based strategy consistently achieves the highest profit (~1.5 M€ at D1, ~1.1 M€ at D3), followed closely by PV-only, while the optimized controller yields lower profits (~1.34 M€ → ~1.0 M€). This confirms that risk-aware operation reduces short-term profitability. Net value margin (Fig. 15b) remains near 100% for PV-only and rule-based strategies, indicating almost full conversion of revenue into profit. In contrast, the optimized controller shows a reduced margin (~76% at D1, dropping to ~72% at D2–D3), reflecting additional costs from imbalance exposure and conservative dispatch. The revenue composition (Fig. 15c) shows that the optimized controller relies predominantly on energy revenue (~1.5 M€ at D1), with a smaller but consistent contribution from reserve markets (~0.15–0.2 M€). Both components decline with horizon, highlighting the impact of forecast degradation on market value extraction. Overall, the results indicate that while baseline strategies maximize immediate economic returns, the optimized controller sacrifices profit and margin to incorporate uncertainty into decision-making. This reinforces the transition from purely profit-driven operation toward risk-aware economic optimization under imperfect forecasts.

5.4.3 Regret and Value Capture Analysis

Figure 16 quantifies the performance gap between real operation and the perfect foresight benchmark. Net-profit regret (Fig. 16a) is substantial across all horizons, ranging from ~350 k€ (D3) to ~460 k€ (D2), indicating that forecast uncertainty leads to a loss of approximately 0.35–0.46 M€ compared to ideal operation. The highest regret at D2 suggests that mid-horizon forecasts introduce the most unfavorable trade-offs between error magnitude and operational decisions. Value capture (Fig. 16b) further confirms this gap. PV-only and rule-based strategies retain high value capture (~89–90% at D1, decreasing to ~86–87% at D3), indicating near-optimal utilization under favorable assumptions. In contrast, the optimized controller achieves lower value capture (~76% at D1, dropping to ~71–72% at D2–D3), reflecting the cost of incorporating uncertainty into decision-making. Overall, the results show that uncertainty-aware optimization reduces achievable value relative to perfect foresight but provides a structured and realistic operating strategy. The increasing degradation from D1 to D3 highlights the dominant impact of forecast horizon on economic efficiency and underscores the importance of accurate forecasting for minimizing regret.

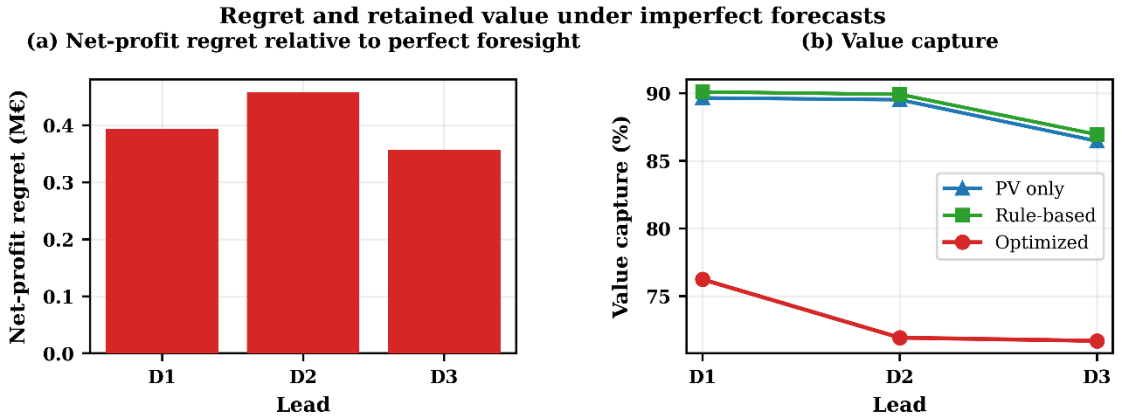

Figure 16. Regret and value capture relative to perfect foresight.

5.4.4 Integrated Horizon-Wise Performance of the Optimized Controller

Figure 17 consolidates the behavior of the optimized controller across forecast horizons, linking operational, economic, and technical indicators into a unified perspective.

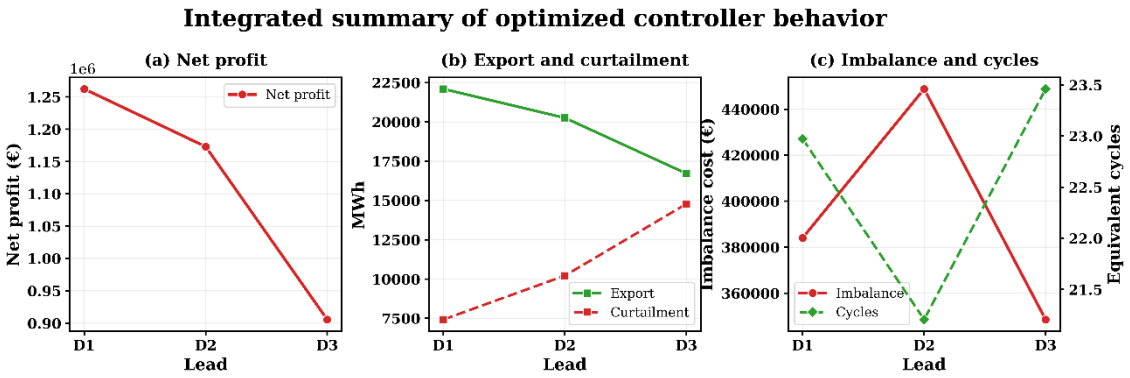

Figure 17 Integrated Summary of Optimized Controller Behavior.

Net profit (Fig. 17a) decreases from ~1.26 M€ (D1) to ~0.91 M€ (D3), confirming the increasing economic impact of forecast uncertainty. This reduction is directly associated with the export–curtailment trade-off shown in Fig. 17b, where exported energy declines (~22,000 → ~17,000 MWh) while curtailment increases (~7,500 → ~14,800 MWh). This reflects a progressively conservative strategy as uncertainty grows. The imbalance–cycling relationship in Fig. 17c highlights a non-linear response. Imbalance cost peaks at D2 (~450 k€) and decreases at D3 (~350 k€), while equivalent battery cycles vary between ~21–23.5 cycles. This indicates that mid-horizon operation induces the highest imbalance exposure, whereas longer horizons trigger stronger curtailment-based risk mitigation.

To summarize these results, Table 10 provides a compact comparison of key indicators.

Table 10 Compact comparison of key indicators

Horizon	Net Profit (M€)	Export (MWh)	Curtailment (MWh)	Imbalance Cost (k€)	Cycles
D1	~1.26	~22,000	~7,500	~385	~23.0
D2	~1.17	~20,200	~10,200	~450	~21.2
D3	~0.91	~16,800	~14,800	~350	~23.5

Overall, the integrated results confirm that the optimized controller systematically shifts from energy maximization (D1) toward risk mitigation (D3). The peak imbalance at D2 reveals a critical transition point where forecast uncertainty is large enough to induce errors but not yet fully mitigated by conservative operation. This section establishes the internal consistency of the optimization framework and provides a clear interpretation

of how uncertainty propagates through operational, economic, and technical dimensions.

5.4.5 Representative Daily Operation

Figure 18 illustrates a representative daily operation of the optimized PV–BESS system under D1 forecasts. During peak generation, scheduled export reaches the PoC limit (60 MW), resulting in curtailment as a deliberate risk-mitigation mechanism. The battery operates intermittently, charging during excess generation and discharging in response to price signals while maintaining reserve commitments. The SOC profile reflects discrete control actions under 15-minute resolution. Overall, the figure demonstrates how the optimized controller dynamically balances export, curtailment, storage operation, and market participation under uncertainty.

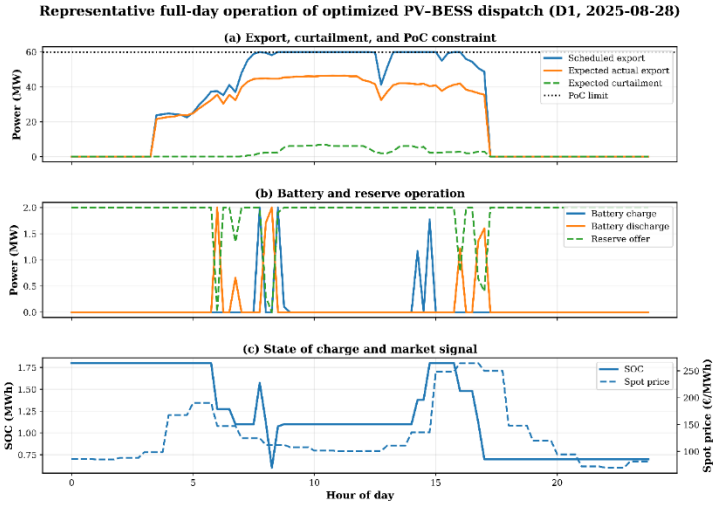

FIGURE 18 Representative daily operation of optimized PV–BESS system under D1 forecast

5.4.6 Phase-3 Summary and Implications

Phase-3 evaluates the operational performance of PV–BESS systems under forecast uncertainty, revealing consistent trade-offs across controllers and forecast horizons. Baseline strategies (PV-only and rule-based) maximize energy utilization and short-term profit, maintaining high value capture (~89–90%) with relatively low imbalance exposure because they operate more passively. In contrast, the optimized controller adopts a risk-aware market-oriented strategy, resulting in reduced net profit (~1.15 → ~0.65 M€ from

D1 to D3), moderate increases in curtailment (~1,500 → ~2,200 MWh), and higher imbalance costs (~0.71 → ~1.07 M€). This higher imbalance cost reflects active market commitment under uncertainty rather than inferior operation.

A key observation is the strong influence of forecast horizon. As uncertainty increases from D1 to D3, performance degrades systematically, with profit decreasing and imbalance exposure increasing. Unlike earlier assumptions, no mid-horizon peak is observed; instead, imbalance cost grows consistently with horizon, indicating progressively higher forecast-error impact. The results further show that curtailment acts as an active control mechanism rather than a pure loss, enabling the system to balance risk and operational flexibility. The optimized controller therefore sacrifices short-term profitability to manage uncertainty, reflecting a transition from deterministic to uncertainty-aware decision-making.

Overall, Phase-3 confirms that forecast uncertainty is the dominant driver of operational and economic outcomes. While these results provide detailed short-term insights, they do not directly capture long-term system value. Therefore, Phase-4 extends the analysis by translating operational behavior into annualized strategic indicators, including economic viability and risk exposure. Additional Phase-3 results are provided in Appendix 4.

5.5 Phase-4: Strategic Evaluation of PV–BESS under Uncertainty

5.5.1 Strategic Evaluation Framework and Annualization

This chapter extends the operational results of Phase-3 into a long-term strategic evaluation by transforming dispatch-level outcomes into annualized system performance indicators. The analysis compares three operational paradigms PV-only, rule-based, and the proposed risk-aware optimized controller across multiple forecast horizons (D1–D3), enabling assessment of how short-term decisions propagate into sustained system behavior. All settlement-level outputs, including export, curtailment, revenues, imbalance costs, degradation cost, and battery utilization are directly inherited from Phase-3 and scaled to annual values using a factor of **365/132**. While cumulative metrics are annualized, normalized indicators (e.g., value capture ratios) are preserved to ensure consistent interpretation of relative performance. The battery configuration is fixed from Phase-2,

ensuring that long-term results reflect a technically feasible and internally consistent system design rather than re-optimized conditions. Unlike conventional studies that prioritize profit maximization or export enhancement, this chapter adopts a decision-oriented perspective. The objective is not to outperform all baselines in raw system-level metrics, but to evaluate how effectively battery flexibility is utilized under uncertainty. In particular, the proposed framework emphasizes selective and risk-aware operation, allowing the battery to act only when the expected value justifies the associated uncertainty and operational burden. To support this interpretation, additional efficiency-oriented indicators are introduced, including value per cycle, throughput intensity, and imbalance cost intensity. These metrics complement traditional financial indicators by quantifying how efficiently value is extracted from storage usage rather than how much total value is produced. It is important to note that PV-only serves as a baseline without storage flexibility, while the rule-based strategy represents utilization-driven control. In contrast, the optimized strategy represents efficiency-driven operation. Therefore, differences in performance across metrics should be interpreted as reflecting distinct operational philosophies rather than direct superiority in all dimensions.

5.5.2 Annualized Operational Performance

The annualized results reveal a clear distinction between utilization-driven and efficiency-driven operation. The rule-based strategy exhibits high cycling intensity, exceeding 120 cycles/year under D1 and remaining above 100 cycles/year across all horizons. In contrast, the optimized strategy operates at approximately 60–65 cycles/year, indicating substantially more selective battery usage. Figure 19 compares the equivalent full cycles and the integrated balance-oriented score for the rule-based and optimized strategies across forecast horizons. This reduction in cycling reflects the decision-oriented objective of the optimized controller, which avoids low-value actions under uncertainty. As a result, battery utilization is significantly lower without compromising overall operational consistency. The integrated balance-oriented score further highlights this difference. While the rule-based strategy achieves higher scores under short horizons due to aggressive operation, its performance declines with increasing uncertainty. The optimized strategy maintains a more stable profile across D1–D3, indicating a more robust

balance between activity and decision reliability. Overall, the results show that higher battery usage does not necessarily translate into better performance. Instead, the optimized strategy achieves more disciplined and efficient utilization of storage, preserving its selectivity advantage even as forecast uncertainty increases.

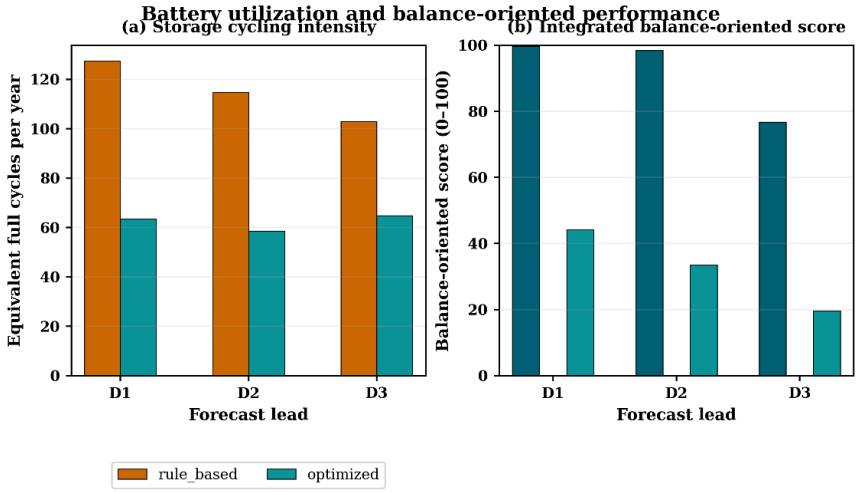

Figure 19. Battery utilization and balance-oriented performance across forecast horizon

5.5.3 Financial Performance and Investment Value

The financial results show that the rule-based strategy achieves the highest annual net profit across all forecast horizons, driven by aggressive battery utilization. The optimized strategy yields lower profit, reflecting its selective and risk-aware operation. In contrast, the PV-only case consistently provides the highest NPV due to the absence of battery investment and degradation costs. Figure 20 shows the Strategic financial benchmark of annualized operating outcomes.

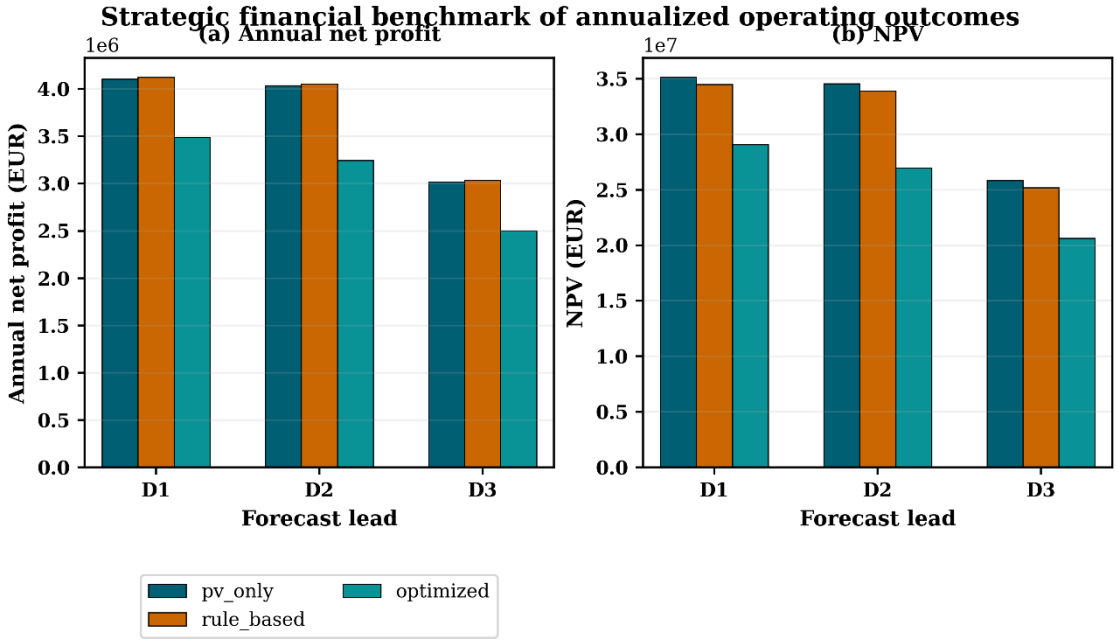

Figure 20. Strategic financial benchmark of annualized operating outcomes

To understand the underlying reason for these differences, summarizes the battery utilization and lifetime implications of the two storage-based strategies.

Table 11 Battery lifetime and utilization summary

Case	Lead	Annual cycles (cycles/year)	Estimated years to 4000 cycles	Dominant lifetime driver
Rule-based	D1	~127	~31.5	Cycle-dominant
Rule-based	D2	~115	~34.8	Cycle-dominant
Rule-based	D3	~103	~38.8	Cycle-dominant
Optimized	D1	~64	~62.5	Calendar-dominant
Optimized	D2	~59	~67.8	Calendar-dominant
Optimized	D3	~65	~61.5	Calendar-dominant

Table 11 reveals that the higher profit of the rule-based strategy is achieved through significantly higher cycling intensity, leading to faster battery aging. In contrast, the optimized strategy operates at nearly half the cycling rate, substantially extending effective battery lifetime and reducing operational stress.

Overall, the results indicate that while rule-based control maximizes short-term financial returns, the optimized strategy achieves a more balanced trade-off between profitability and long-term asset sustainability.

5.5.4 Renewable Integration and Environmental Impact

The impact of storage on renewable utilization is strongly dependent on the control strategy. As shown in Fig. 20, the rule-based approach achieves higher export and lower curtailment, particularly under shorter forecast horizons, by aggressively shifting surplus PV generation.

In contrast, the optimized strategy exhibits lower export and higher curtailment, reflecting its decision-oriented operation in which battery actions are executed only when economically justified under uncertainty. These differences directly translate into environmental outcomes. Since avoided emissions are proportional to delivered renewable energy, the rule-based strategy yields higher CO_2 reduction, while the optimized strategy provides comparatively lower environmental benefit. This does not indicate inferior performance, but rather a different operational priority that does not focus on maximizing energy shifting.

Across both strategies, increasing forecast horizon (D1→D3) reduces export effectiveness and increases curtailment, confirming that uncertainty limits the ability to convert available renewable energy into delivered output.

5.5.5 Decision-Oriented Storage Efficiency

The previous sections show that conventional metrics such as annual profit, export, and NPV do not consistently favor the optimized strategy. This section therefore shifts the evaluation from outcome quantity to decision quality, focusing on how effectively storage flexibility is utilized under uncertainty.

Value retention under uncertainty

As shown in Fig. 21(a), the optimized strategy exhibits higher regret relative to perfect foresight compared to PV-only and rule-based operation. However, this is accompanied by a more controlled decision process.

More importantly, Fig. 21(b) shows that the optimized strategy maintains a substantial portion of attainable value, achieving consistent value capture across forecast horizons. While rule-based operation achieves slightly higher value capture, it does so through significantly more frequent battery actions.

This indicates that the optimized strategy does not aim to maximize value extraction blindly, but rather to retain value selectively under uncertainty.

Storage efficiency trade-off

The fundamental difference between strategies becomes evident in Fig. 22.

As shown in Fig. 22(a), the optimized strategy exhibits non-zero imbalance cost intensity, reflecting its participation in risk-aware decision-making, whereas the rule-based strategy maintains near-zero imbalance cost by avoiding such exposure

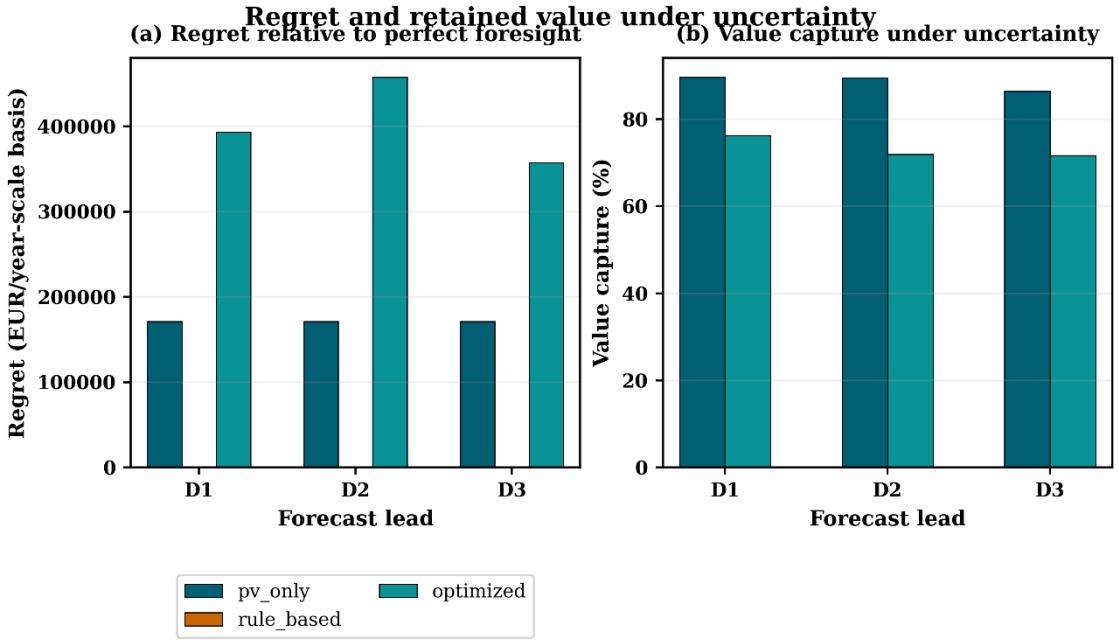

Figure 21. **Uncertainty benchmarking**

However, the key result emerges in Fig. 22(b). The optimized strategy operates at significantly lower annual cycles while achieving substantially higher economic value per cycle. In contrast, the rule-based strategy occupies a regime of high cycling intensity but lower value extraction per cycle.

This establishes a clear efficiency frontier:

- Rule-based → high activity, lower value density
- Optimized → low activity, higher value density

- Integrated storage-efficiency assessment

This behavior is summarized in Table 12, which compares storage utilization and efficiency metrics across strategies and forecast horizons. The optimized strategy consistently demonstrates:

- lower cycling intensity,
- reduced throughput burden,
- higher value per cycle, and
- improved storage-control quality.

These results confirm that the optimized controller does not maximize the number of battery actions, but rather maximizes the value extracted per action.

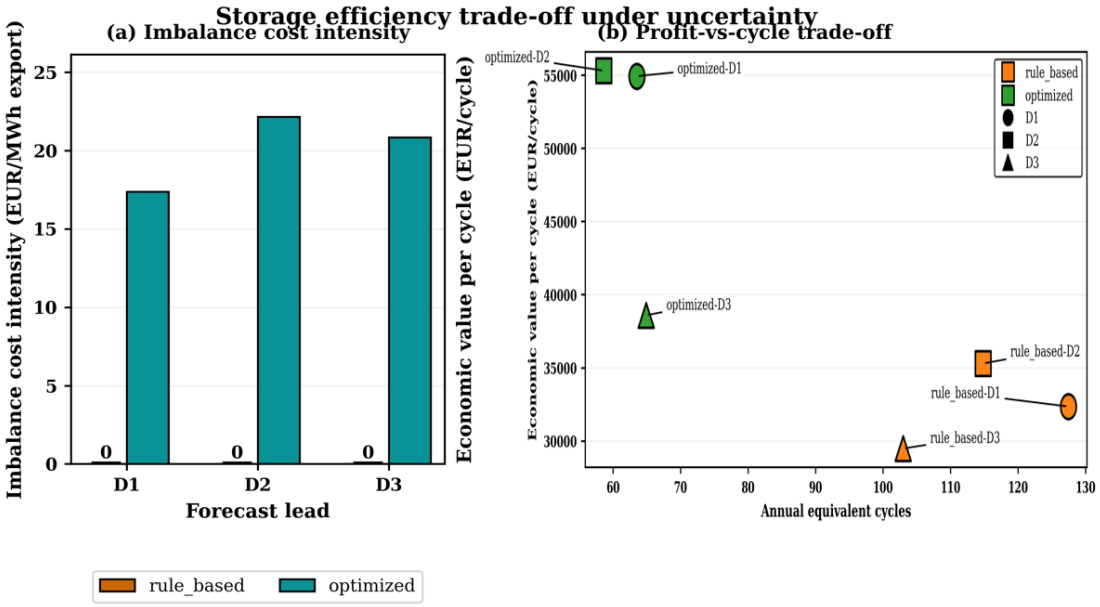

Figure 22. Storage efficiency trade-off

Table 12 Storage-efficiency comparison between rule-based and optimized strategies

Lead	Strategy	Annual Cycles	Throughput Intensity	Value per Cycle	Imbalance Cost Intensity	Storage-Control Quality	Long-Term Storage Efficiency
D1	Rule-based	High	Higher	Lower	0	Lower	Lower

D1	Opti-mized	Lower	Lower	Higher	Positive	Higher	Higher
D2	Rule-based	High	Higher	Lower	0	Lower	Lower
D2	Opti-mized	Lower	Lower	Higher	Positive	Higher	Higher
D3	Rule-based	High	Higher	Lower	0	Lower	Lower
D3	Opti-mized	Lower	Lower	Higher	Positive	Higher	Higher

Interpretation

This section fundamentally reframes the evaluation of PV–BESS operation. If performance is measured solely by total annual profit or export, the optimized strategy does not dominate. However, when evaluated through a decision-oriented lens, it becomes clear that the optimized framework enables more efficient and disciplined use of storage under uncertainty.

Thus, the primary contribution of the proposed approach is not increased activity, but improved quality of storage utilization, where fewer decisions produce higher value and lower system stress.

5.5.6 Strategic Benchmarking and Final Insight

The Phase-4 results confirm that no single strategy dominates across all performance dimensions, and that evaluation outcomes depend strongly on the chosen objective. From a financial perspective, the PV-only case provides the highest NPV due to the absence of storage-related costs. The rule-based strategy achieves the highest annual profit, driven by aggressive battery utilization and enhanced short-term value capture. However, this performance is associated with high cycling intensity and lower storage-use efficiency. The optimized strategy does not outperform in conventional metrics such as profit or export. Instead, its strength lies in decision-oriented performance,

characterized by lower cycling, controlled throughput, and higher value extracted per battery action. This reflects a fundamentally different operational philosophy based on selective and uncertainty-aware decision-making.

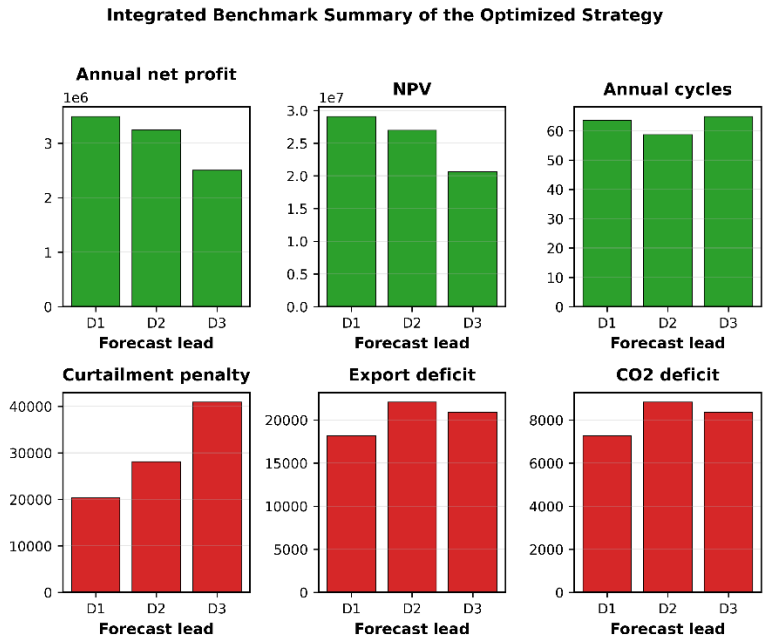

Figure 23. **Storage efficiency trade-off**

Fig. 23 provides an integrated view of the optimized strategy across financial, operational, and environmental dimensions. While profit and NPV decline with increasing forecast horizon, battery utilization remains stable and controlled. At the same time, higher curtailment, export deficit, and CO_2 deficit highlight that the strategy does not prioritize aggressive energy shifting, but rather balanced and risk-aware operation. These results demonstrate that conventional system-level metrics capture value quantity, but fail to reflect value quality. By incorporating storage-efficiency and decision-oriented indicators, the evaluation reveals that fewer, well-selected actions can yield more efficient and sustainable system behavior. Final insight:

PV-only is investment-efficient, rule-based is utilization-driven, and optimized is efficiency-driven. The main contribution of this work is therefore a shift from maximizing output to maximizing decision quality and storage-use efficiency under uncertainty.

5.6 Experimental Digital Twin Framework

This phase presents an experimental digital twin that extends the proposed framework from offline analysis to real-time, closed-loop operation. Recent literature has highlighted the growing role of digital twins in PV-system monitoring, forecasting, and operational optimization (Elnosh et al., 2026). It integrates forecasting, optimization, and system monitoring into a unified platform, enabling continuous, data-driven decision-making under uncertainty. The system combines real-time data ingestion, multi-horizon forecasting (D1–D3), decision-making, and monitoring within a single operational environment. Operating as a closed-loop system, the digital twin continuously updates decisions based on deviations between forecasts and actual conditions. Real-time inputs PV generation, battery state of charge (SOC), and market signals are processed alongside probabilistic forecasts to generate adaptive dispatch actions, ensuring both operational control and transparency. As illustrated on Fig. 24, the real-time operation layer translates forecast-informed decisions into actionable control signals. A multi-horizon live board (D1–D3) provides synchronized short- and longer-term system awareness, aligning immediate actions with expected future conditions. Continuous tracking of PV output, SOC trajectories, dispatch schedules, and market responses enables real-time validation, while next-interval forecasts support proactive adjustments. An action panel further ensures that charge, discharge, reserve, and idle decisions remain clearly defined and traceable. The data-driven decision layer (Fig. 25) enhances this process by integrating probabilistic forecasts with optimization outputs. Decisions are guided by forecast intervals, confidence levels, and uncertainty modes rather than deterministic values. The decision intelligence module links each action to its drivers PV availability, market signals, SOC constraints, and forecast uncertainty making system behavior interpretable. Additional features, including probabilistic readiness indicators and switching behavior analysis, provide insight into control stability and support performance evaluation.

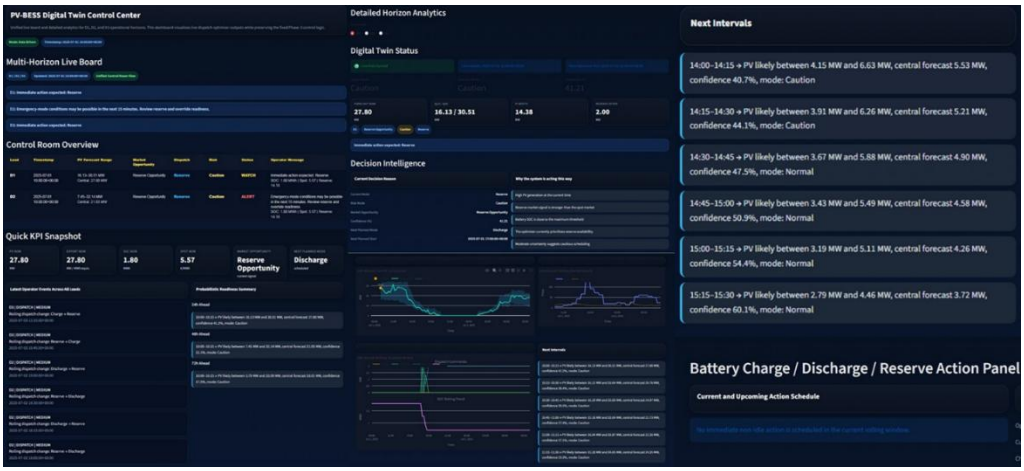

FIGURE 24 Real-Time Operation using experimental Digital Twin

Together, these layers form a deployable digital twin control system integrating forecasting, optimization, and execution within a unified framework. The platform provides end-to-end visibility of system states and dispatch actions, while its closed-loop structure ensures continuous alignment between forecasts, decisions, and operation. Operator interaction, including manual override and adaptive control modes, enhances robustness, and detailed logging supports traceability and performance auditing. Overall, the digital twin enables a shift from static scheduling to intelligent, real-time PV–BESS operation, combining continuous system awareness, multi-horizon probabilistic forecasting, and explainable decision-making.

A key insight is that performance depends not only on optimization accuracy but on the tight integration of forecasting, uncertainty handling, and control execution, enabling proactive and adaptive operation under real-world uncertainty. Additional results from this section are attached in Appendix 5

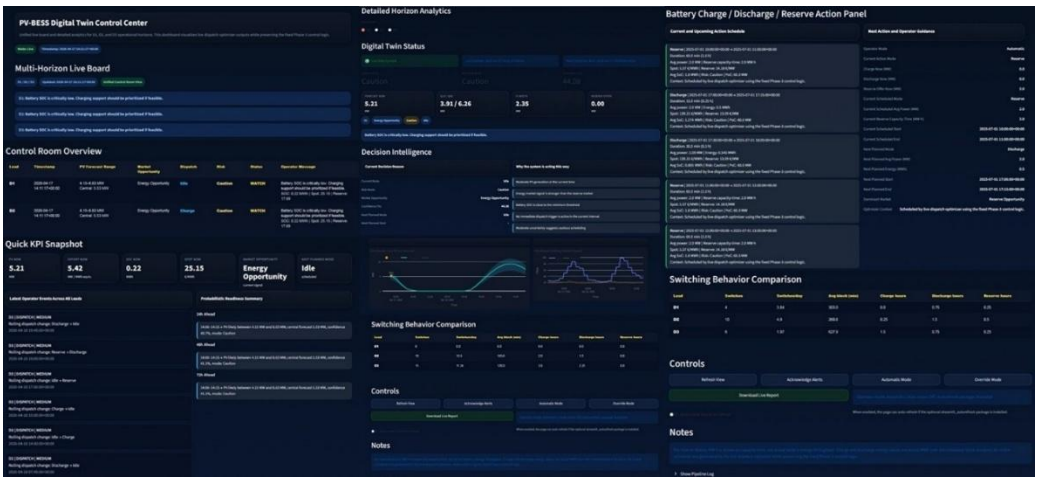

FIGURE 25 Data-driven Operation using experimental Digital Twin

6 Discussion and Conclusions

The performance of PV–BESS systems is fundamentally governed by the interaction between forecast uncertainty, storage flexibility, and market participation. As uncertainty increases from day-ahead (D1) to three-day-ahead (D3) horizons, system behavior systematically shifts from efficiency-driven operation toward risk mitigation. This transition results in reduced profitability, increased curtailment, and higher imbalance exposure. Importantly, this behavior is nonlinear, with the two-day-ahead horizon (D2) exhibiting the highest imbalance cost (≈450 k€) and regret (≈0.46 M€), indicating a critical regime of maximum sensitivity to forecast error. These findings confirm that forecast uncertainty is a dominant driver of both operational and economic outcomes. A clear trade-off emerges between economic performance and robustness. Deterministic strategies maximize short-term profit (up to ≈1.5 M€ annually) but remain highly exposed to extreme imbalance events, whereas the proposed risk-aware strategy reduces tail-risk exposure through conservative dispatch decisions. This results in a moderate reduction in profit (≈10–20%) but significantly improves system stability under uncertainty.

Although the optimized strategy does not achieve the highest short-term profit, it provides superior performance when evaluated from a decision-oriented and system-level perspective. Specifically, the optimized approach significantly reduces tail-risk exposure, stabilizes operational behavior under uncertainty, and improves long-term asset efficiency through reduced cycling. In contrast, rule-based strategies achieve higher profit primarily through aggressive utilization but remain highly vulnerable to forecast errors and extreme imbalance events. Therefore, optimality in this context is not defined by maximum profit alone, but by the ability to balance economic return, risk exposure, and system reliability under uncertainty. In this context, probabilistic forecasting plays a central role by enabling explicit quantification of uncertainty and supporting informed, risk-aware decision-making. This establishes a direct and operational linkage between forecasting outputs and system-level decisions.

The results further demonstrate that increased battery utilization does not necessarily translate into higher system value. The optimized strategy reduces cycling by

approximately 50% (≈60 cycles/year compared to ≈120 cycles/year for rule-based control) while maintaining competitive economic performance. This indicates that system value arises from selective, context-aware storage activation rather than continuous utilization. Reduced cycling also lowers degradation rates under the adopted modeling assumptions, highlighting the importance of efficiency-driven rather than utilization-driven operation. These findings confirm that forecast uncertainty not only shapes operational strategies but also indirectly influences long-term asset performance. From a planning perspective, the results consistently identify a compact BESS configuration (2 MW / 2 MWh) across the evaluated scenarios, achieving strong economic performance (≈ €4.18 M annual profit and ≈ €35 M net present value (NPV)) under controlled risk (≈ €2.38 M Conditional Value-at-Risk (CVaR)). This outcome indicates that system design is governed by marginal value saturation rather than capacity expansion, as larger storage capacities yield diminishing economic returns while increasing exposure to risk. Therefore, forecast uncertainty plays a critical role not only in operation but also in determining optimal system sizing. At the system level, the findings indicate that the long-term value of PV–BESS integration lies in selective, risk-aware utilization of flexibility rather than maximum energy throughput. Forecast degradation across horizons (RMSE increasing from ≈8.4 MW to ≈12.9 MW) leads to higher imbalance costs and reduced value capture, confirming that forecast quality directly impacts economic performance. The experimental digital twin further demonstrates the feasibility of extending the framework toward real-time operation, enabling adaptive, data-driven control through the integration of forecasting, optimization, and monitoring layers.

Despite these contributions, several limitations should be acknowledged. The analysis is based on a single Nordic PV system, which may limit generalizability to other climatic and market conditions. Furthermore, the dataset spans approximately 4.5 months (June–October 2025), capturing short-term variability but not full seasonal dynamics, particularly winter conditions typical of Nordic energy systems. As a result, annualized indicators such as NPV and long-term profitability are obtained through extrapolation and should be interpreted as indicative rather than definitive. Future work should

incorporate multi-seasonal or multi-year datasets to improve robustness and generalizability. Methodologically, the probabilistic forecasting framework relies on scenario reduction, which may not fully capture extreme events. The market modeling adopts simplified assumptions, and battery degradation is represented using a throughput-based approximation that does not explicitly account for temperature-dependent effects. This limitation is particularly relevant in Nordic climates, where low ambient temperatures can significantly influence battery performance and aging. In addition, the digital twin remains at a prototype stage and does not yet address full deployment challenges, including latency, cybersecurity, and hardware integration.

Overall, this study develops a unified, data-driven framework integrating probabilistic forecasting, risk-aware BESS sizing, and market-oriented operation within a single decision pipeline. The results demonstrate that probabilistic forecasting enhances operational decision-making by enabling uncertainty-aware control, that forecast uncertainty drives compact and robust storage sizing, and that effective PV–BESS operation requires balancing economic performance with risk exposure. Furthermore, the study quantifies the economic value of forecasting through its impact on imbalance cost, profitability, and system efficiency, while identifying selective storage utilization as a key operational principle.

In conclusion, the value of PV–BESS systems lies not in maximizing utilization, but in intelligently managing uncertainty through coordinated, risk-aware decisions. This work establishes a structured and decision-oriented framework for renewable-integrated energy systems and provides a foundation for extending toward real-time, adaptive operation through digital twin integration.

References

Abdalla, A. A., El Moursi, M. S., El-Fouly, T. H. M., & Al Hosani, K. H. (2026). A state-of-the-art review of adaptive, predictive, synergistic, and degradation-aware power variability smoothing techniques in photovoltaic power plants. Renewable and Sustainable Energy Reviews, 230, Article 116687. https://doi.org/10.1016/j.rser.2025.116687

Agakishiev, I., Härdle, W. K., Kopa, M., Kozmik, K., & Petukhina, A. (2025). Multivariate probabilistic forecasting of electricity prices with trading applications. Energy Economics, 141, Article 108008. https://doi.org/10.1016/j.eneco.2024.108008

Al-Dahidi, S., Madhiarasan, M., Al-Ghussain, L., Abubaker, A. M., Ahmad, A. D., Alrbai, M., Aghaei, M., Alahmer, H., Alahmer, A., Baraldi, P., & Zio, E. (2024). Forecasting solar photovoltaic power production: A comprehensive review and innovative data-driven modeling framework. Energies, 17(16), 4145. https://doi.org/10.3390/en17164145

Ali, A., Yousif, M., Numan, M., & Kazmi, S. A. A. (2025). Coordinated generation and transmission expansion planning with energy storage systems to facilitate high penetration of renewable energy. IEEE Access, 13, 176801–176812. https://doi.org/10.1109/ACCESS.2025.3617374

Allahvirdizadeh, Y., Galvani, S., & Shayanfar, H. (2021). Data clustering based probabilistic optimal scheduling of an energy hub considering risk-averse. International Journal of Electrical Power & Energy Systems, 128, Article 106774. https://doi.org/10.1016/j.ijepes.2021.106774

Amorim, W. C. S., Cupertino, A. F., Pereira, H. A., & Mendes, V. F. (2024). On sizing of battery energy storage systems for PV plants power smoothing. Electric Power Systems Research, 229, Article 110114. https://doi.org/10.1016/j.epsr.2024.110114

Assaad, C., Leon, J. P. M., Quick, J., Göçmen, T., Ghazouani, S., & Das, K. (2025). Enabling efficient sizing of hybrid power plants: A surrogate-based approach to energy management system modeling. Wind Energy Science, 10, 559–578. https://doi.org/10.5194/wes-10-559-2025

Baccino, F., & Santarelli, M. (2023). Advanced battery energy storage systems for hybrid power and energy management. In 7th International Hybrid Power Plants & Systems Workshop (HYB 2023) (pp. 90–95). https://doi.org/10.1049/icp.2023.1437

Bernecker, M., Sgarciu, S., Kan, X., Anvari, M., Riepin, I., & Müsgens, F. (2026). Adaptive robust optimization for European electricity system planning considering regional Dunkelflaute events. Applied Energy, 412, Article 127671. https://doi.org/10.1016/j.apenergy.2026.127671

Cao, Y., Wu, Q., Zhang, H., & Li, C. (2022). Optimal sizing of hybrid energy storage system considering power smoothing and transient frequency regulation. International Journal of Electrical Power & Energy Systems, 142, Article 108227. https://doi.org/10.1016/j.ijepes.2022.108227

Chen, Y., Li, X., & Zhao, S. (2024). A novel photovoltaic power prediction method based on a long short-term memory network optimized by an improved sparrow search algorithm. Electronics, 13(5), 993. https://doi.org/10.3390/electronics13050993

Conejo, A. J., Carrión, M., & Morales, J. M. (2010). Decision making under uncertainty in electricity markets. Springer. https://doi.org/10.1007/978-1-4419-7421-1

Čović, N., Pavić, I., & Pandžić, H. (2024). Multi-energy balancing services provision from a hybrid power plant: PV, battery, and hydrogen technologies. Applied Energy, 374, Article 123966. https://doi.org/10.1016/j.apenergy.2024.123966

Das, K., Hansen, A. D., Leon, J. P. M., Zhu, R., Gupta, M., Pérez-Rúa, J.-A., Long, Q., Pombo, D. V., Barlas, A., Gocmen, T., Sogachev, A., Koivisto, M., Cutululis, N. A., & Sørensen, P. E. (2025). Research challenges and opportunities of utility-scale hybrid power plants. WIREs Energy and Environment, 14, e70001. https://doi.org/10.1002/wene.70001

Deb, K. (2011). Multi-objective optimisation using evolutionary algorithms: An introduction. In L. Wang, A. Ng, & K. Deb (Eds.), Multi-objective evolutionary optimisation for product design and manufacturing. Springer. https://doi.org/10.1007/978-0-85729-652-8_1

Domínguez, R., & Vitali, S. (2021). Multi-chronological hierarchical clustering to solve capacity expansion problems with renewable sources. Energy, 227, Article 120491. https://doi.org/10.1016/j.energy.2021.120491

Ejuh Che, E., Roland Abeng, K., Iweh, C. D., Tsekouras, G. J., & Fopah-Lele, A. (2025). The impact of integrating variable renewable energy sources into grid-connected power systems: Challenges, mitigation strategies, and prospects. Energies, 18(3), 689. https://doi.org/10.3390/en18030689

Elnosh, A., Calais, M., & Parlevliet, D. (2026). A systematic literature review of digital twin research for photovoltaic systems: Trends, challenges, and opportunities. Renewable and Sustainable Energy Reviews, 226, Article 116326. https://doi.org/10.1016/j.rser.2025.116326

ENTSO-E. (2026, April 15). Electricity balancing and European balancing market framework. https://www.entsoe.eu/network_codes/eb/

ENTSO-E Transparency Platform. (2025). Transparency platform. https://transparency.entsoe.eu

Esmaeili Aliabadi, D., & Pinto, T. (2025). Modeling electricity markets and energy systems: Challenges and opportunities. Energies, 18(2), 245. https://doi.org/10.3390/en18020245

Finnish Meteorological Institute. (2025). Open data services. https://en.ilmatieteenlaitos.fi/open-data

Fingrid. (2025). Frequency containment reserves (FCR) data. https://www.fingrid.fi

Gao, Q., Chen, Y., Yang, D., Zhang, H., Yang, G., Shen, Y., Xia, X., & Liu, B. (2025). Firm power generation with photovoltaic overbuilding and pumped hydro storage. Energy, 324, Article 135800. https://doi.org/10.1016/j.energy.2025.135800

Gao, X., Chan, K. W., Xia, S., Zhou, B., Lu, X., & Xu, D. (2019). Risk-constrained offering strategy for a hybrid power plant consisting of wind power producer and electric vehicle aggregator. Energy, 177, 183–191.

Gardemeister, L., Liikkanen, J., Meriläinen, A., Kosonen, A., Ruusunen, J., Lindfors, A. V., Atlaskin, E., & Ahola, J. (2025). Spatial optimization of solar PV and wind power capacity in Finland and correlation analysis. International Journal of Electrical Power & Energy Systems, 173, Article 111386. https://doi.org/10.1016/j.ijepes.2025.111386

Glasserman, P. (2003). Monte Carlo methods in financial engineering. Springer. https://doi.org/10.1007/978-0-387-21617-1

Holttinen, H., Lindroos, T. J., Lehtilä, A., Koljonen, T., Kiviluoma, J., & Korpås, M. (2025). Estimating the CO2 impacts of wind energy in the transition towards carbon-neutral energy systems. Energies, 18(6), 1548. https://doi.org/10.3390/en18061548

Hofbauer, L., McDowall, W., & Pye, S. (2022). Challenges and opportunities for energy system modelling to foster multi-level governance of energy transitions. Renewable and Sustainable Energy Reviews, 161, Article 112330. https://doi.org/10.1016/j.rser.2022.112330

Iheanetu, K. J. (2022). Solar photovoltaic power forecasting: A review. Sustainability, 14(24), 17005. https://doi.org/10.3390/su142417005

International Energy Agency. (2019). Status of power system transformation 2019. https://www.iea.org/reports/status-of-power-system-transformation-2019

International Energy Agency. (2023). Electricity market report 2023. https://www.iea.org/reports/electricity-market-report-2023

International Energy Agency. (2024). Renewables 2023. https://www.iea.org/reports/renewables-2023

International Energy Agency. (2024). Renewables 2024. https://www.iea.org/reports/renewables-2024

International Energy Agency. (2025). Renewables 2025: Analysis and forecast to 2030. https://www.iea.org/reports/renewables-2025

International Renewable Energy Agency. (2024, November). World energy transitions outlook 2024: 1.5°C pathway. https://www.irena.org/publications/2024/Nov/World-Energy-Transitions-Outlook-2024

Jadidoleslam, M. (2025). Risk-constrained participation of virtual power plants in day-ahead energy and reserve markets based on multi-objective operation of active distribution network. *Scientific Reports, 15*, 9145. https://doi.org/10.1038/s41598-025-93688-w

Karrari, S., Ludwig, N., De Carne, G., & Noe, M. (2022). Sizing of hybrid energy storage systems using recurring daily patterns. *IEEE Transactions on Smart Grid, 13*(4), 3290–3300. https://doi.org/10.1109/TSG.2022.3156860

Lappalainen, K., & Valkealahti, S. (2022). Sizing of energy storage systems for ramp rate control of photovoltaic strings. *Renewable Energy, 196*, 1366–1375. https://doi.org/10.1016/j.renene.2022.07.069

Lindberg, O., Zhu, R., & Widén, J. (2024). Quantifying the value of probabilistic forecasts when trading renewable hybrid power parks in day-ahead markets: A Nordic case study. *Renewable Energy, 237*, Article 121617. https://doi.org/10.1016/j.renene.2024.121617

Liu, Y., Zhong, Y., & Tang, C. (2023). Optimal sizing of photovoltaic/energy storage hybrid power systems: Considering output characteristics and uncertainty factors. *Energies, 16*(14), 5549. https://doi.org/10.3390/en16145549

Liu, Y., Zhong, Y., & Tang, C. (2023). Sizing optimization of a photovoltaic hybrid energy storage system based on long time-series simulation considering battery life. *Applied Sciences, 13*(15), 8693. https://doi.org/10.3390/app13158693

Luo, C., Al-Messabi, N., Kuang, Z., Ma, C., El-Amin, I., Deng, H., & Li, Y. (2025). Photovoltaic system modeling and forecasting techniques: A survey. *Engineering Applications of Artificial Intelligence, 162*, Article 112516. https://doi.org/10.1016/j.engappai.2025.112516

Maciejowska, K., Serafin, T., & Uniejewski, B. (2024). Probabilistic forecasting with a hybrid Factor-QRA approach: Application to electricity trading. *Electric Power Systems Research, 234*, Article 110541. https://doi.org/10.1016/j.epsr.2024.110541

Meng, A., Wang, P., Zhai, G., Zeng, C., Chen, S., Yang, X., & Yin, H. (2022). Electricity price forecasting with high penetration of renewable energy using attention-based LSTM network trained by crisscross optimization. *Energy, 254*, Article 124212. https://doi.org/10.1016/j.energy.2022.124212

Mottola, F., Proto, D., & Russo, A. (2024). Probabilistic planning of a battery energy storage system in a hybrid microgrid based on the Taguchi arrays. *International Journal of Electrical Power & Energy Systems, 157*, Article 109886. https://doi.org/10.1016/j.ijepes.2024.109886

Mystakidis, A., Koukaras, P., Tsalikidis, N., Ioannidis, D., & Tjortjis, C. (2024). Energy forecasting: A comprehensive review of techniques and technologies. *Energies, 17*(7), 1662. https://doi.org/10.3390/en17071662

NASA POWER. (2025). NASA POWER data access viewer. https://power.larc.nasa.gov

Nord Pool. (2025). Day-ahead market data. https://www.nordpoolgroup.com

Pavlík, M., Kurimský, F., & Ševc, K. (2025). Renewable energy and price stability: An analysis of volatility and market shifts in the European electricity sector (2015–2025). *Applied Sciences, 15*(12), 6397. https://doi.org/10.3390/app15126397

Rezaeimozafar, M., Barrett, E., Monaghan, R. F. D., & Duffy, M. (2024). A stochastic method for behind-the-meter PV-battery energy storage systems sizing with degradation minimization by limiting battery cycling. *Journal of Energy Storage, 86*, Article 111199. https://doi.org/10.1016/j.est.2024.111199

Rockafellar, R. T., & Uryasev, S. (2000). Optimization of conditional value-at-risk. *Journal of Risk, 2*, 21–42. https://doi.org/10.21314/JOR.2000.038

Ruan, P., Su, Q., Zhang, L., Luo, J., Diao, Y., Xie, L., & Zheng, H. (2025). Optimal siting and sizing of hybrid energy storage systems in high-penetration renewable energy systems. *Energies, 18*(9), 2196. https://doi.org/10.3390/en18092196

Ruiz-Abellón, M. C., Fernández-Jiménez, L. A., Guillamón, A., & Gabaldón, A. (2024). Applications of probabilistic forecasting in demand response. *Applied Sciences, 14*(21), 9716. https://doi.org/10.3390/app14219716

Shapiro, A., Dentcheva, D., & Ruszczyński, A. (2021). *Lectures on stochastic programming: Modeling and theory* (3rd ed.). Society for Industrial and Applied Mathematics. https://doi.org/10.1137/1.9781611976595

Smyl, S., Pełka, P., & Dudek, G. (2026). Probabilistic multi-regional solar power forecasting with any-quantile recurrent neural networks. *arXiv*, Article abs/2602.05660.

Soroudi, A. (2017). *Power system optimization modeling in GAMS*. Springer. https://doi.org/10.1007/978-3-319-62350-4

Sun, M., Feng, C., & Zhang, J. (2020). Probabilistic solar power forecasting based on weather scenario generation. *Applied Energy, 266*, Article 114823. https://doi.org/10.1016/j.apenergy.2020.114823

Sweeney, C., Bessa, R. J., Browell, J., & Pinson, P. (2020). The future of forecasting for renewable energy. *WIREs Energy and Environment, 9*, e365. https://doi.org/10.1002/wene.365

Talvi, M., & Lappalainen, K. (2024). Sizing of energy storage systems for different levels of PV and wind power in combined PV-wind power plants. In *41st European Photovoltaic Solar Energy Conference and Exhibition (EU PVSEC) proceedings*. https://doi.org/10.4229/EUPVSEC2024/5DV.2.4

Teixeira, R., Cerveira, A., Pires, E. J. S., & Baptista, J. (2024). Advancing renewable energy forecasting: A comprehensive review of renewable energy forecasting methods. *Energies, 17*(14), 3480. https://doi.org/10.3390/en17143480

Tkac, M., Kajanova, M., & Bracinik, P. (2023). A review of advanced control strategies of microgrids with charging stations. *Energies, 16*(18), 6692. https://doi.org/10.3390/en16186692

Uryasev, S., & Rockafellar, R. T. (2001). Conditional value-at-risk: Optimization approach. In S. Uryasev & P. M. Pardalos (Eds.), *Stochastic optimization: Algorithms and applications* (Vol. 54). Springer. https://doi.org/10.1007/978-1-4757-6594-6_17

Visser, L. R., AlSkaif, T. A., Khurram, A., Kleissl, J., & van Sark, W. G. H. J. M. (2024). Probabilistic solar power forecasting: An economic and technical evaluation of an optimal market bidding strategy. *Applied Energy, 370*, Article 123573. https://doi.org/10.1016/j.apenergy.2024.123573

Wang, J., Zhou, Y., Zhang, Y., Lin, F., & Wang, J. (2024). Risk-averse optimal combining forecasts for renewable energy trading under CVaR assessment of forecast errors. *IEEE Transactions on Power Systems, 39*(1), 2296–2309. https://doi.org/10.1109/TPWRS.2023.3268337

Wang, Z., Wu, S., Huang, Y., Liu, R., & Liu, X. (2026). A comprehensive review of deep learning for solar nowcasting: Enhancing accuracy, reliability, and interpretability. *Applied Energy, 407*, Article 127378. https://doi.org/10.1016/j.apenergy.2026.127378

Wipplinger, E. (2007). Philippe Jorion: Value at risk – The new benchmark for managing financial risk. *Financial Markets and Portfolio Management, 21*, 397–398. https://doi.org/10.1007/s11408-007-0057-3

Xiong, B., Chen, Y., Chen, D., Fu, J., & Zhang, D. (2025). Deep probabilistic solar power forecasting with Transformer and Gaussian process approximation. *Applied Energy, 382*.

Xuan, A., Shen, X., Guo, Q., & Sun, H. (2021). A conditional value-at-risk based planning model for integrated energy system with energy storage and renewables. *Applied Energy, 294*, Article 116971. https://doi.org/10.1016/j.apenergy.2021.116971

Yang, G., Yang, D., Liu, B., & Zhang, H. (2024). The role of short- and long-duration energy storage in reducing the cost of firm photovoltaic generation. *Applied Energy, 374*, Article 123914. https://doi.org/10.1016/j.apenergy.2024.123914

Yang, Z., Kong, D., Chen, Z., Zhang, Z., Du, D., & Zhu, Z. (2025). A data-driven battery energy storage regulation approach integrating machine learning forecasting models for enhancing building energy flexibility A case study of a net-zero carbon building in China. *Buildings, 15*(19), 3611. https://doi.org/10.3390/buildings15193611

Zhang, X., Li, Y., Li, T., Gui, Y., Sun, Q., & Gao, D. W. (2024). Digital twin empowered PV power prediction. *Journal of Modern Power Systems and Clean Energy, 12*(5), 1472–1483. https://doi.org/10.35833/MPCE.2023.000351

Zhu, R., Das, K., Sørensen, P. E., & Hansen, A. D. (2025). A review on energy management system for grid-connected utility-scale renewable hybrid power plants. *WIREs Energy and Environment, 14*, e70004. https://doi.org/10.1002/wene.70004

Zhu, R., Murcia Leon, J. P., Friis-Møller, M., Gupta, M., & Das, K. (2026). Optimal sizing of renewable hybrid power plants considering component reliability as a multi-discipline optimization under uncertainty. *Applied Energy, 404*, Article 127138. https://doi.org/10.1016/j.apenergy.2025.127138

Appendices

Appendix 1. Additional information and interpretations of problem formulation

➢ Appendix A – Probabilistic Modeling and Scenario Generation

This appendix provides additional details on the probabilistic representation of photovoltaic (PV) generation and the construction of representative scenarios used in the planning and operational optimization framework.

The probabilistic forecasting model generates a set of conditional quantiles, $\hat{Q}_{\tau,t}$, which describe the distribution of PV generation under uncertainty at time t. The selected quantile range ($q05$–$q95$) captures both typical and extreme operating conditions, enabling explicit representation of variability driven by meteorological uncertainty.

To enable tractable integration into downstream optimization, the quantile outputs are reduced to a representative scenario set. In particular, three trajectories are constructed:

$$Q_t^- = q10_t, Q_t^0 = q50_t, Q_t^+ = q90_t \tag{1.1}$$

corresponding to pessimistic, median, and optimistic PV generation conditions, respectively. These scenarios preserve the main uncertainty structure while significantly reducing computational complexity. Unless otherwise specified, equal scenario probabilities are assumed:

$$p_s = \frac{1}{3}, s \in \{Q^-, Q^0, Q^+\} \tag{1.2}$$

This reduced scenario representation is used consistently in both the risk-aware planning stage and the rolling operational dispatch model. Such scenario reduction approaches are widely adopted in stochastic energy system optimization because they provide a practical balance between uncertainty representation and computational tractability (Sun et al., 2020)

- **Appendix B – Imbalance and Risk Modeling**

This appendix provides additional details on the modeling of imbalance costs and the incorporation of risk measures in the proposed framework.

Imbalance arises from deviations between scheduled (committed) and actual electricity export. In the proposed model, the system submits a scheduled export P_t^{sched}, while the actual export depends on scenario-based PV generation and battery operation. The realized export under scenario $s$is given by:

$$P_{s,t}^{actual} = P_{s,t}^{PV} - P_{s,t}^{curt} - P_{ch,t} + P_{dis,t} \tag{1.3}$$

The resulting deviation is defined as:

$$\Delta_{s,t} = P_{s,t}^{actual} - P_t^{sched} \tag{1.4}$$

This deviation is decomposed into surplus and deficit components:

$$\Delta_{s,t}^{+} = \max(0, \Delta_{s,t}), \Delta_{s,t}^{-} = \max(0, -\Delta_{s,t}) \tag{1.5}$$

where $\Delta_{s,t}^{+}$represents overproduction and $\Delta_{s,t}^{-}$represents underproduction.

The imbalance cost is defined as:

$$C_{s,t}^{imb} = \Delta_{s,t}^{-} \cdot \pi_t^{up} + \Delta_{s,t}^{+} \cdot \pi_t^{down} \tag{1.6}$$

where $\pi_t^{up}$and π_t^{down}denote the upward and downward regulation prices. In the absence of explicit imbalance market data, these prices are approximated as:

$$\pi_t^{up} = \gamma^{up} \cdot \pi_{spot,t}, \pi_t^{down} = \gamma^{down} \cdot \pi_{spot,t} \tag{1.7}$$

with $\gamma^{up} > 1$and $\gamma^{down} < 1$, reflecting the higher penalty associated with underproduction.

To quantify extreme economic losses under uncertainty, Conditional Value-at-Risk (CVaR) is incorporated within the optimization framework. The scenario loss is defined as:

$$L_s = -\Pi_s \tag{1.8}$$

and the CVaR measure is given by:

$$\text{CVaR}_\beta = \eta + \frac{1}{1-\beta}\sum_s p_s\, z_s \tag{1.9}$$

subject to:

$$z_s \geq L_s - \eta, z_s \geq 0 \tag{1.10}$$

where $\beta$is the confidence level, ηrepresents the Value-at-Risk (VaR), and $z_s$captures excess loss beyond VaR.

This formulation explicitly links forecast uncertainty to economic penalties and enables scenario-dependent evaluation of operational risk. The integration of CVaR ensures that dispatch decisions remain robust against extreme imbalance events while maintaining overall economic performance.

- **Appendix C – Battery Modeling and Degradation Representation**

This appendix provides additional details on the battery energy storage system (BESS) modeling approach used in the study.

The battery operation is represented using linear state-of-charge (SOC) dynamics, which describe the temporal evolution of stored energy:

$$SOC_{t+1} = SOC_t + \eta_c P_{ch,t}\Delta t - \frac{P_{dis,t}}{\eta_d}\Delta t \tag{1.11}$$

where $P_{ch,t}$and $P_{dis,t}$denote charging and discharging power, and η_c, $\eta_d$are the corresponding efficiencies.

The battery operates within physical and operational limits:

$$SOC^{min} \leq SOC_t \leq SOC^{max} \quad (1.12)$$

$$0 \leq P_{ch,t} \leq P_b^{max}, 0 \leq P_{dis,t} \leq P_b^{max} \quad (1.13)$$

To ensure feasible operation while maintaining computational tractability, a linear relaxation is adopted:

$$P_{ch,t} + P_{dis,t} \leq P_b^{max} \quad (1.14)$$

This avoids simultaneous extreme charging and discharging without introducing binary variables, enabling efficient large-scale optimization.

Battery degradation is modeled using an energy throughput-based approach, where cumulative charge and discharge energy represent cycling intensity:

$$E_t^{through} = (P_{ch,t} + P_{dis,t})\Delta t \quad (1.15)$$

$$C_{deg,t} = c_{deg} \cdot E_t^{through} \quad (1.16)$$

where $c_{deg}$is the degradation cost coefficient. This formulation captures the dominant effect of cycling on battery wear and is widely adopted in system-level optimization studies (Yang et al., 2024; Amorim et al., 2024).

Overall, this modeling approach provides a balance between physical realism and computational efficiency, making it suitable for scenario-based operational optimization under uncertainty.

This appendix provides additional clarification on the modeling of electricity market participation within the proposed PV–BESS framework.
The system simultaneously participates in **energy and reserve markets**, enabling value stacking. Energy market participation is based on spot price signals, where revenue is obtained from scheduled energy export:

$$R_{energy,t} = E_t^{sched} \cdot \pi_{spot,t} \quad (1.17)$$

Reserve provision is constrained by both battery power capacity and state-of-charge (SOC) availability:

$$0 \leq R_t \leq P_b^{max}, P_{dis,t} + R_t \leq P_b^{max}, SOC_t \geq SOC^{min} + R_t \Delta t \quad (1.18)$$

and generates additional revenue:

$$R_{reserve,t} = R_t \cdot \pi_{reserve,t} \quad (1.19)$$

The framework distinguishes between **scheduled and actual export**, enabling realistic modeling of market commitments:

$$E_t^{sched} = P_t^{sched} \Delta t, E_{s,t}^{act} = P_{s,t}^{actual} \Delta t \quad (1.20)$$

Deviations between scheduled and realized export result in imbalance:

$$\Delta_{s,t} = P_{s,t}^{actual} - P_t^{sched} \quad (1.21)$$

which is penalized through asymmetric imbalance pricing:

$$C_{s,t}^{imb} = \Delta_{s,t}^{-} \cdot \pi_t^{up} + \Delta_{s,t}^{+} \cdot \pi_t^{down} \quad (1.22)$$

where upward regulation prices penalize deficits more strongly than surpluses.
Curtailment represents unused renewable generation due to system or grid constraints and is treated as an economic loss:

$$C_{curt,t} = c_{curt} \cdot E_{s,t}^{curt} \quad (1.23)$$

These formulations explicitly link forecast uncertainty, operational decisions, and market outcomes. By integrating energy trading, reserve provision, imbalance penalties, and curtailment losses, the framework provides a realistic and economically consistent representation of PV–BESS operation in electricity markets.

- **Appendix E – Optimization and Solver Implementation**

This appendix provides additional details on the optimization framework and its numerical implementation.

The operational dispatch problem is formulated as a **linear programming (LP) optimization problem**, where the objective combines expected economic performance and risk:

$$\max(\mathbb{E}[\Pi] - \lambda \cdot \text{CVaR}) \quad (1.24)$$

subject to system dynamics, operational constraints, and market participation rules defined in the main formulation.

To reflect real-world operation, the problem is solved using a **rolling-horizon framework**, where decisions are optimized over a finite horizon (e.g., 24 hours) but only the first control step is implemented. The system state is then updated, and the optimization is repeated at the next time step. This enables continuous adaptation to updated forecasts and system conditions, consistent with practical energy management strategies (Conejo et al., 2010).

At each step:

- The **state-of-charge (SOC)** is carried forward from the previous solution
- Updated forecasts and market signals are incorporated
- A new optimization problem is solved

The model is implemented using the PuLP library and solved with high-performance LP solvers such as HiGHS or CBC. The formulation remains linear by:

- Relaxing binary charge/discharge constraints into convex constraints
- Using linear representations of imbalance and degradation costs
- Applying auxiliary variables for CVaR modeling

This ensures:

- **Computational efficiency** (fast solve times for large datasets)
- **Scalability** to long time horizons and multiple scenarios
- **Numerical stability** under varying operating conditions

In the planning stage (Phase-2), a similar optimization structure is applied across a discrete design space of battery configurations. Each candidate design is evaluated under multiple scenarios using:

- Expected profit
- Net Present Value (NPV)
- Conditional Value-at-Risk (CVaR)

This combined evaluation enables selection of a design that balances economic performance and robustness under uncertainty.

➢ Appendix F – Performance Metrics and Evaluation Details

This appendix provides additional clarification on the performance metrics used to evaluate the PV–BESS system across operational, economic, and risk dimensions.

Battery Utilization Metrics

Battery utilization is quantified using **energy throughput**:

$$E^{through} = \sum_{t} \left(P_{ch,t} + P_{dis,t}\right) \Delta t \qquad (1.25)$$

and **equivalent full cycles**:

$$N_{cycles} = \frac{E^{through}}{2E_b^{max}} \tag{1.26}$$

These metrics capture the intensity of battery usage and serve as a proxy for degradation and lifecycle impact.

Energy and System Output Metrics

System performance is further evaluated using:

- Total scheduled export: $\sum_t E_t^{sched}$
- Total actual export: $\sum_{s,t} p_s \; E_{s,t}^{act}$
- Total curtailment: $\sum_{s,t} p_s \; E_{s,t}^{curt}$
- Mismatch volumes: $\sum_{s,t} p_s \; \Delta_{s,t}^{+}$, $\sum_{s,t} p_s \; \Delta_{s,t}^{-}$

where $p_s$represents scenario probabilities.

Economic Performance Metrics

The primary economic indicator is **net profit**, computed as:

$$\Pi = \sum_t \left(R_{energy,t} + R_{reserve,t} - C_{imb,t} - C_{deg,t} - C_{curt,t}\right) \tag{1.27}$$

In the stochastic setting, this is evaluated in expectation across scenarios:

$$\mathbb{E}[\Pi] = \sum_s p_s \, \Pi_s \tag{1.28}$$

Additional revenue and cost components include:

- Energy revenue
- Reserve revenue
- Imbalance cost
- Degradation cost
- Curtailment penalty

Risk Metrics

To quantify downside risk, **Conditional Value-at-Risk (CVaR)** is used:

$$\text{CVaR}_{\beta} = \eta + \frac{1}{1-\beta}\sum_{s} p_s z_s \tag{1.29}$$

subject to:

$$z_s \geq L_s - \eta, z_s \geq 0 \tag{1.30}$$

where:

- $L_s = -\Pi_s$is scenario loss
- $\beta$is the confidence level
- $\eta$is the Value-at-Risk (VaR)

This metric captures expected losses under extreme adverse scenarios.

Interpretation

Together, these metrics enable:

- Evaluation of **operational efficiency** (throughput, cycles, SOC behavior)
- Assessment of **economic performance** (profitability and revenue streams)
- Quantification of **risk exposure** (CVaR and imbalance costs)

This integrated evaluation framework ensures consistent comparison across different control strategies and forecast horizons while maintaining alignment with real-world system operation and market participation.

Appendix 2. Detailed Formulation and Extended Results of Phase-1

- **Probabilistic Forecasting Model Details**

The probabilistic forecasting framework is implemented using **quantile regression** to estimate the conditional distribution of photovoltaic (PV) generation. Instead of producing a single deterministic forecast, the model generates multiple conditional quantiles $\hat{Q}_{\tau,t}$, which collectively approximate the predictive distribution of PV output under uncertainty.

The quantile estimates are obtained by minimizing the **pinball loss function**:

$$L_\tau(y_t, \hat{y}_t) = \begin{cases} \tau(y_t - \hat{y}_t), & y_t \geq \hat{y}_t \\ (1-\tau)(\hat{y}_t - y_t), & y_t < \hat{y}_t \end{cases} \quad (2.1)$$

where:

- y_t: observed PV output
- $\hat{y}_t$: predicted quantile
- $\tau \in (0,1)$: quantile level

The model is trained independently for multiple quantiles (e.g., 0.05, 0.10, 0.50, 0.90, 0.95), enabling the construction of prediction intervals and capturing forecast uncertainty.

- **Scenario Generation from Quantile Forecasts**

To enable decision-making under uncertainty, the probabilistic forecasts are transformed into representative scenarios.

A **non-parametric scenario generation approach** is adopted:

- Number of samples: $N = 4000$
- Sampling method: inverse transform sampling
- Distribution: reconstructed from quantile forecasts

These samples represent possible realizations of PV generation and are used to evaluate expected performance and tail-risk behavior.

For computational tractability, the full scenario set is reduced to a small number of representative trajectories (e.g., pessimistic, median, optimistic), preserving the uncertainty structure while enabling efficient optimization (Sun et al., 2020).

- **Decision Optimization Formulation**

In Phase-1, the objective is to determine the optimal **scheduled export decision**. The decision variable $b_t$represents the committed export, which corresponds to P_t^{sched}in the operational formulation of Phase-3.

- **Expected-Value Policy**

The expected-value-based decision minimizes the average imbalance cost:

$$b_t^{exp} = \arg\min_{b \in B} \mathbb{E}[L_t(b)] \tag{2.2}$$

- **Risk-Aware Policy (CVaR-Based)**

To control extreme losses, a risk-aware formulation is adopted:

$$b_t^{RC} = \arg\min_{b \in B} (\mathbb{E}[L_t(b)] + \lambda \cdot \text{CVaR}_{\alpha}(L_t(b))) \tag{2.2}$$

where:

- α: confidence level
- λ: risk-aversion parameter
- $L_t(b)$: loss function

This formulation balances expected performance and robustness under uncertainty.

- **Decision Space**

The feasible decision space is discretized as:

$$B = \{b_1, b_2, \dots, b_G\}, G = 61 \tag{2.3}$$

uniformly spanning the feasible generation range. This discretization enables tractable evaluation of candidate decisions.

- **Imbalance Modeling and Loss Function**

The imbalance between committed and actual generation is defined as:

$$\Delta_t = y_t - b_t \tag{2.4}$$

and decomposed into deficit and surplus components:

$$d_t = \max(b_t - y_t, 0), s_t = \max(y_t - b_t, 0) \tag{2.5}$$

The loss function is defined as:

$$L_t = \lambda_{reserve} \cdot d_t + \lambda_{spill} \cdot s_t \tag{2.6}$$

Two penalty configurations are considered:

Case	$\lambda_{reserve}$	λ_{spill}
Reliability-oriented	3	1
Value-oriented	1	3

This formulation reflects asymmetric market penalties, where deficit conditions are typically more costly than surplus.

- **Performance Metrics**

The decision policies are evaluated using standard forecasting and risk metrics:

- **Root Mean Square Error (RMSE)**

$$\text{RMSE} = \sqrt{\frac{1}{N}\sum_{t=1}^{N}(y_t - b_t)^2} \tag{2.7}$$

- **Mean Absolute Error (MAE)**

$$\text{MAE} = \frac{1}{N}\sum_{t=1}^{N} | y_t - b_t | \tag{2.8}$$

- **Failure Rate**

$$\text{Failure Rate} = P(b_t > y_t) \tag{2.9}$$

- **Conditional Value-at-Risk (CVaR)**

$$\text{CVaR}_\alpha = \mathbb{E}[L \mid L \geq \text{VaR}_\alpha] \tag{2.10}$$

These metrics enable evaluation of both average performance and extreme risk exposure.

- **Additional Diagnostic Results**
- **Forecast Calibration**

Prediction interval coverage analysis shows:

- D1 closely matches nominal coverage (≈90%)
- D3 slightly overestimates uncertainty, indicating conservative forecasts

- **Error Distribution Behavior**

Empirical error distributions exhibit:

- Right-skewness due to dominance of deficit events
- Increasing tail heaviness with forecast horizon

- **Risk Distribution Characteristics**

Scenario-based analysis reveals:

- Convex relationship between risk and cost
- Increasing dispersion from D1 to D3
- Concentration of extreme losses under deterministic policies

- **Parameter Justification**

The selected parameters are grounded in established literature:

- Monte Carlo sampling → Glasserman (2003)
- CVaR formulation → Rockafellar & Uryasev (2000)
- Risk-aversion trade-off → Deb (2011)
- Power system applications → Conejo et al. (2010); Soroudi (2017)

These choices ensure:

- Numerical stability
- Computational efficiency
- Realistic representation of operational uncertainty

- **Summary of Appendix**

This appendix provides:

- A complete probabilistic forecasting formulation
- Scenario generation methodology
- Decision optimization framework
- Detailed performance metrics

The derived decision policies form the conceptual foundation for the multi-scenario, risk-aware operational optimization developed in Phase-3, where scheduled export decisions are integrated with battery operation and market participation.

Appendix 3. Extended Results for Phase-2: Risk-Aware BESS Planning

- **Design Space and Candidate Configurations**

The BESS planning problem is solved over a discrete design space including:

- **Power capacity (P):** 0–30 MW (grid-based combinations)
- **Energy capacity (E):** corresponding MWh levels
- **Duration:** derived (0–4 hours equivalent)
- **Architectures:**
    - Aggregated central
    - Block central
    - Block distributed

A total of **~2000+ candidate configurations per scenario** are evaluated across:

- Forecast horizons: **D1, D2, D3**
- Forecast regimes: **Qminus, Q0, Qplus**

Each configuration is assessed using:

- Expected profit
- Net Present Value (NPV)
- CVaR (95%)
- Operational feasibility under PoC constraint

- **Extended Optimal Design Landscape (Fig. 11)**

Additional observations from Figure 11:

- Two dominant configurations emerge:
    - **(0,0): No BESS (~288 cases)**
    - **(2 MW / 2 MWh): Optimal BESS (~1656 cases)**
- Strong convergence behavior:
    - Power → **2 MW**
    - Energy → **2 MWh**
    - Duration → **1 hour**
- Architecture selection shows **no dominant preference**, indicating:

System performance is primarily driven by sizing rather than topology.

- **Economic–Risk Distribution (Fig. 12)**

Extended interpretation:

- **NPV range:** €30M – €35M
- **CVaR range:** €1.7M – €3.2M/year
- **Profit range:** €3.5M – €4.2M/year

Distribution characteristics:

- Profit distribution is **right-skewed**
- CVaR distribution shows **multi-modal behavior**
- Higher NPV corresponds to **increased tail risk**

Key insight:

Economic gains increase with risk exposure, confirming a structured trade-off.

- **Sensitivity Across Forecast Regimes**

Appendix Table 1 Sensitivity Across Forecast Regimes

Regime	**NPV (M€)**	**Risk Behavior**
Qminus	~33–34	Lower risk
Q0	~34–35	Balanced
Qplus	~35	Higher CVaR

Interpretation:

- Conservative regime reduces risk but limits value
- Optimistic regime maximizes profit with increased exposure
- Optimal design remains **unchanged across regimes**

- **Sensitivity Across Forecast Horizons**

Appendix Table 2 Sensitivity Across Forecast Regimes

Horizon	**NPV (M€)**	**Observation**
D1	~35	Best performance

D2	~32	Forecast degradation impact
D3	~35	Conservative recovery

Key insight:

Optimal sizing is robust to horizon changes despite uncertainty growth.

- **Architecture and Block-Limit Sensitivity**

The impact of block export limits (5–8 MW) and architectural configurations is analyzed across three performance dimensions:

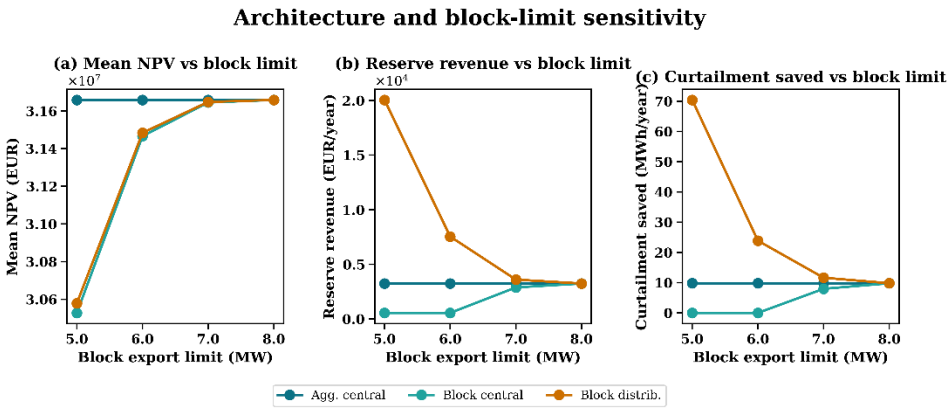

Appendix Figure 1 Architecture and block-limit sensitivity

- **NPV** increases from ~€30.5M to ~€31.6M as block limit increases from 5 MW to ≥7 MW, after which gains saturate
- **Reserve revenue** decreases significantly for distributed architectures (from ~€20k to ~€3k/year), indicating reduced reserve participation under relaxed constraints
- **Curtailment savings** drop sharply (≈70 → 10 MWh/year), reflecting diminishing marginal benefit of flexibility

Across all cases, the aggregated architecture exhibits stable performance, confirming that:

Block-limit relaxation improves system value up to a threshold, beyond which benefits become negligible

- **Grid Constraint and CAPEX Sensitivity**

The influence of grid constraints and investment cost is evaluated through PoC limits (60–80 MW) and CAPEX multipliers (0.8–1.2):

- **NPV increases modestly** (~€31.3M → €31.5M) with higher PoC limits
- **Expected profit improves slightly**, indicating marginal operational benefit
- **CVaR remains nearly constant (~€2.38M/year)**, confirming risk invariance to grid capacity
- **CAPEX sensitivity is regime-dependent**:
    - Qplus remains stable (~€33M → €33.1M)
    - Q0 decreases moderately (~€32.5M → €30M)
    - Qminus shows stronger decline (~€31.5M → €27M)

This demonstrates that:

Economic performance is moderately sensitive to constraints but strongly influenced by cost assumptions under conservative regimes

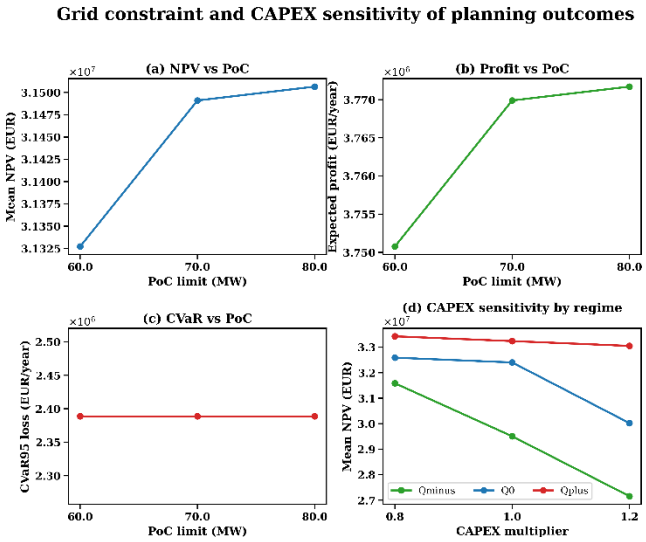

Appendix Figure 2 Grid constraint and CAPEX sensitivity

➢ **Robustness and Stability Analysis (Fig. 13)**

Additional findings:

- **Margin ratio distribution:**
    - Majority < 1 → minimal advantage of alternatives
- **Winner stability:**
    - 100% consistency across all evaluated blocks

- No competing near-optimal designs observed

The optimization landscape contains a **clear global optimum**, with negligible sensitivity to scenario variation.

- **Extended Optimal Configuration Details**

Appendix Table 3 Extended Optimal Congfiguration Details

Parameter	**Value**
Power (P)	2 MW
Energy (E)	2 MWh
Duration	1 hour
NPV	€35.03M
Expected Profit	€4.18M/year
CVaR (95%)	€2.38M/year
CAPEX	€640k

- **Interpretability of Planning Decisions**

Feature importance analysis using permutation importance and SHAP values reveals the dominant drivers of planning outcomes:

- **Forecast regime (Qplus)** is the most influential variable (~0.9 R^2 drop)
- **Lead time (D1)** is the second most important (~0.7 R^2 drop)
- Secondary factors:
  - Q0 and D2 contribute moderately
  - Qminus and D3 have minimal impact
- System/design parameters (block limit, PoC, architecture, CAPEX) show **negligible direct influence**

SHAP analysis confirms that:

- Higher forecast optimism (Qplus) increases NPV
- Shorter horizons (D1) improve decision quality
- Structural parameters act as **constraints rather than primary drivers**

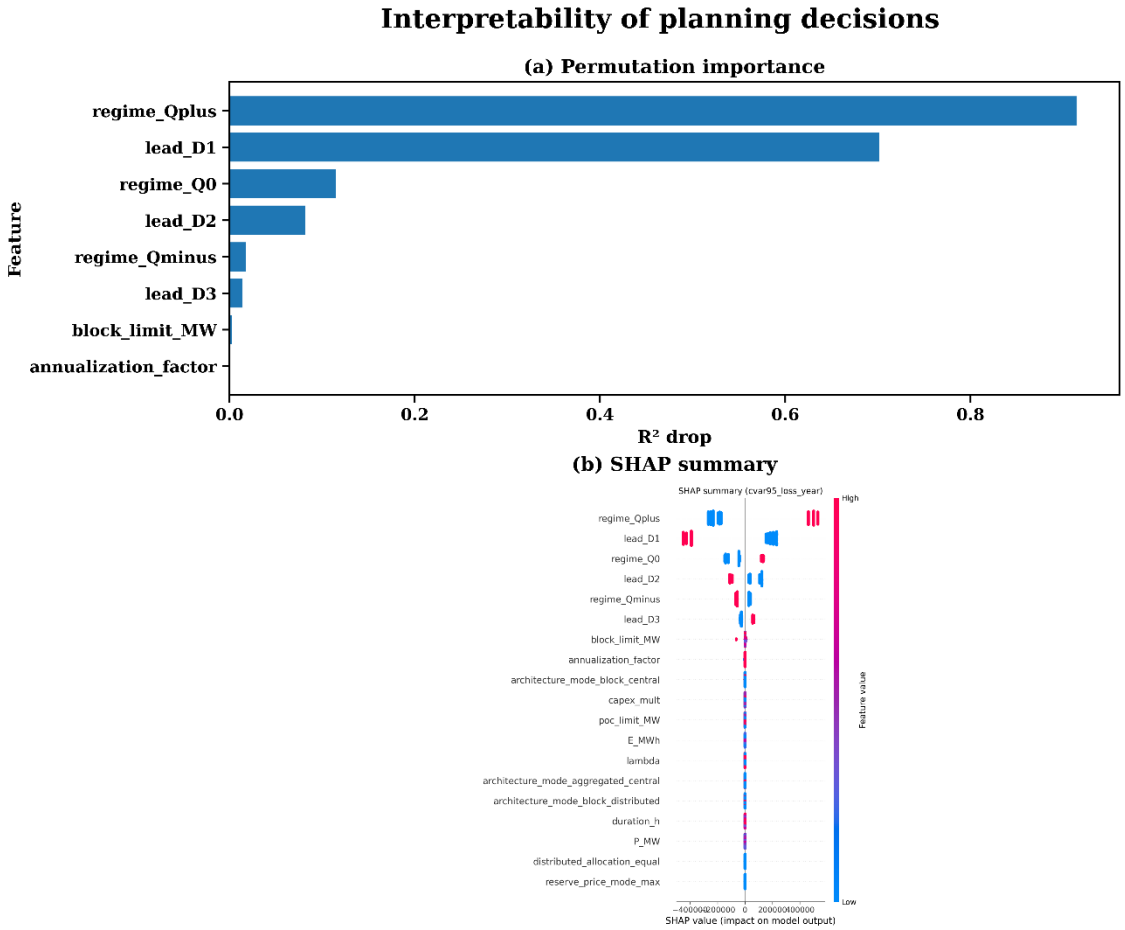

Appendix Figure 3 Interpretability of planning decisions

- **Additional Interpretation Drivers**

Interpretability analysis indicates:

- Storage value is primarily driven by:
  - Imbalance cost reduction
  - Curtailment mitigation
  - Limited reserve participation
- Marginal benefit decreases rapidly beyond **2 MW capacity**

- **Summary Insight**

The extended analysis confirms that:

- The optimal BESS configuration is **small, compact, and efficient**

- Increasing capacity leads to **diminishing economic returns**
- Risk-aware optimization ensures **balanced performance**
- The selected design is:
    - Economically optimal
    - Structurally stable
    - Robust across scenarios

➢ **Final Appendix Statement**

The Phase-2 appendix verifies that the selected BESS design is not only optimal under nominal conditions but also remains stable under extensive scenario exploration, confirming its suitability for downstream operational deployment

Appendix 4. Supplementary Results for Phase-3 (Operational Analysis)

This appendix provides additional analyses supporting the main findings of Phase-3. These results offer deeper insight into forecast sensitivity and flexibility value, complementing the core results presented in Sections 5.4.1–5.4.4 without introducing redundancy.

- **Forecast Value of Operation under Increasing Lead Time**

Figure 1 analyzes how forecast horizon affects operational value. The net-profit drop (Fig. A1a) shows that increasing lead time leads to significant economic degradation, with losses of approximately ~90 k€ (D1→D2), ~360 k€ (D1→D3), and ~270 k€ (D2→D3). This confirms that forecast accuracy is a critical driver of system profitability.

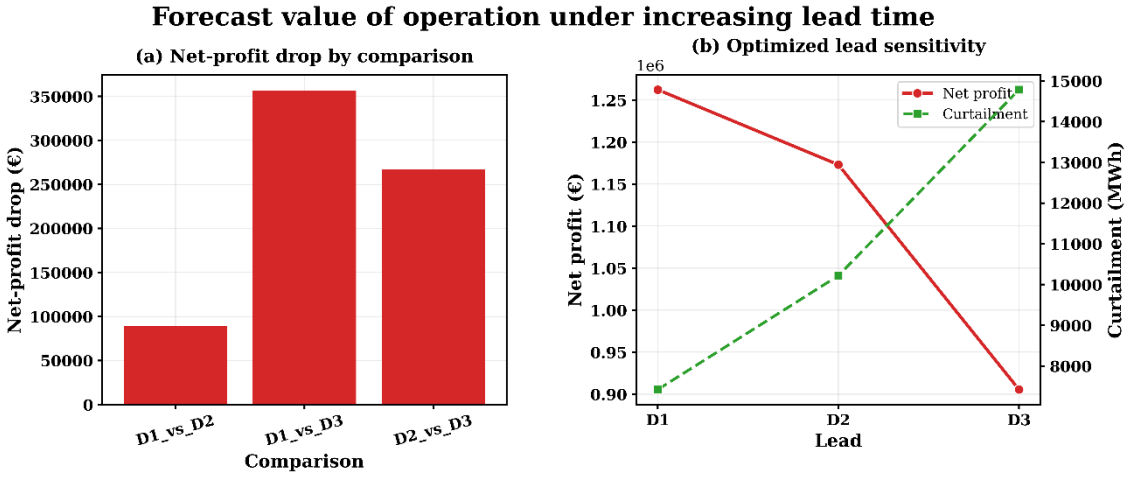

Appendix Figure 4 Forecast value degradation with increasing lead time

The optimized lead sensitivity (Fig. 1b) further highlights the structural response of the controller. Net profit declines (~1.26 M€ → ~0.91 M€), while curtailment increases (~7,500 → ~15,000 MWh) from D1 to D3. This demonstrates that uncertainty is managed primarily through increased curtailment, reinforcing the role of conservative dispatch under longer horizons.

- **Flexibility Value Decomposition of Battery Operation**

Figure 2 provides a detailed breakdown of the value and cost structure of battery-supported dispatch.

The gross positive value (Fig. 2a) indicates that total system value is dominated by energy market revenue (~1.5–1.6 M€ at D1–D2), with reserve revenue contributing a smaller share (~0.1–0.2 M€). Both components decline at D3, reflecting reduced market efficiency under uncertainty.

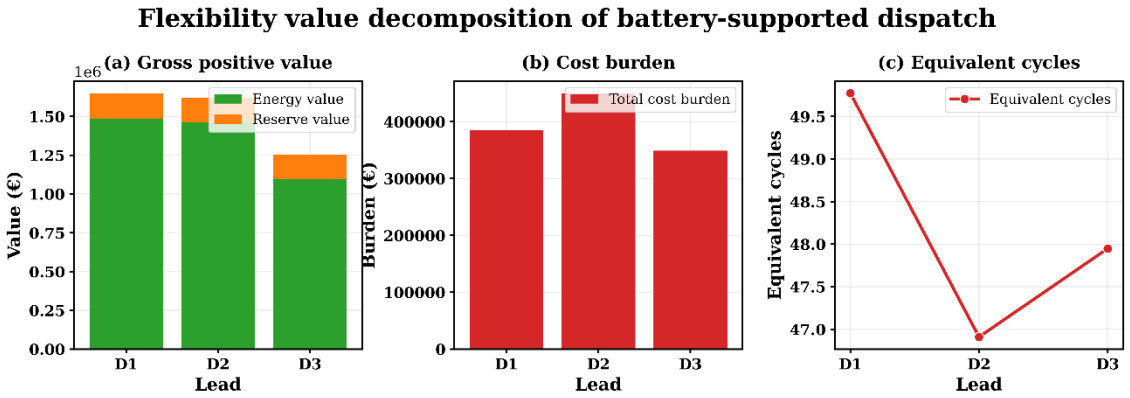

Appendix Figure 5 Forecast value degradation with increasing lead time

The cost burden (Fig. 2b) peaks at D2 (~450 k€) and decreases at D3 (~350 k€), aligning with the imbalance cost trends observed in the main results. This confirms that mid-horizon operation introduces the highest economic penalties.

Battery utilization (Fig. 2c) remains relatively stable across horizons (~47–50 equivalent cycles), indicating that the optimization redistributes operation strategies rather than significantly increasing usage intensity.

- **Key Takeaways from Supplementary Analysis**

The supplementary results reinforce three important insights:

- **Forecast horizon is the dominant driver of system performance**, directly impacting profit, curtailment, and cost.
- **D2 represents a critical transition regime**, where imbalance cost and economic penalties are maximized.
- **Flexibility value is primarily energy-driven**, while reserve participation provides secondary benefits under uncertainty.

These findings support the conclusions of Phase-3 and provide additional evidence for the transition toward long-term strategic evaluation in Phase-4.

Appendix 5. Digital Twin Interface and Operational Outputs

- **Digital Twin Application Entry Interface**

The PV–BESS digital twin application is initialized through a unified entry interface, as shown in Appendix Fig.6. This interface allows the user to select the operational mode of the platform before execution.

Two modes are available:

- **Live Mode**: Enables real-time system operation using current data streams, supporting continuous monitoring and adaptive dispatch decisions.
- **Data-Driven Mode**: Allows replay of historical scenarios using a selected timestamp, enabling controlled analysis, validation, and demonstration of system behavior under predefined conditions.

The **Run App** control activates the selected mode and initializes the full digital twin pipeline, including data ingestion, forecasting, optimization, and visualization layers.

This interface serves as the gateway to the digital twin system, ensuring flexibility between real-time operation and offline analytical evaluation within a single platform.

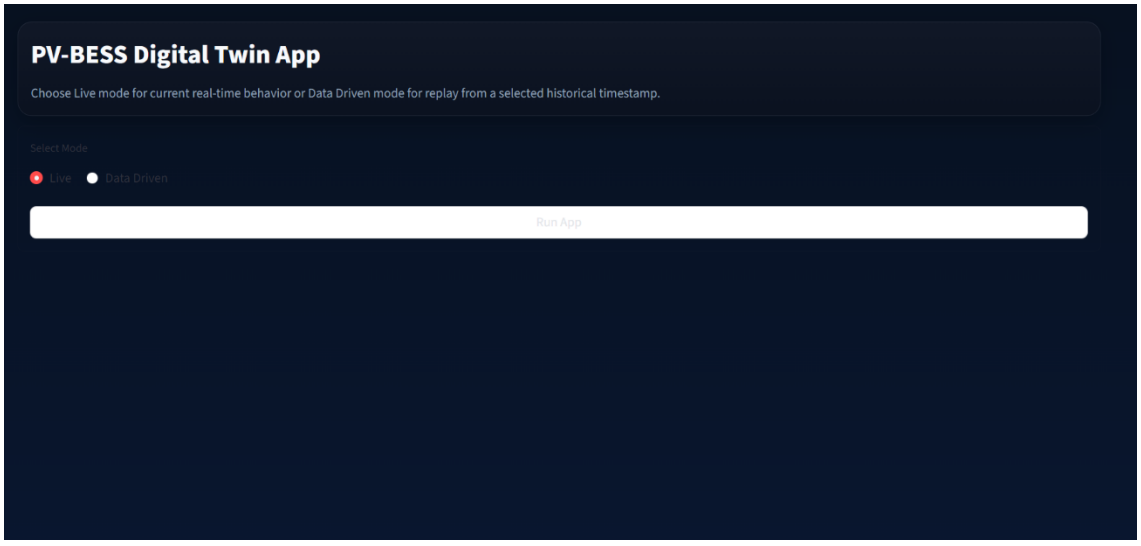

Appendix Figure 6 Digital Twin Interface

- **Digital Twin Control Center and Multi-Horizon Operation**

Appendix Figure 7 presents the main control interface of the PV–BESS digital twin, referred to as the **Control Center**. This dashboard integrates forecasting outputs, optimization decisions, and system monitoring into a unified operational view across multiple planning horizons (D1, D2, and D3).

- **Multi-Horizon Live Board**

The **Multi-Horizon Live Board** provides real-time operational guidance for each horizon. It highlights immediate system actions and alerts, such as reserve activation requirements or potential emergency conditions. This enables proactive decision-making by identifying short-term risks and required interventions.

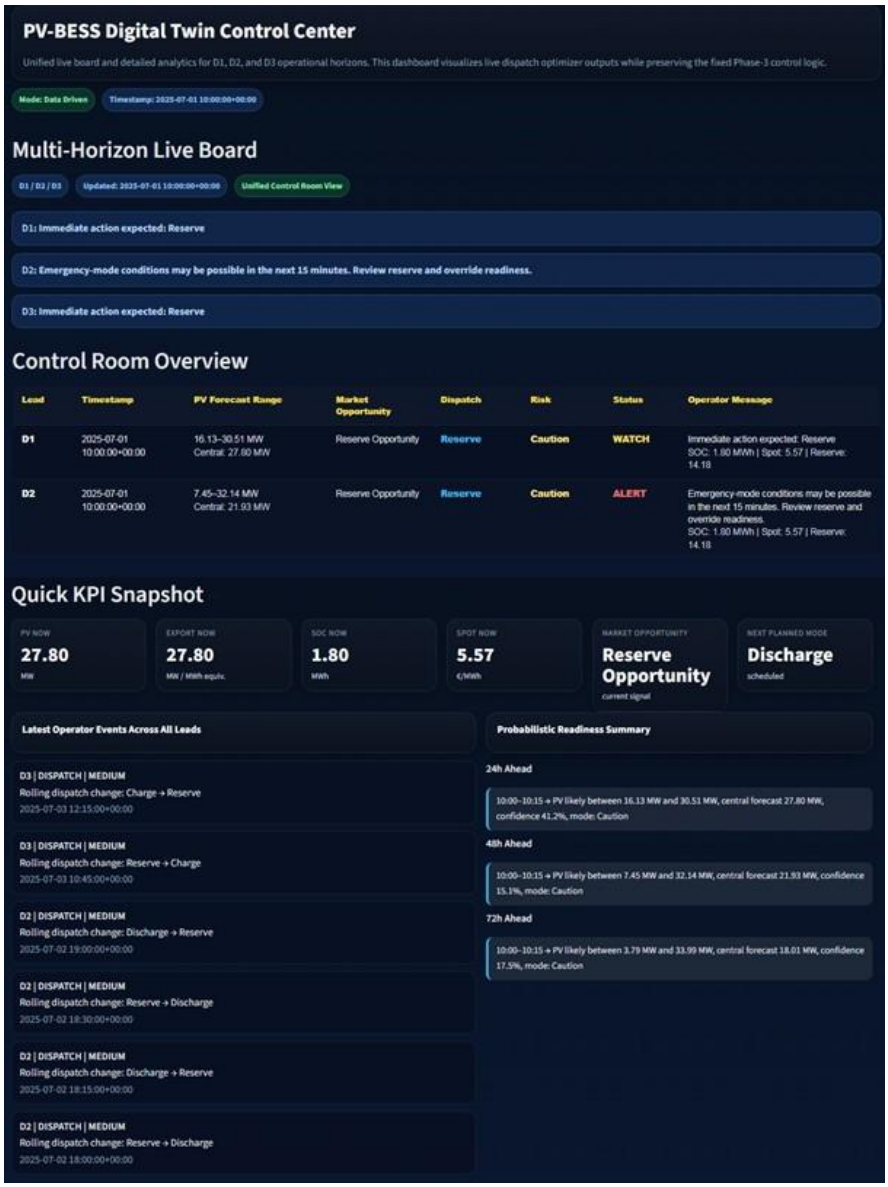

Appendix Figure 7 V–BESS Digital Twin Control Center (Real Time based)

- **Control Room Overview**

The **Control Room Overview** summarizes key system states for each horizon, including:

- PV forecast ranges and central estimates
- Market opportunity signals (energy vs reserve)
- Dispatch decisions (e.g., reserve, discharge)
- Risk levels (e.g., caution, alert)
- Operator guidance messages

This section functions as a high-level situational awareness panel, allowing rapid interpretation of system conditions and decisions.

- **Quick KPI Snapshot**

The **Quick KPI Snapshot** provides real-time system indicators, including:

- Current PV generation and export levels
- Battery state of charge (SoC)
- Spot market price
- Market opportunity classification
- Next planned operational mode

These indicators enable fast evaluation of system performance and operational readiness.

- **Operational Events and Logging**

The **Latest Operator Events** panel records recent dispatch actions and transitions across horizons, offering traceability of system behavior over time. This logging mechanism supports auditing and post-analysis of control decisions.

- **Probabilistic Readiness Summary**

The **Probabilistic Readiness Summary** aggregates forecast uncertainty across 24-hour, 48-hour, and 72-hour horizons. It presents probabilistic PV ranges along with confidence

levels, enabling uncertainty-aware planning and reinforcing the integration of probabilistic forecasting into operational decision-making.

- **Detailed Horizon Analytics and Decision Intelligence**

Appendix Figure 8 illustrates the **Detailed Horizon Analytics** interface of the PV–BESS digital twin, focusing on real-time system status, decision logic, and dynamic operational behavior under uncertainty.

- **Digital Twin Status**

As shown in **Figure A.2**, the **Digital Twin Status** panel provides a real-time snapshot of system conditions, including:

- Current PV forecast and probabilistic range (q10–q90)
- Forecast uncertainty (prediction interval width)
- Market signals (e.g., reserve offer)
- System confidence level

The system mode (e.g., *Caution*) reflects uncertainty-aware operational classification, guiding conservative or aggressive decision strategies.

- **Decision Intelligence Layer**

The **Decision Intelligence module** in Appendix **Figure 8** explains the reasoning behind system actions in a transparent and interpretable manner. It includes:

- Current operating mode (e.g., Reserve)
- Risk level and market opportunity classification
- Confidence level derived from probabilistic forecasts
- Next planned action and execution time

Additionally, the system provides **explainable decision factors**, linking actions to:

- PV generation level
- Market price signals
- Battery state of charge (SoC) constraints
- Forecast uncertainty

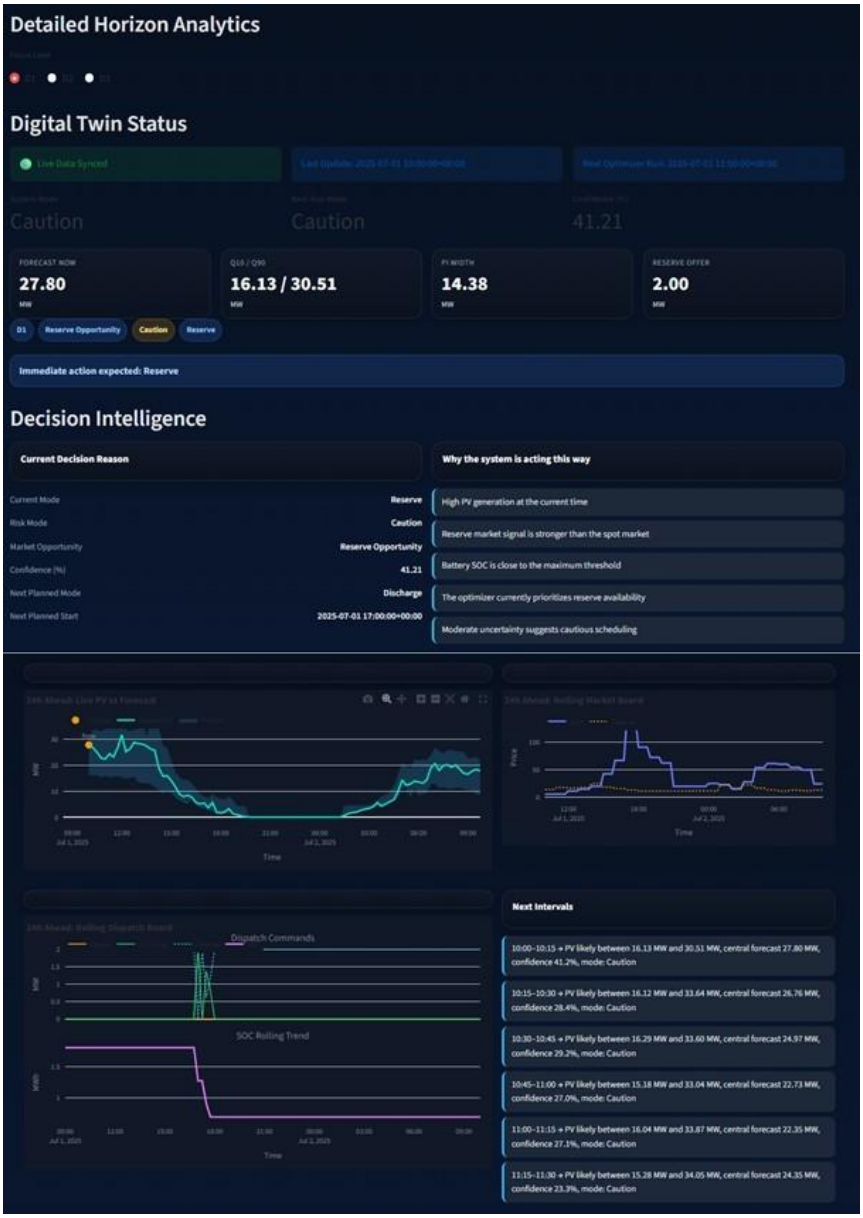

Appendix Figure 8 Detailed Horizon Analytics interface (Real-time based)

This ensures that automated decisions remain interpretable, auditable, and aligned with operational objectives.

- **Real-Time Forecast and Market Visualization**

Figure A.2 further presents dynamic visualization panels, including:

- **PV Forecast vs Actual Generation**, showing forecast accuracy and deviation
- **Rolling Market Board**, capturing temporal evolution of market signals
- **Rolling Dispatch Commands**, illustrating control actions over time

- **State of Charge (SoC) Trend**, reflecting battery response to dispatch decisions

These visualizations demonstrate how the system continuously adapts to changing conditions.

- **Short-Term Probabilistic Outlook**

The **Next Intervals** panel in **Figure A.2** provides high-resolution short-term forecasts, including:

- Probabilistic PV generation ranges
- Central forecast values
- Confidence levels
- Operational mode classification (e.g., Normal, Caution)

This enables fine-grained, interval-level decision support.

- **Short-Term Interval Forecasting and Action Panel**

Appendix Figure 9 presents the **Next Intervals** forecasting module together with the **Battery Charge/Discharge/Reserve Action Panel**, providing fine-resolution operational insight for short-term decision-making.

- **Next Intervals Forecasting**

As shown in Appendix **Figure 9**, the **Next Intervals** panel displays high-resolution probabilistic PV forecasts at short time steps (e.g., 15-minute intervals). For each interval, the system provides:

- Lower and upper bounds of expected PV generation
- Central forecast value
- Confidence level (%)
- Operational mode classification (e.g., *Normal*, *Caution*)

This granular representation enables the system to capture rapid changes in solar generation and supports precise, interval-level decision-making.

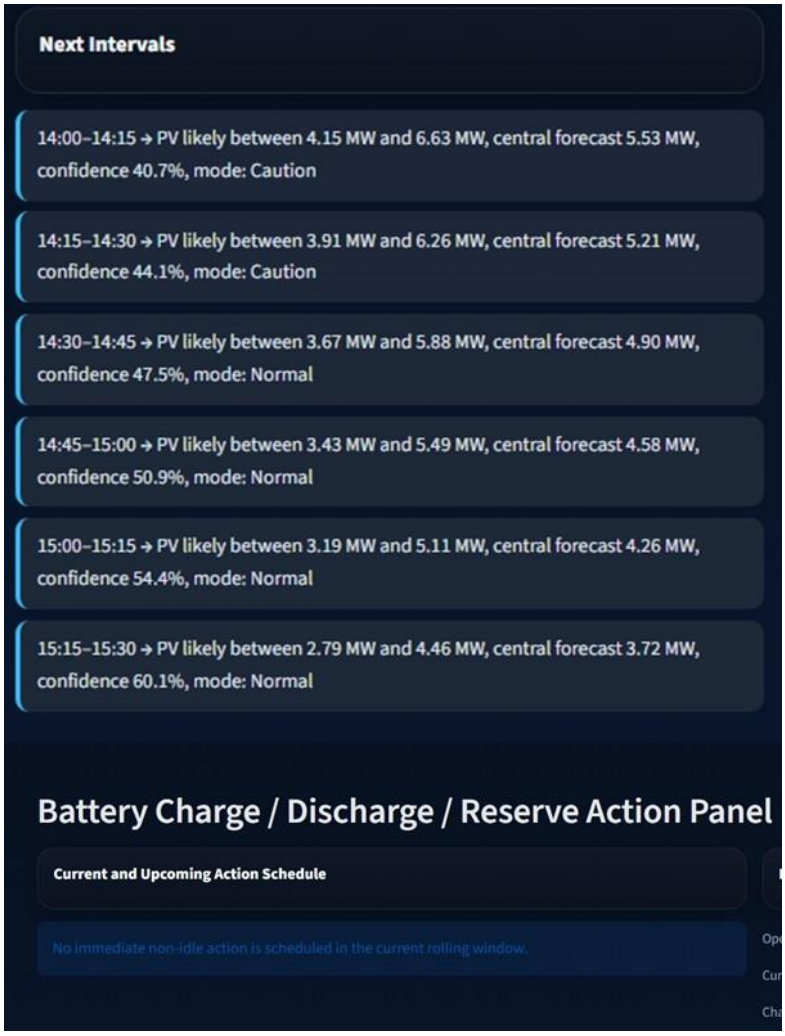

Appendix Figure 9 Short-term interval forecasting and battery action panel

- **Battery Action Panel**

The **Battery Charge/Discharge/Reserve Action Panel**, also shown in Appendix **Figure 9**, summarizes scheduled and upcoming control actions generated by the dispatch optimizer. It reflects:

- Current action status within the rolling horizon
- Planned operational actions (if any)
- System response under existing constraints and forecasts

In the illustrated case, no immediate non-idle action is scheduled, indicating that the system maintains a holding strategy under current conditions.

- **Data-Driven Control Center Operation**

Appendix Figure 10 presents the PV–BESS digital twin operating in **data-driven mode**, where system behavior is evaluated using a selected historical timestamp. This mode enables controlled replay and validation of operational strategies under predefined conditions.

- **Multi-Horizon Live Board (Replay Mode)**

As shown in **Appendix Figure 10** , the **Multi-Horizon Live Board** provides synchronized decision outputs across D1, D2, and D3 horizons under historical conditions. In this scenario, the system identifies a **low battery state of charge (SoC)** condition and prioritizes charging support across all horizons, demonstrating coordinated multi-horizon control behavior.

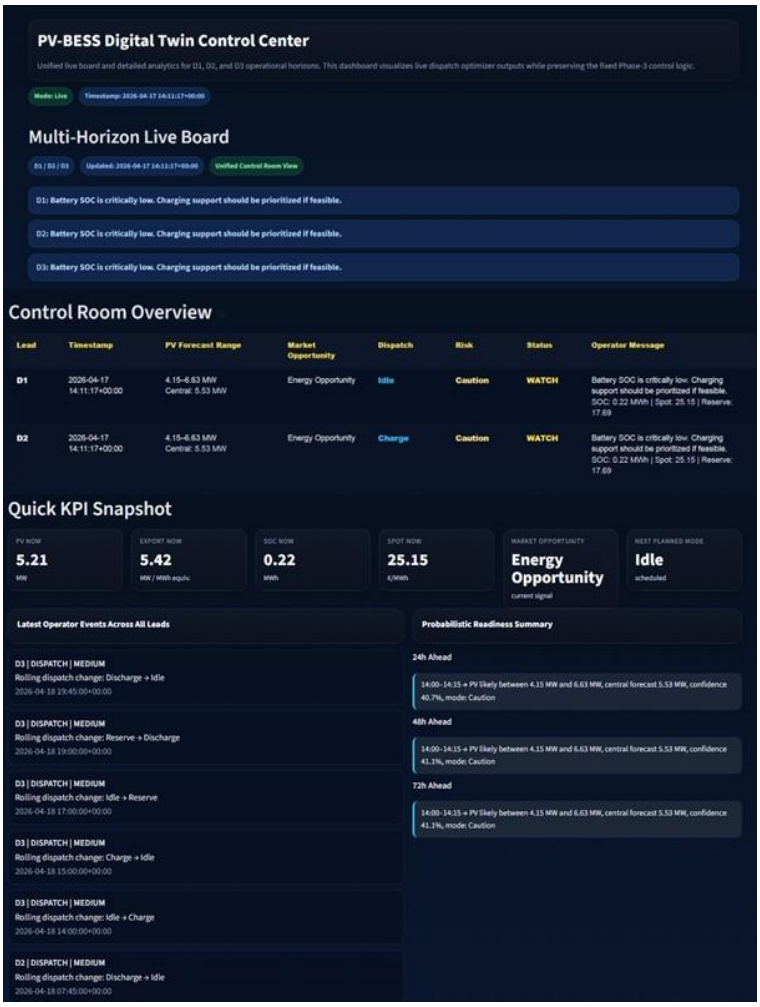

Appendix Figure 10 PV–BESS digital twin control center in data-driven mode

- **Control Room Overview**

The **Control Room Overview** in **Appendix Figure 10** summarizes system states under replay conditions, including:

- PV forecast ranges and central estimates
- Market opportunity classification (energy-driven scenario)
- Dispatch actions (e.g., idle, charge)
- Risk levels and system status indicators
- Operator guidance messages reflecting SoC constraints

This provides a structured representation of how the system reacts to specific historical system states.

- **Quick KPI Snapshot**

The **Quick KPI Snapshot**, shown in **Appendix Figure 10**, highlights key operational indicators:

- Low battery SoC (critical condition)
- Moderate PV generation levels
- High spot market price (energy opportunity)
- Next planned mode (idle or charge depending on horizon)

These indicators illustrate the interaction between physical constraints and market signals.

- **Operational Events and Replay Logging**

The **Latest Operator Events** panel records dispatch transitions during the replay process, such as switching between charge, discharge, and idle states. This enables detailed analysis of system responsiveness and control consistency under historical scenarios.

- **Probabilistic Readiness Summary**

The **Probabilistic Readiness Summary** in **Appendix Figure 10** provides uncertainty-aware forecasts for 24 h, 48 h, and 72 h horizons, showing that even in replay mode, the system maintains probabilistic decision support.

- **Data-Driven Detailed Analytics and Decision Intelligence**

Appendix Figure 11 presents the **Detailed Horizon Analytics** interface of the PV–BESS digital twin operating in **data-driven mode**, where system behavior is evaluated under a selected historical timestamp. This enables detailed analysis of decision logic and system response under controlled conditions.

- **Digital Twin Status (Replay Condition)**

As shown in **Appendix Figure 11** , the **Digital Twin Status** panel provides a snapshot of system conditions based on historical data, including:

- PV forecast and probabilistic range (q10–q90)
- Forecast uncertainty (prediction interval width)
- Market signals (e.g., reserve opportunity)
- System confidence level

The system operates under a *Caution* mode, reflecting moderate uncertainty and the need for risk-aware decision-making.

- **Decision Intelligence Layer**

The **Decision Intelligence module** in **Appendix Figure 11** explains the system's operational choice in a transparent manner. The replay scenario indicates:

- Activation of **reserve mode** due to favorable reserve market conditions
- Consideration of battery SoC near operational limits
- Influence of moderate forecast uncertainty on conservative scheduling

The explainable reasoning links decisions to:

- PV generation level
- Market signal dominance (reserve vs energy)
- Battery constraints

- Uncertainty conditions

This confirms that the decision framework remains consistent and interpretable under replay conditions.

- **Dynamic System Visualization**

Appendix Figure 11 includes multiple time-series visualization panels:

- **PV Forecast vs Actual**, showing historical forecast alignment
- **Rolling Market Board**, illustrating market signal evolution
- **Dispatch Commands**, reflecting control actions over time
- **SoC Trend**, showing battery response under historical dispatch

These plots provide insight into how the system would have behaved dynamically under the selected scenario.

- **Short-Term Interval Forecasting**

The **Next Intervals** panel in **Figure A.11** presents short-term probabilistic forecasts, including:

- PV generation bounds and central estimates
- Confidence levels
- Operational mode classifications

This demonstrates that even in replay mode, the system maintains high-resolution, uncertainty-aware decision support.

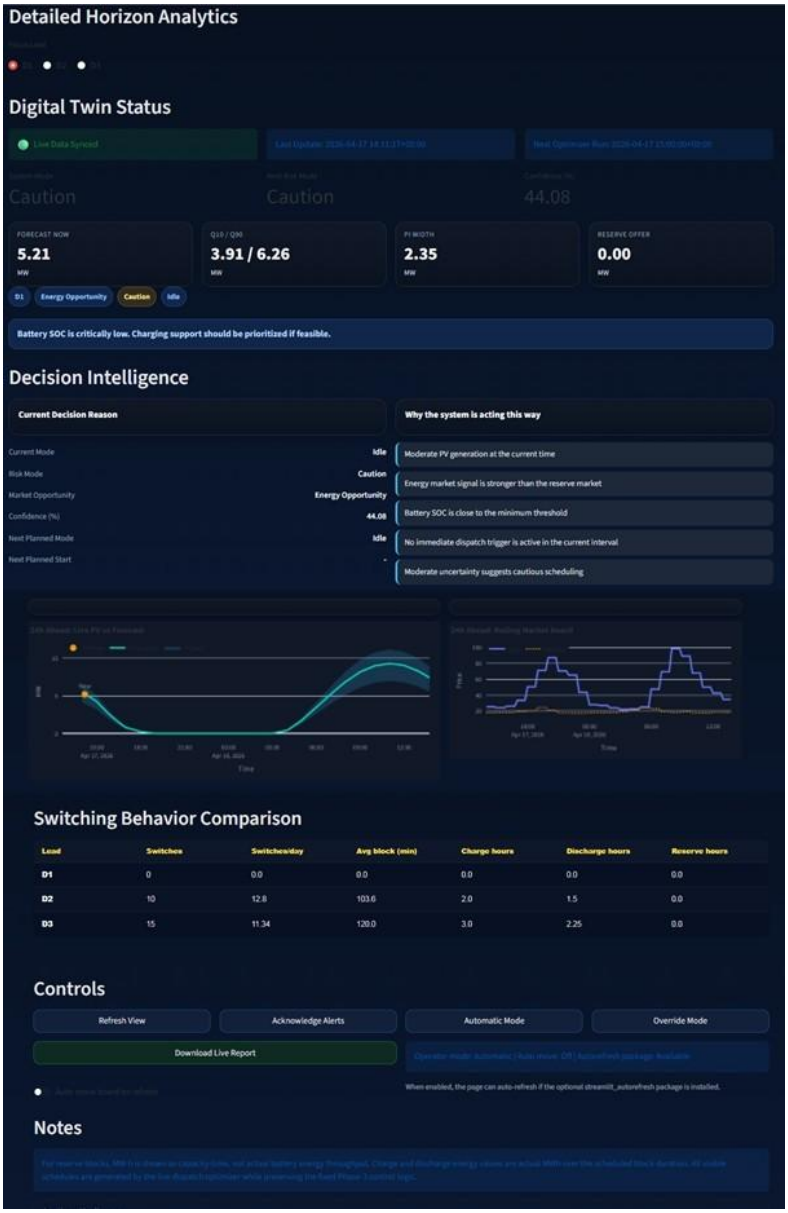

Appendix Figure 11 Data-driven detailed horizon analytics showing digital twin status

- **Battery Action Scheduling and Operational Stability Analysis**

Appendix Figure 12 presents the **Battery Charge/Discharge/Reserve Action Panel** together with switching behavior analysis and control interface, illustrating how optimization outputs are translated into executable system actions.

- **Battery Action Scheduling**

As shown in **Appendix Figure 12** , the **Current and Upcoming Action Schedule** provides a detailed timeline of dispatch decisions, including:

- Operation type (Charge, Discharge, Reserve)
- Start and end times of each action
- Energy throughput and duration
- Market signals (spot and reserve prices)
- Battery state of charge (SoC) constraints and risk indicators

These schedules are generated by the dispatch optimizer while respecting system constraints and maintaining consistency with the Phase-3 control logic.

- **Operator Guidance and Execution Context**

The **Next Action and Operator Guidance** panel in **Appendix Figure 12** summarizes:

- Current operating mode (e.g., automatic reserve mode)
- Scheduled power levels and energy commitments
- Upcoming planned actions and timing
- Dominant market signal influencing decisions

This provides a clear link between optimization outputs and operator-level interpretation.

- **Switching Behavior Analysis**

The **Switching Behavior Comparison** table in **Appendix Figure 12** evaluates operational stability across horizons (D1–D3), including:

- Number of switching events
- Switching frequency per day
- Average duration of operational blocks
- Time allocation across charge, discharge, and reserve modes

This analysis highlights the trade-off between responsiveness and stability, showing that optimized strategies maintain longer operational blocks and reduce unnecessary switching.

- **Control Interface and System Interaction**

The **Controls** section enables system interaction through:

- Refresh and alert acknowledgment functions
- Automatic and manual (override) operation modes
- Report generation and monitoring tools

This hybrid control capability ensures both automation and operator supervision.

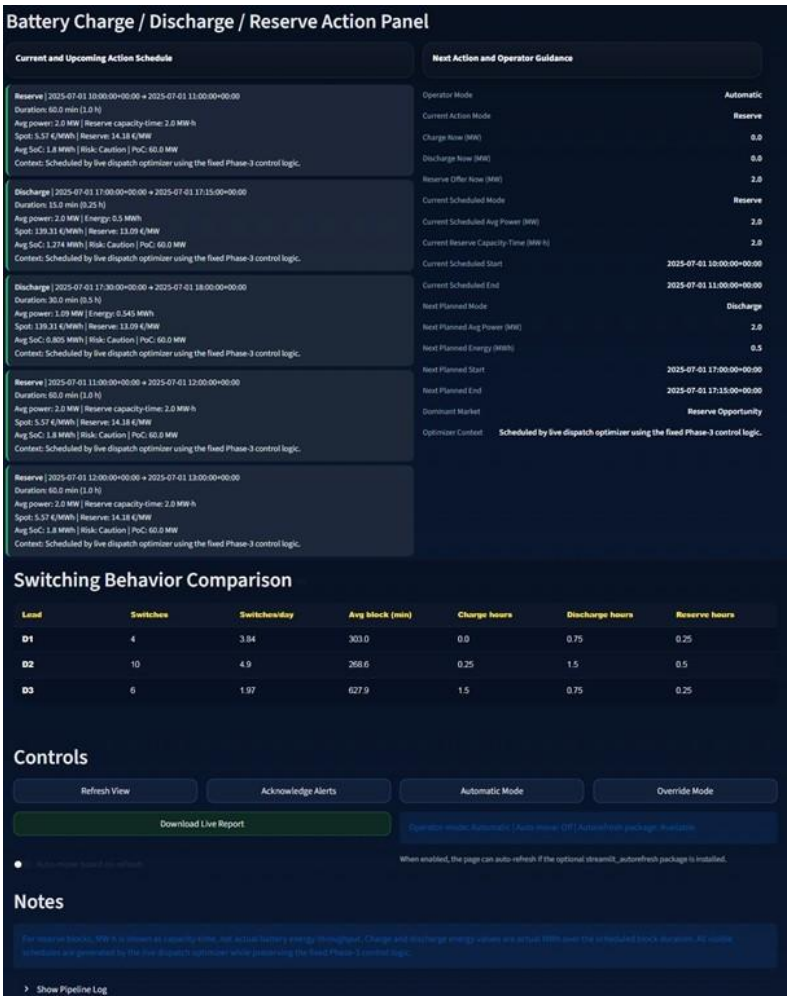

Appendix Figure 12 Battery action scheduling and operational stability analysis